

Aus dem Institut für Humanernährung und Lebensmittelkunde
der Christian-Albrechts-Universität zu Kiel

**Loss of function mutation in the
S-adenosylmethionine synthetase 1 gene (sams-1) increases
lipogenesis, enlarges lipid droplets and reduces lipolysis efficiency
in *Caenorhabditis elegans***

Dissertation

zur Erlangung des Doktorgrades
der Agrar- und Ernährungswissenschaftlichen Fakultät
der Christian-Albrechts-Universität zu Kiel

vorgelegt von

M.Sc. Madeleine Ehmke

aus Eberswalde

Kiel, 2013

Dekan: Prof. Dr. Dr. h.c. Rainer Horn

1. Berichterstatter: Prof. Dr. Frank Döring

2. Berichterstatter: Prof. Dr. Gerald Rimbach

Tag der mündlichen Prüfung: 11.07.2013

Gedruckt mit Genehmigung der Agrar- und
Ernährungswissenschaftlichen Fakultät der
Christian-Albrechts-Universität zu Kiel

Table of contents

Table of contents	I
List of Figures and Tables	IV
Abbreviations	VI
Summary	1
Zusammenfassung	2
1 Introduction	4
1.1 Lipid droplets are evolutionary conserved organelles important for intracellular lipid homeostasis.....	4
1.2 Lipid droplets are versatile organelles important for temporal protein storage.....	5
1.3 The biogenesis of lipid droplets is coupled to the synthesis of phosphatidylcholine	6
1.4 Basic aspects of lipid metabolism and lipid droplet size have been unravelled in the model organism <i>Caenorhabditis elegans</i>	7
1.5 Aims of the study.....	9
2 Materials and Methods	11
2.1 Worm strains and culture.....	11
2.2 EMS mutagenesis and isolation of the mutant <i>sams-1(t5669)</i>	11
2.3 Strategy of mutant identification.....	12
2.4 Outcrossing of <i>sams-1(t5669)</i> with wild type N2.....	13
2.5 Crossing of <i>sams-1(t5669)</i> with the Hawaiian strain CB4856.....	14
2.6 Isolation of genomic DNA.....	14
2.7 One-step WGS/ SNP mapping.....	14
2.8 Traditional chromosome mapping.....	15
2.9 Traditional interval mapping.....	15
2.10 Genetic complementation testing.....	16
2.11 Sequencing of the postulated mutation site.....	16
2.12 RFLP analysis.....	17
2.13 Analysis of body size.....	17
2.14 Determination of hatching rates and number of progenies.....	17
2.15 Lipid extraction for phospholipid and triacylglycerol quantification via thin-layer chromatography.....	18
2.16 Separation and quantification of phospholipids and triacylglycerol using thin-layer chromatography.....	18
2.17 BODIPY™ 493/503 staining and fluorescence imaging.....	19
2.18 Colocalization experiments.....	20

2.19	Design of starvation experiments.....	20
2.20	Quantification of triacylglycerol and protein level using colorimetric assays	20
2.21	Analysis of number and size of lipid droplets	21
2.22	Determination of surviving rates of worms exposed to arsenite and osmotic stress..	22
2.23	Total RNA isolation and whole genome gene expression analysis	23
2.24	Statistical analysis	23
3	Results	24
3.1	Identification of a the <i>sams-1(t5669)</i> mutant showing enlarged vacuoles in the embryo.....	24
3.2	<i>In silico</i> analysis predicts impairment of protein function due to A105V substitution in SAMS-1	25
3.3	Vulnerability to arsenite, a glutathione-depleting agent, is similar in <i>sams-1(t5669)</i> mutants, <i>sams-1(RNAi)</i> worms and <i>sams-1(ok3033)</i> mutants.....	26
3.4	<i>sams-1</i> adults but not <i>sams-1</i> larvae show a reduced proportion of phosphatidylcholine and an elevated triacylglycerol proportion	28
3.5	<i>sams-1</i> adults but not <i>sams-1</i> larvae show higher expression of genes involved in the synthesis of both phosphatidylcholine and triacylglycerol	30
3.6	<i>sams-1</i> mutants exhibit a small body size and a reduced number of progenies....	33
3.7	<i>sams-1</i> mutants exhibit enlarged lipid droplets in embryos as well as in the anterior and posterior intestine of L4 larvae and adults	35
3.8	<i>sams-1</i> larvae show a 2 fold enrichment of LDs that are $\geq 5 \mu\text{m}^3$ in size and are located in the anterior and the posterior intestine	40
3.9	In response to starvation, <i>sams-1</i> larvae show diminished depletion of triacylglycerol stores.....	41
4	Discussion	45
4.1	A missense mutation in <i>sams-1</i> most likely impairs protein function.....	45
4.2	SAMS-1 deficiency lowers phosphatidylcholine level - SAM-dependent synthesis of phosphatidylcholine may be of quantitative importance for growth and fertility	45
4.3	SAMS-1 deficiency lowers phosphatidylcholine level – this phenotype may be coupled to increased synthesis of triacylglycerol in order to reduce toxic effects of free fatty acids	46
4.4	SAMS-1 deficiency enlarges lipid droplets – a possible adaption to economize phosphatidylcholine.....	49
4.5	SAMS-1 deficiency reduces lipolysis efficiency under starvation conditions – an indication of inefficient liberation of lipid droplet-derived fatty acids	50
4.6	SAMS-1 deficiency reflects symptoms of non-alcoholic steatohepatitis	52

4.7	SAMS-1 deficiency mimics a dietary restriction state - a possible role of SAM-levels as gauge for nutrient availability	53
4.8	Conclusion	54
5	References	56
6	Supporting Information	69
7	Appendix	83
	Danksagung	IX
	Lebenslauf	X

List of Figures and Tables

Figure 1: Schematic depiction of structural and functional characteristics of LDs.	5
Figure 2: Biosynthesis of phosphatidylcholine in mammals, yeast, bacteria, plants and nematodes.....	7
Figure 3: Overview of methods used for mutant identification.....	13
Figure 4: Identification of a putative loss-of-function mutation in <i>sams-1</i> in <i>C. elegans</i>	24
Figure 5: <i>In silico</i> analysis of SAMS-1.	26
Figure 6: Vulnerability of <i>sams-1</i> mutants to arsenite and NaCl.....	28
Figure 7: TLC analysis of TAG, PC and PE fractions of wild type worms and <i>sams-1</i> mutants.	29
Figure 8: Genes involved in PC synthesis and lipogenesis are differentially expressed in wild types and <i>sams-1</i> mutants.....	31
Figure 9: Body size, hatching rate and number of progenies of wild type worms and <i>sams-1</i> mutants.....	34
Figure 10: Lipid droplets in wild type and <i>sams-1</i> embryos.....	36
Figure 11: Lipid droplets in wild type and <i>sams-1</i> L4 larvae.....	37
Figure 12: Lipid droplets in 5-day-old wild type worms and <i>sams-1</i> mutants.	39
Figure 13: Total number and mean volume of lipid droplets in wild type and <i>sams-1</i> L4 larvae.....	41
Figure 14: Starvation-induced LD breakdown and TAG consumption in wild type worms and <i>sams-1</i> mutants.	42
Figure 15: Size classification of LDs from <i>ad libitum</i> fed and starved wild type and <i>sams-1</i> larvae.....	44
Figure 16: Physiological consequences of <i>sams-1</i> inhibition.	55
Supporting information figure S1: Presentation of WGS/ SNP mapping data and SNP mapping data.	69
Supporting information figure S2: Wild type and <i>t5669</i> sequences of an amplified genomic PCR product harbouring the mutation site in the <i>sams-1</i> gene.....	75
Supporting information figure S3: Schematic representation of the connection between the one-carbon cycle and the transsulfuration pathway.....	76

Supporting information figure S4: TAG level adjusted to body volume of <i>sams-1</i> mutants and wild type worms.	77
Supporting information figure S5: Time of flight and extinction values of wild type worms and <i>sams-1</i> mutants.	78
Supporting information figure S6: ATGL-1::GFP as marker for lipid droplets in <i>sams-1(t5669)</i> mutants.	79
Supporting information figure S7: Starvation-induced alterations in LD size and LD number in wild type worms and <i>sams-1</i> mutants.....	80
Supporting information figure S8: Alterations of LD number and LD size during starvation in wild type worms and <i>sams-1</i> mutants.	81
Table 1: Genes contributing to lipid droplet size in <i>Caenorhabditis elegans</i>	10
Table 2: Expression level of genes involved in PL synthesis and lipogenesis compared in wild type worms and <i>sams-1</i> mutants.....	32
Supporting information table S1: <i>t5669</i> variants within the linked region derived from the WGS/ SNP method.	71
Supporting information table S2: List of primers used for chromosome and interval mapping.....	72
Supporting information table S3: Relative number of lipid droplets classified by size in <i>ad libitum</i> fed and starved wild type worms and <i>sams-1</i> mutants.	82

Abbreviations

°C	Degree celcius
µg	Microgram
µl	Microlitre
µm	Micrometre
1CC	One-carbon-cycle
3D	Three dimensional
5d ad	fifth day of adulthood
<i>acbp</i>	<i>Acyl-CoA binding protein</i>
ACC	Acetyl-CoA carboxylase
<i>acl</i>	<i>Acyltransferase-like</i>
<i>acs</i>	<i>Acyl-CoA synthetase</i>
<i>ahcy</i>	<i>S-adenosylhomocysteine hydrolase</i>
Apo B100	Apolipoprotein B100
ATGL	Adipose triglyceride lipase
BCA	Bicinchoninic acid
bp	base pair
BSA	Bovine serum albumine
<i>C. elegans</i>	<i>Caenorhabditis elegans</i>
<i>cbl</i>	<i>Cystthionine β-lyase</i>
<i>cbs</i>	<i>Cystathionine β-synthase</i>
CCT	CTP:phosphocholine cytidyltransferase
CDP-choline	Cytidin 5-Diphosphocholine
<i>cds</i>	<i>CDP-diglyceride synthetase</i>
<i>cept</i>	<i>Choline/ ethanolamine phosphotransferase</i>
CHO	Chinese hamster ovary
CIDE	Cell death-inducing DFF45-like effector
<i>cka</i>	<i>Choline kinase B</i>
<i>ckb</i>	<i>Choline kinase A</i>
<i>ckc</i>	<i>Choline kinalse C</i>
	CDP:choline
CPT	diacylglycerol choline phosphotransferase
cRNA	complementary RNA
<i>cth</i>	<i>Cystathionine γ-lyase</i>
<i>cyp</i>	<i>cytochrome P450</i>
<i>D. melanogaster</i>	<i>Drosophila melanogaster</i>
<i>daf</i>	<i>Dauer defective</i>
DAG	Diacylglycerol
<i>dgat</i>	<i>acyl-CoA:DiacylGlycerol AcylTransferase</i>
<i>dhs</i>	<i>Dehydrogenase</i>
DIC	Differential interference contrast
DR	Dietary restriction
<i>drr</i>	<i>DR-responsive</i>
<i>E. coli</i>	<i>Escherichia coli</i>
e.g.	exempli gratia

<i>elo</i>	<i>elongase</i>
EMS	Ethyl methanesulfonate
EXT	Extinction
FA	Fatty acids
<i>fasn</i>	<i>Fatty acid synthase</i>
<i>fat</i>	<i>fatty acid desaturase</i>
FSP27	Fat-specific protein of 27 kDA
<i>gcs-1</i>	γ -glutamine cysteine synthetase
gDNA	Genomic deoxyribonucleic acid
GPAT	Glycerol-3-phosphate transferase
gpx	Glutathione peroxidase
GSH	Reduced glutathione
gsr	Glutathione disulfide reductase
<i>gss</i>	<i>Glutathione synthetase</i>
HOPE	Have your protein explained
hr	Hours
i.e.	id est
<i>ino</i>	<i>Inositol requiring</i>
IPTG	Isopropyl- β -D-thiogalactopyranosid
<i>klf-3</i>	<i>Krüppel-like transcription factor 3</i>
L4	fourth larval stage
<i>lbp</i>	<i>Lipid binding protein</i>
LD	Lipid droplet
<i>let</i>	<i>lethal</i>
<i>lpin</i>	<i>lipin homolog</i>
LT	Lipidtropfen
<i>maoc</i>	MAO-C-like dehydratase domain
MAT	Methionine adenosyltransferase
<i>mboa</i>	<i>Membrane bound O-acyl transferase</i>
MeOH	Methanol
metr	5-Methyltetrahydrofolate-homocysteine methyltransferase
min	Minutes
ml	Mililitre
mm	Milimetre
mRNA	messenger RNA
MTBE	Methyl-tert-butyl ether
mTOR	mammalian target of rapamycin
MutPred	Mutation prediction
NAFLD	Non-alcoholic fatty liver disease
NASH	Non-alcoholic steatohepatitis
NGM	Nematode growth medium
NHR-49	Nuclear hormone receptor 49
<i>odc</i>	<i>Ornithine decarboxylase</i>
PC	Phosphatidylcholine
PCR	Polymerase chain reaction
<i>pcyt</i>	<i>Phosphocholine cytidyltransferase</i>

PDB	Protein data bank
PE	Phosphatidylethanolamine
PEAMT	Phosphoethanolamine methyltransferase
PEMT	Phosphatidylethanolamine methyltransferase
<i>pept</i>	<i>Peptide transporter</i>
<i>pisy</i>	<i>Phosphatidylinositol synthase</i>
PL	Phospholipid
<i>pmt</i>	<i>Phosphoethanolamine methyltransferase</i>
<i>pod</i>	<i>Polarity and osmotic sensitivity defect</i>
PolyPhen	Polymorphism phenotyping
PPAR α	Peroxisome proliferator-activated receptor α
<i>prx</i>	<i>Peroxisome assembly factor</i>
<i>psd</i>	<i>Phosphatidylserine decarboxylase</i>
<i>pssy</i>	<i>Phosphatidylserine synthase</i>
RFLP	Restriction fragment length polymorphism
RNA	Ribonucleic acid
RNAi	RNA interference
rpm	Rounds per minute
<i>S. cerevisiae</i>	<i>Saccharomyces cerevisiae</i>
SAM	S-adenosylmethionine
SAMS	S-adenosylmethionine synthetase
SBP	Sterol regulatory element binding protein
sec	Seconds
SEM	Standard error of the mean
SIFT	Sorting intolerant from tolerant
<i>smd</i>	<i>SAM decarboxylase</i>
SNARE	N-ethylmaleimide-sensitive-factor attachment receptor
SNP	Single nucleotide polymorphism
<i>spds</i>	<i>Spermidine synthase</i>
<i>sptl</i>	<i>serine palmitoyltransferase</i>
SREBP	Sterol regulatory element-binding protein
TAG	Triacylglycerol
TGF- β	transforming growth factor- β
TLC	Thin layer chromatography
TOF	Time of flight
VLDL	Very low-density lipoprotein
WGS	Whole genome sequencing

Summary

Cytosolic lipid droplets (LDs) are evolutionary conserved and versatile organelles important for storage and utilization of lipids in almost all cell types. In order to gain insights into the functional connection between LD size and lipid homeostasis we isolated, identified and finally characterized an S-adenosylmethionine synthetase (SAMS-1) deficient *Caenorhabditis elegans* (*C. elegans*) mutant showing enlarged LDs throughout the life cycle. SAMS-1 belongs to a family of evolutionary conserved enzymes, which catalyze the only known route of S-adenosylmethionine (SAM) synthesis. SAM-dependent methylation is of quantitative importance for the synthesis of phosphatidylcholine (PC), a major phospholipid of membranes. Syntheses of PC and triacylglycerol (TAG) are intimately coupled to each other due to common intermediates, shared biosynthetic routes and mutual regulatory mechanisms. The present study shows that SAMS-1 is necessary for homeostasis of PC and TAG synthesis and that SAMS-1 deficiency results in excessive TAG storage in *C. elegans*.

Thin layer chromatography based analysis of lipid extracts revealed that SAMS-1 deficiency reduces PC level but increases TAG proportions. Microarray-based expression profiling identified up-regulation of several lipogenic genes due to SAMS-1 deficiency, which is supposed to contribute to increased TAG proportions. Vital fat staining via BODIPY™ 493/503 revealed that increased TAG level are stored in fewer but larger LDs in *sams-1* mutants. A reduced surface area of few large-sized LDs is supposed to represent a mechanism to economize PC. On the other hand, it may limit the accessibility of TAG hydrolyzing lipases to LDs, since starvation experiments unveiled inefficient TAG hydrolysis and diminished LD breakdown of especially large-sized LDs in *sams-1* mutants. Moreover, *sams-1* mutants displayed a reduced body size and an impaired reproductive capability. Both, a reduced PC availability and the inefficient liberation of fatty acids are supposed to contribute to reduced growth and reproduction.

In summary, our data reveal a mechanism of how SAMS-1 deficiency mediates increased fat storage through impaired PC synthesis, LD expansion, increased lipogenesis and reduced lipolysis efficiency. We therefore conclude that synthesis of the methyl group donor SAM is necessary to limit fat storage.

Zusammenfassung

Lipidtropfen (LT) sind evolutionär konservierte, vielseitige cytosolische Organellen. Hauptfunktion der LT ist die kontrollierte Speicherung und Freisetzung von Lipiden. Ziel dieser Arbeit war es, einen tieferen Einblick in den funktionellen Zusammenhang zwischen LT-Größe und Lipidhomöostase zu erlangen. Zu diesem Zweck wurde eine S-adenosylmethioninsynthase (SAMS-1) defiziente *Caenorhabditis elegans* Mutante isoliert, identifiziert und charakterisiert, die sich durch die Ausprägung stark vergrößerter LT auszeichnet. SAMS-1 gehört zu einer Familie evolutionär konservierter Enzyme, die die Synthese von S-adenosylmethionin (SAM) katalysieren. SAM fungiert als der wichtigste Methylgruppendonor für eine Vielzahl physiologischer Reaktionen. SAM-abhängige Methylierungen sind unter anderem für die Synthese von Phosphatidylcholin (PC) von quantitativer Bedeutung. PC stellt eines der Hauptphospholipide biologischer Membranen dar. Die Synthese von PC ist mit der Triacylglyceridsynthese gekoppelt. Beide Stoffwechselwege teilen gemeinsame Substrate und unterliegen gleichen regulatorischen Mechanismen. Diese Studie zeigt die Bedeutung von SAMS-1 für die PC- und für die Triacylglyceridsynthese, und daß ein SAMS-Mangel in *C. elegans* zu einer exzessiven Speicherung von Triacylglyceriden (TAG) führt.

Mithilfe von Dünnschichtchromatographieverfahren konnte gezeigt werden, daß *sams-1* Mutanten zwar deutlich geringe PC Level besitzen, aber einen erhöhten TAG-Anteil aufweisen. Genexpressionsanalysen haben gezeigt, daß zahlreiche Gene der Lipogenese in *sams-1* Mutanten hochreguliert sind und es wird vermutet, daß dies zur verstärkten TAG-Synthese beiträgt. Vitalfettfärbungen haben zudem gezeigt, daß der erhöhte TAG-Anteil in *sams-1* Mutanten in insgesamt weniger, aber dafür deutlich größeren LT gespeichert wird. Eine Vergrößerung der LT verringert das Verhältnis von Oberfläche zu Volumen und bietet somit die PC-sparsamste Form große Mengen Fett zu speichern. Andererseits bietet eine geringere LT-Oberfläche weniger Angriffsfläche für Lipasen. In Hungerexperimenten konnte gezeigt werden, daß ein SAMS-1 Mangel in einer verminderten Hydrolyse von TAG und einem reduzierten Abbau von insbesondere großen LT resultiert. SAMS-1 defiziente Würmer wiesen eine deutlich geringere Körpergröße und eine stark reduzierte Anzahl an Nachkommen auf. Sowohl die die verminderte Verfügbarkeit

von PC, als auch die ineffiziente Lipolyse tragen höchstwahrscheinlich zu den Beeinträchtigungen im Wachstum und in der Reproduktion bei.

Zusammenfassend konnte in dieser Arbeit gezeigt werden, daß eine SAMS-1 Defizienz zu einer verminderten PC Synthese, einer verstärkten Lipogenese, einer Vergrößerung der LT und einer Verringerung der Lipolyseeffizienz beiträgt, und daß diese Mechanismen in einer exzessiven Fettspeicherung resultieren. Aufgrund dieser Daten wird vermutet, daß die Synthese von SAM für die Limitation der Fettspeicherung von essentieller Bedeutung ist.

1 Introduction

1.1 Lipid droplets are evolutionary conserved organelles important for intracellular lipid homeostasis

Lipid droplets (LDs) are cytosolic organelles, which have been identified in a huge number of species ranging from bacteria to humans [1-6]. In eukaryotic organisms, LDs are present in most cell types. The structural characteristics of LDs are similar in all species and cell types. LDs comprise a hydrophobic core, predominantly composed of triacylglycerols (TAG) and sterol esters, and a phospholipid monolayer surrounding the core. Phosphatidylcholine (PC) and phosphatidylethanolamine (PE) are the major surface phospholipids (PL) of LDs [7]. A high diversity of proteins is embedded into the LD membrane or adherent to the LD surface [8, 9]. These include structural proteins, like perilipin and CIDE proteins, which are critical regulators of lipid storage and utilization [10-14], SNARE proteins that mediate vesicle fusion [15], and key enzymes of PL and TAG synthesis [16-19]. The decoration of LDs with structural and lipid metabolizing proteins is the basis for their versatile functions.

The most prominent and evolutionary conserved function of LDs is storage of neutral lipids to regulate intracellular lipid homeostasis and to protect cells from lipotoxicity [20-23]. Under conditions of lipid overload, cells respond by increasing the number or the size of LDs to elevate lipid storage capacity [16, 24]. Contrary, during times of increased energy demand, including cell growth, dietary restriction or fasting, fatty acids (FA) are effectively delivered from LDs [25]. These FA are used for β -oxidation, biogenesis of membrane lipids and synthesis of lipoproteins, steroids and other lipid mediators [26, 27]. Lipid hydrolysis is mediated by LD associated lipases, like adipose triglyceride lipase (ATGL) [28-30]. Activation of these lipases depends on regulatory proteins such as perilipin. In adipocytes, perilipin functions as barrier to protect LDs from lipolysis under resting conditions. However, upon lipolytic stimulation, perilipin is phosphorylated and promotes lipolysis by activating ATGL [31-33]. The biological significance of LD associated lipases has been studied in mouse, yeast, fly and nematodes using mutants that are deficient in their respective ATGL homologs. These studies showed that inefficient lipolysis of LDs is associated with

proteolytic stress on many organs, a delay in cell-cycle entry, embryonic lethality as well as reduced motility and survival rates during starvation [34-37].

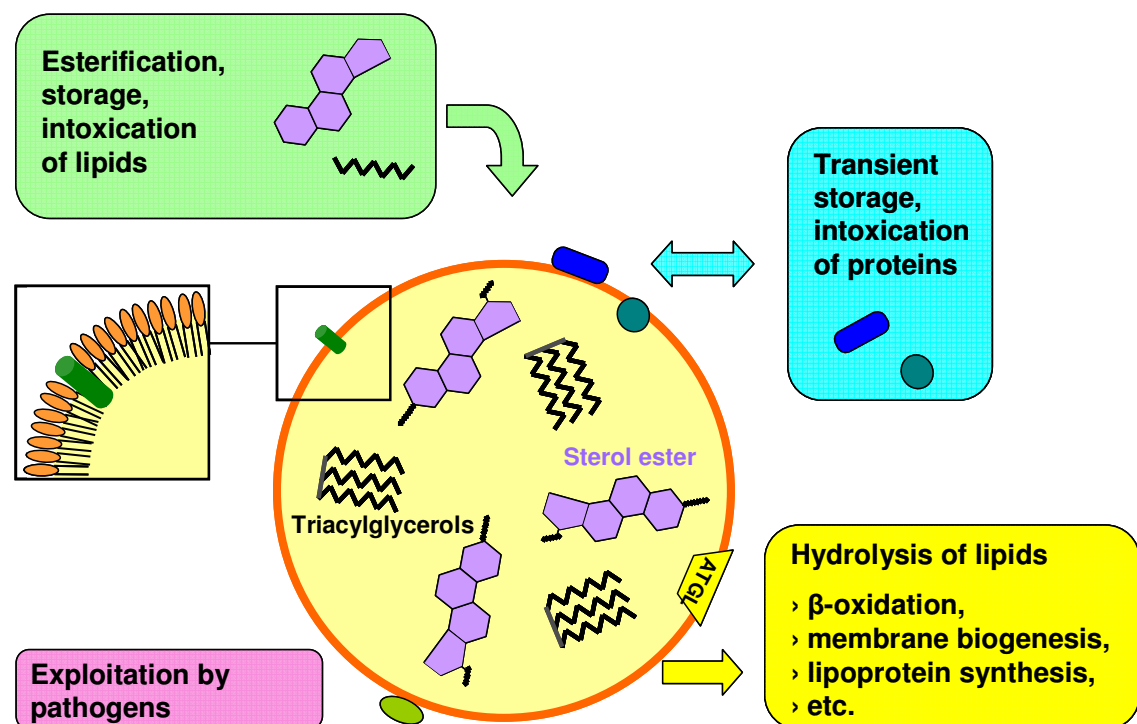


Figure 1: Schematic depiction of structural and functional characteristics of LDs. The neutral core of LDs is mainly composed of triacylglycerols and sterol esters. The core is surrounded by a phospholipid monolayer. Diverse structural and functional proteins cover the LD surface or are embedded within the LD membrane. Storage of lipid esters builds an energetic reservoir and protects cells from lipotoxicity (green box). In times of demand, lipids are hydrolyzed and free fatty acids are used for various functions (yellow box). Transient sequestration of proteins modulates availability according to systemic demand and protects from proteotoxicity (blue box). Some pathogens use host LDs for their own survival (purple box). The figure was adapted from Suzuki *et al.* [38].

1.2 Lipid droplets are versatile organelles important for temporal protein storage

More recently, LDs have been implicated in various activities, which are not directly related to lipid metabolism. For instance, LDs are sites for replication of pathogens. *Chlamydia trachomatis*, the hepatitis C virus and the dengue virus effectively utilize host LDs for growth and survival [39-44]. LDs are also transient storage sites for proteins intended for degradation or hydrophobic proteins such as Apo B100 or α -synuclein, a Parkinson's disease related protein. Thereby, LDs represent a buffering system that protects cells from proteotoxicity, since hydrophobic proteins

would aggregate in the aqueous environment [45-47]. Additionally, instead of being removed by degradation, a subset of LD proteins is stored for future use. For example, in *D. melanogaster*, histones are sequestered on embryonic LDs and they are only released to enter the nucleus when histone demand is highest in development [48]. Moreover, in the presence of bacterial lipopolysaccharides, LD-associated histones are released from the LD surface and kill bacteria efficiently *in vitro* and *in vivo* [49]. Structural and functional aspects of LDs are highlighted in figure 1.

1.3 The biogenesis of lipid droplets is coupled to the synthesis of phosphatidylcholine

PC is one of the major PLs composing the LD membrane [7]. Importance of proper PC synthesis for LD formation arises from the observation that key enzymes of PC biogenesis are present on the LD surface [16]. PC can be synthesized by each one of three metabolic pathways: The Kennedy pathway, the Bremer-Greenberg pathway and the PEAMT pathway (Figure 2). The presence and the relative importance of each pathway differ from organism to organism and even from tissue to tissue in the latter case [50]. The Kennedy pathway represents *de novo* PC synthesis and is present in mammals, yeast, fungi, plants and nematodes [51-60]. Herein, free choline is converted to PC via the intermediates phosphocholine and CDP-choline. Choline kinase, CTP:phosphocholine cytidyltransferase (CCT) and CDP:choline diacylglycerol choline phosphotransferase (CPT) are the sequential enzymes catalyzing the reactions of the Kennedy route [61, 62]. In the Bremer-Greenberg pathway, PC is formed by three successive methylation steps of PE [63, 64]. Methylations are catalyzed by PE-methyltransferases (PEMTs). Monomethylphosphatidylethanolamine and dimethylphosphatidylethanolamine are the intermediates of this route. Genes encoding PEMTs have been cloned from yeast and from mammalian liver cells [65, 66]. In the PEAMT pathway phosphoethanolamine methyltransferases (PEAMTs) catalyze the multiple methylation of phosphoethanolamine to phosphocholine, thereby providing nearly all of the metabolic flux into the Kennedy route. The PEAMT pathway was found in plants and nematodes, including *C. elegans* [67-70]. Both, PEMTs (within the Bremer-Greenberg route) as well as PEAMTs use SAM as methyl donor. Interruption

of both, SAM synthesis and PC formation has been shown to influence LD size and function [71-73].

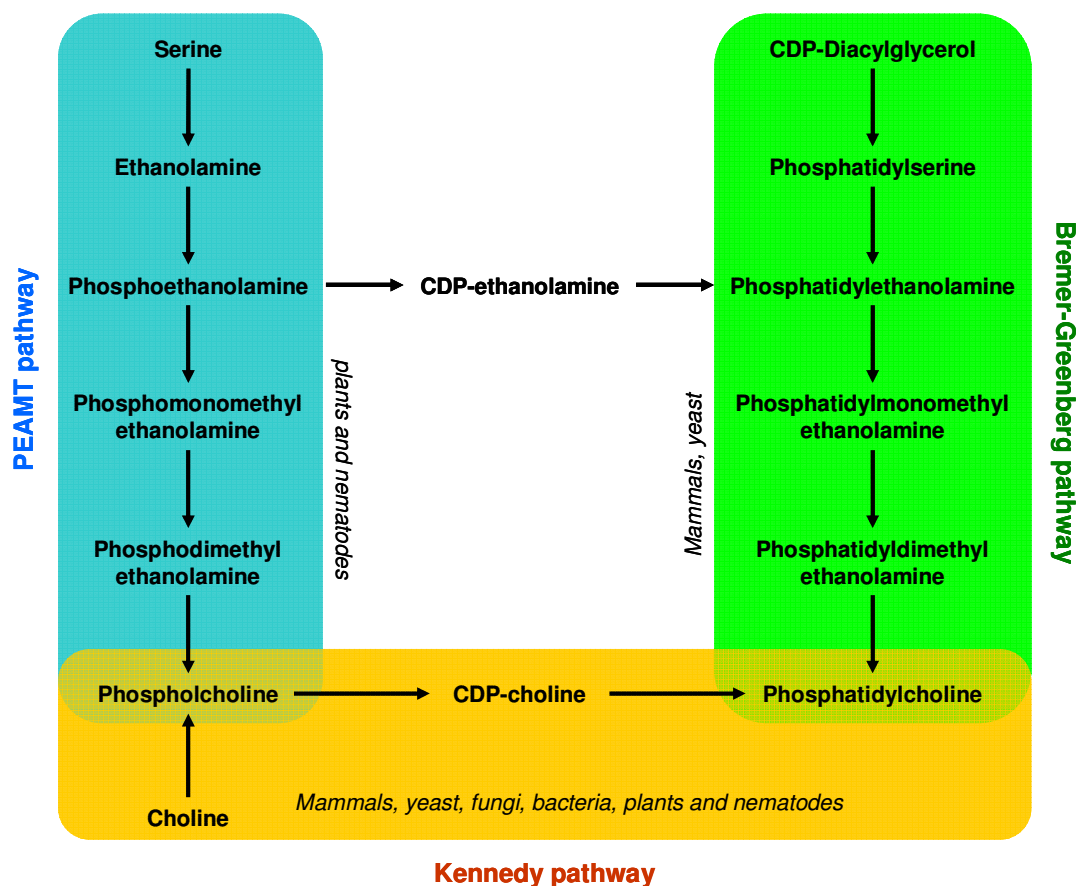


Figure 2: Biosynthesis of phosphatidylcholine in mammals, yeast, bacteria, plants and nematodes. The three routes of PC synthesis are schematically depicted. The Kennedy pathway is highlighted in orange, the Bremer-Greenberg pathway is indicated in the green box and the PEAMT pathway is shown in blue. The figure was modified from Palavalli *et al.* [70].

1.4 Basic aspects of lipid metabolism and lipid droplet size have been unravelled in the model organism *Caenorhabditis elegans*

During the last decade, several genes involved in synthesis, storage and utilization of lipids were identified in *C. elegans* and found to be highly conserved [74-76]. Moreover, conserved pathways regulating fat metabolism have been initially described in *C. elegans*. Serotonin, insulin, TGF- β (transforming growth factor- β) and mTOR (mammalian target of rapamycin) signalling as well as nematode homologs for the mammalian transcription factors SREBP and PPAR α were uncovered to regulate fat storage [77-85]. Moreover, novel microscopic techniques and staining methods enable visualization of LDs throughout life cycle at single-cell resolution [86-89].

Therefore, *C. elegans* has been established as a useful model to study basic aspects of lipid metabolism.

C. elegans lacks a specialized adipose tissue, but it stores fat in LDs, mainly present in its intestinal and hypodermal cells [5]. Both, mutant analysis and RNA interference (RNAi) screens in *C. elegans*, revealed a couple of evolutionary conserved genes, which are linked to LD size. Most of these genes encode proteins that participate in lipid metabolism (Table 1). Loss of *pept-1* abolishes intestinal proton-coupled peptide transport accompanied by a higher uptake of FA that are deposited in enlarged LDs [90, 91]. Increased intestinal uptake of FA, elevated *de novo* fat synthesis and accumulation of enlarged LDs were also shown in *acs-3* deficient mutants [92]. *acs-3* encodes a long chain acyl-CoA synthetase and ACS-3 derived acyl-CoAs are supposed to modulate the action of respective transcription factors, which regulate fat uptake and metabolism [92].

Genes encoding proteins for lipid binding and transport are also involved in determining LD size in *C. elegans*. Loss of *acbp-1*, encoding an acyl-CoA binding protein, reduces total TAG levels and number of LDs, but leads to a dramatic increase in the size of remaining LDs [93]. *lbp-5* encodes another lipid binding protein. *lbp-5* knock-down increases TAG storage and concomitantly LD size by reduced activation of the transcription factor NHR-49, due to defective transport of FA as ligands into the nucleus [94]. NHR-49 is a *C. elegans* homolog for PPAR α and LD expansion was found in *nhr-49* mutants, too [94]. The Krüppel-like transcription factor 3 is a further key regulator of fat metabolism in *C. elegans* and was associated with excessive lipid deposition when mutated [95-97]. LD enlargement is also induced by defective fatty acid breakdown. Loss of genes that mediate peroxisomal β -oxidation, namely *prx-10*, *maoc-1*, *dhs-28* and *daf-22*, results in TAG accumulation in expanded LDs [98, 99]. In contrast, genes that mediate TAG synthesis, like *acs-22* and *dgat-2*, were shown to be necessary for LD expansion [18]. *sams-1* and *pmt-1* encode SAMS-1 and PEAMT-1, respectively. Both proteins are involved in PC synthesis. Loss of either *sams-1* or *pmt-1* has been shown to increase LD size in adult worms [100, 101].

Recently, Zhang *et al.* identified nine additional genes that contribute to LD size [102]. RNAi inhibition of C05D11.7, *mboa-7*, *dhs-16* and *let-767* has been shown to enlarge LDs in *C. elegans*. C05D11.7 represents an ortholog of the human patatin-like phospholipase, which catalyzes the hydrolysis of TAG in the adipose tissue [102]. *mboa-7* encodes a membrane-bound acyltransferase and is required for incorporation of polyunsaturated fatty acids into phosphatidylinositol [103]. DHS-16 was identified as novel 3-hydroxysteroid dehydrogenase that regulates the formation of bile acid-like steroids called dafachronic acids [104]. *let-767* encodes a 3-ketoacyl-CoA reductase required for the bulk production of monomethyl branched and long chain fatty acids [105]. Interestingly, RNAi knock-down of *lpin-1*, *sptl-1*, *acs-1*, *cyp-29A2* and *fat-6* reduced the LD size, suggesting that these genes are important for LD growth [102]. *lpin-1* and *sptl-1* encode a putative phosphatidic acid phosphatase and a putative serine palmitoyltransferase, respectively [106-109]. CYP-29A2 belongs to the cytochrome P450 family and ACS-1 (acyl-CoA synthetase) mediates the incorporation of branched chain fatty acids into phospholipids [96, 110]. *fat-6* encodes a palmitoyl-CoA specific Δ -9 fatty acid desaturase [111-114].

1.5 Aims of the study

In this study, a new *C. elegans* mutant was isolated, which is characterized by enlarged lipid droplets. Aims of the present study were: (a) Identification of the phenotype causing mutation by whole genome sequencing and SNP mapping; (b) Characterization of LD size, LD number and LD distribution by fat staining methods and 3D fluorescence microscopy; (c) Monitoring LD breakdown and lipolysis efficiency under conditions of starvation; (d) Analysis of the lipid composition with special attention to TAG and PL fractions by thin layer chromatography; (e) Determination of development, growth and reproduction of the new mutant; (f) Identification of differentially expressed genes in the mutant and the wild type by comparative microarray analysis.

Table 1: Genes contributing to lipid droplet size in *Caenorhabditis elegans*.

Gene name	Gene ID	LD size ^a	metabolic process	Reference
<i>pept-1</i>	K04E7.2	↑	uptake of peptides from intestine	[90, 91]
<i>acs-3</i>	T08B1.6	↑	synthesis of long chain acyl CoA esters	[92]
<i>acbp-1</i>	C44E4.6	↑	binding and transport of acyl CoA esters	[93]
<i>lbp-5</i>	W02D3.7	↑	binding and transport of small lipophilic molecules	[94]
<i>acs-22</i>	D1009.1	↑	synthesis of very long chain acyl CoA esters	[18]
<i>dgat-2</i>	F59A1.10	↑	triacylglycerol synthesis	[18]
<i>prx-10</i>	C34E10.4	↑	import of peroxisomal matrix proteins	[98]
<i>maoc-1</i>	E04F6.3	↑	peroxisomal β -oxidation	[98]
<i>dhs-28</i>	M03A8.1	↑	peroxisomal β -oxidation	[98, 99]
<i>daf-22</i>	Y57A10C.6	↑	peroxisomal β -oxidation	[98, 99]
<i>nhr-49</i>	K10C3.6	↑	transcription factor, regulating fat metabolism	[94]
<i>klf-3</i>	F54H5.4	↑	transcription factor, regulating fat metabolism	[95-97]
<i>sams-1</i>	C49F5.1	↑	synthesis of S-adenosylmethionine; phosphatidylcholine synthesis	[100, 101]
<i>pmt-1</i>	ZK622.3	↑	phosphatidylcholine synthesis	[101]
	C05D11.7	↑	glycerolipid metabolism	[102]
<i>mboa-7</i>	F14F3.3	↑	phosphatidylinositol synthesis	[103]
<i>dhs-16</i>	C10F3.2	↑	short chain dehydrogenase	[104]
<i>let-767</i>	C56G2.6	↑	fatty acid metabolism	[105]
<i>lpin-1</i>	H37A05.1	↓	synthesis of triacylglycerol and phospholipids	[107, 108]
<i>sptl-1</i>	C23H3.4	↓	sphingolipid metabolism	[109]
<i>acs-1</i>	F46E10.1	↓	fatty acid metabolism	[96, 110]
<i>cyp-29A2</i>	T19B10.1	↓	arachidonic acid metabolism	[102]
<i>fat-6</i>	VZK822L.1	↓	Δ -9 fatty acid desaturase	[111-114]

^a LD size after inhibition of gene function with exception of *dgat-2* and *acs-22*, which are necessary for LD expansion.

2 Materials and Methods

2.1 Worm strains and culture

Bristol N2 and Hawaiian CB4856 were a gift from Ralf Schnabel (Developmental Genetics, TU Braunschweig, Germany). *sams-1(ok3033)* and VS20(hjls67) were obtained from the Caenorhabditis Genetics Center (Minneapolis, MN, USA). *sams-1(t5669)* was isolated from an EMS mutagenesis screen (section 2.2). Nematodes were cultured on Nematode Growth Medium (NGM) agar plates seeded with *Escherichia coli* var. OP50 as food source at 15°C. For all experiments gravid adult worms were hypochlorite treated to obtain synchronized populations. In general, culture and handling of worms were performed according to standard protocols [115, 116].

2.2 EMS mutagenesis and isolation of the mutant *sams-1(t5669)*

In collaboration with the laboratory of Ralf Schnabel (Developmental Genetics, TU Braunschweig, Germany), ethyl methanesulfonate (EMS) mutagenesis was performed in accordance to Jorgensen & Mango [117]. Wild type N2 L4 larvae were incubated in a EMS/ M9 buffer solution for 4 hr in a glass test tube. During incubation larvae were shortly spun on a vortexer in an interval of 15 min. Larvae were washed by eight cycles of sedimentation through 1 ml M9 buffer in a glass test tube and were transferred to NGM plates thereafter. After a recovery period of three hours at 15°C, EMS exposed L4 larvae were separated to 25-30 worms per plate by picking. Up-growing heterozygous progenies (F₁) were separated from P₀ worms by picking them on fresh plates (25-30 F₁ larvae/ plate). Using large particle flow cytometry (COPAS Biosort system, Union Biometra), their ensuing homozygous progeny (F₂) was dispensed in separate wells of 96-well plates. Therein, singled F₂ worms were cultured in liquid medium (for recipe see [118]) until screening for temperature-sensitive embryonic lethal mutant lines. By accident, mutant strain *sams-1(t5669)* was isolated, because the embryos of this strain contained large vacuoles. This phenotype was considered as interesting. Temperature-sensitivity of this strain could not be verified, but large vacuoles in *sams-1(t5669)* embryos were observed during further analysis.

2.3 Strategy of mutant identification

In the first instance, *sams-1(t5669)* was outcrossed with N2 to reduce background mutations (section 2.4). After that, *sams-1(t5669)* was crossed with polymorphic Hawaiian strain CB4856 (section 2.5). F₂ progenies carrying the “vacuole” phenotype represented recombinants between Hawaiian and Bristol N2 chromosomes. The progenies (F₃ and subsequent generations) of 45 F₂ recombinants were used to generate a recombinant DNA pool (section 2.6). This DNA pool was subjected to the one-step Whole Genome Sequencing and SNP mapping (WGS/ SNP mapping) procedure [119] (section 2.7). In parallel, traditional SNP mapping was performed. The recombinant DNA pool was used for chromosome mapping to identify the mutation bearing chromosome (section 2.8). Individual recombinant lines were used for interval mapping to locate the mutation between to snip-SNPs on the X chromosome (section 2.9). By both, one-step WGS/ SNP mapping and traditional SNP mapping, the mutation was located to the chromosomal region X: 11-12 Mb. Moreover, by use of WGS data, the mutation could be identified as C→T transition in the *sams-1* gene. Verification of *sams-1* as mutation bearing gene was done by genetic complementation testing (section 2.10) The C→T transition was verified by sequencing of an amplified genomic PCR product that includes the postulated mutation site (section 2.11) and subsequent restriction fragment length polymorphism (RFLP) analysis (section 2.12). An overview is given in figure 3.

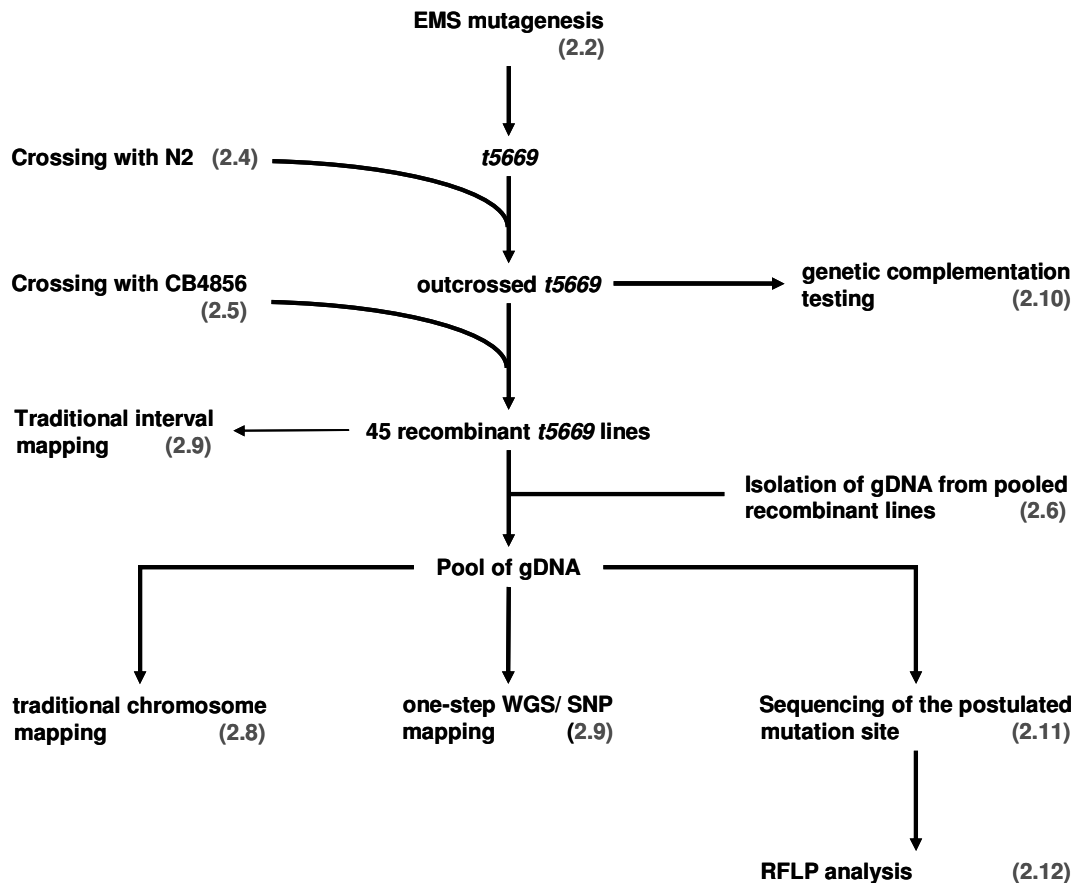


Figure 3: Overview of methods used for mutant identification. A schematic representation of methods that have been used for location, identification and verification of the phenotype causing mutation in *sams-1(t5669)* mutants is shown. Abbr.: EMS = ethyl methanesulfonate; gDNA = genomic DNA; WGS = whole genome sequencing.

2.4 Outcrossing of *sams-1(t5669)* with wild type N2

To reduce background mutations, the mutant strain *sams-1(t5669)* was crossed with wild type N2. Single *sams-1(t5669)* L4 hermaphrodites were placed on small NGM plates (3.5 cm in diameter) together with 4 N2 males. F₁ generation was scored for male frequency to ensure cross-fertilization. Individual F₁ cross-progenies were separated on small plates and allowed to self-fertilize. F₂ individuals carrying the droplet phenotype were singled and their progenies were used for a further crossing with N2 males. In total, *sams-1(t5669)* was outcrossed five times. The outcrossed *sams-1(t5669)* mutant was used for phenotypic analysis.

2.5 Crossing of *sams-1(t5669)* with the Hawaiian strain CB4856

For mutant mapping, the *sams-1(t5669)* mutant was crossed with males of the polymorphic Hawaiian strain CB4856 by analogy to outcrosses with N2. F₁ cross-progenies were singled onto 6 cm NGM plates. In a total, 45 F₂ recombinants carrying the droplet phenotype were singled and allowed to self-fertilize. The 45 recombinant lines were used for one-step WGS/ SNP mapping (section 2.7) as well as for traditional chromosome (section 2.8) and interval mapping (section 2.9)

2.6 Isolation of genomic DNA

One-step WGS/ SNP mapping and traditional chromosome SNP mapping required genomic DNA of pooled recombinant lines. Therefore, pooled progenies of the 45 F₂ recombinants were washed with M9 buffer three times. To remove the food in the gut, worms were incubated in M9 buffer on a nutator mixer for 2 hr. After three additional washing steps worms were centrifuged at 3153 rpm for 2 min and as much as possible M9 was removed without disturbing the worm pellet. The worm pool was stored at -80°C overnight (http://hobertlab.org/wp-content/uploads/2013/02/Worm_Genomic_DNA_Prep.pdf). Finally, the Genra Puregene Tissue Kit was used for isolation of genomic DNA according to manufactures instructions (protocol: DNA Purification From Tissue; QIAGEN, Hilden, Germany). Additionally, DNA solution was subjected to phenol extraction followed by ethanol precipitation to increase purity of DNA. Quality and yield of the extracted DNA were assessed spectrophotometrically (BioPhotometer, Eppendorf, Hamburg, Germany).

2.7 One-step WGS/ SNP mapping

For combined mutant mapping and mutant identification the genomic DNA of pooled recombinants (20 ng/μl) was subjected to the one-step WGS/ SNP mapping procedure [119]. Sequencing was done on an Illumina GA2 sequencing platform. The WGS dataset was analyzed using the CloudMap software pipeline (<http://usegalaxy.org/cloudmap>) [120]. Accordingly, the genome of the N2 strain used for mutational generation of *sams-1(t5669)* was sequenced, thereby providing the genuine mutational background of *sams-1(t5669)*. WGS/ SNP mapping procedure

and data analysis were carried out by the Oliver Hobert laboratory (Department of Biochemistry & Molecular Biophysics, Columbia University, New York, USA). Sequences were aligned to the WS220 release of the *C. elegans* genome.

2.8 Traditional chromosome mapping

For chromosome mapping, pooled DNA of *sams-1(t5669)* recombinants as well as wild type N2 and CB4856 reference DNA templates were used. Preparation of reference templates was done as follows: 20 N2 worms and 20 CB4856 animals were picked in separate 0.2 ml tubes, containing 20 μ l single-worm-lysis buffer (50 mM KCL, 10 mM Tris-HCL pH 8.3, 2.5 mM MgCl₂, 0.45 % NP-40, 0.45 % Tween20, 0.01 % gelatine, 0.2 mg/ml Proteinase K). Worms were lysed by freezing in liquid nitrogen for 30 min and incubation at 65°C for 1 h in a thermocycler. Proteinase K was inactivated by incubation at 95°C for 15 min. N2, CB4856 and recombinant *t5669* DNA templates were added in a volume of 1 μ l to a PCR master mix, containing 12.5 μ l MangoMix™ (Bioline, Luckenwalde, Germany), 10.5 μ l water and 1 μ l primer pair (0.5 μ l each primer). For each chromosome, three primer pairs were used that enabled amplification of snip-SNP regions at the end of both arms and in the central region of a chromosome, respectively (Table S2). Amplification of PCR products was done in a thermocycler using the following cycling conditions: 2 min 95°C; 30 sec 95°C, 30 sec 54°C, 90 sec 72°C (35x). PCR products were digested with the respective restriction enzyme (Fermentas Life Science) at 37°C overnight (Table S2). Digestion reactions comprised 1.5 μ l 10 \times enzyme buffer, 6 μ l water, 0.1 μ l restriction enzyme and 7.5 μ l PCR product. Samples were loaded on a 2 % agarose gel (SeaKem® LE agarose, Biozym®, Hessisch Oldendorf, Germany), containing ethidium bromide (5 μ l/ 50 ml gel). After electrophoresis, gels were visualized with the Alphaimager HP (Biozym, Hessisch Oldendorf, Germany).

2.9 Traditional interval mapping

For interval mapping, single-worm-lysates for each of the 45 recombinant lines were prepared according to the preparation of N2 and CB4856 reference DNA templates (section 2.8). All recombinants were analyzed for 21 snip-SNPs along the entire X chromosome. Amplification and restriction of the PCR products as well as digestion and gel electrophoresis were done according to chromosome mapping. Each

snip-SNP loci was scored for frequency of CB4856 alleles. Snip-SNP loci showing only N2 alleles were considered as mutation bearing region. A complete list of primers used for interval mapping is given in table S2. Primer designs used for chromosome and interval mapping derived from Davis et al. [121], from the *C. elegans* Single Nucleotide Polymorphism Data base (<http://genome.wustl.edu/services/c-elegans-snpdata>) [122], and from Wormbase Release 235.

2.10 Genetic complementation testing

To verify *sams-1* as mutation bearing gene, a genetic complementation test was performed. *sams-1(t5669)* L4 hermaphrodites were crossed with males of a known *sams-1* mutant (RB2240), harbouring a 480 bp deletion allele of *sams-1 (ok3033)*. Cross-fertilization was ensured by 50 % male frequency in the F₁ generation. F₁ cross progeny was examined for the occurrence of the droplet phenotype. Since both *sams-1* alleles are recessive, the presence of the droplet phenotype in heterozygous F₁ animals indicated that they fail to complement each other.

2.11 Sequencing of the postulated mutation site

To further verify the C→T transition at position 11966380 we amplified by PCR 742 bp of genomic *sams-1(t5669)* and N2 DNA that contained the loci of interest within the *sams-1* gene. Primers used for the amplification were CCTTTTCACCAAGTGAATCTGTG and CCTTCTTGATAACATCAGCGAG (figure S2). PCR products were purified by gel electrophoresis using a 1.2 % low melting agarose gel (NuSieve® GTG® agarose, Biozym®, Hessisch Oldendorf, Germany). A gel extraction kit (GENAXXON, Ulm, Germany) was used to extract DNA fragments from the gel according to manufactures instructions. Quality and yield of the extracted DNA were assessed spectrophotometrically (BioPhotometer, Eppendorf, Hamburg, Germany). Sequencing was done by Eurofins MWG Operon using the value read service.

2.12 RFLP analysis

PCR products were also used for RFLP analysis, since C→T transition at position X: 11966380 alters the recognition site of the restriction enzyme Fnu4HI (Figure 1C). Digestion reactions comprised 1.5 µl 10× FastDigest reaction buffer, 6 µl water, 0.1 µl FastDigest® Fnu4HI (Fermentas Life Science, Ulm, Germany) and 7.5 µl PCR product and were incubated at 37°C for 10 min. DNA fragments were separated by gel electrophoresis (2 % agarose gel). Allele-specific restriction was visualized with the Alphaimager HP.

2.13 Analysis of body size

Parameters of body size were determined in L4 larvae and five-day-old adults, respectively. TOF (time of flight) and extinction (EXT), determined by large particle flow cytometry using the COPAS Biosort system, were used as approximate values for length and volume of the worms, respectively [86]. 2000 to 4000 individual animals were analyzed for each strain and developmental stage in at least three independent experiments. Based on analysis of microscopic images, body volume of the worms was calculated from area and perimeter using an adapted cylinder volume formula [123, 124]. Worms were imaged by the bright field optics of a Zeiss SteREO Discovery.V8 microscope (Achromat S 1,5x FWD 28 mm objective; 8x manual zoom), fitted with a AxioCam ICc 1 (Zeiss). Area and perimeter were determined by encircling worms with the AxioVision software (release 4.8, Zeiss, Jena, Germany). At least 10 worms per strain, developmental stage and experiment were analyzed. The experiment was repeated twice.

2.14 Determination of hatching rates and number of progenies

To determine hatching rate, L4 larvae of each strain were individualized on single small NGM agar plates (3.5 cm in diameter) and cultivated until they laid the first ~50 eggs. A total number of at least 30 freshly laid eggs per worm were picked on new small NGM agar plates and analysed for hatching. Hatched F₁ larvae were scored at the late L2/ early L3 stage. Hatching rate was expressed as percentage of hatched F₁ larvae from the total number of eggs that were analyzed per worm. Ten worms per strain were analyzed in two individual experiments, respectively. To determine the

number of progenies, L4 larvae (P_0) of each strain were individualized on single small NGM agar plates and screened for viable progenies during entire reproductive phase. To prevent an intermixture of F_1 and F_2 progenies adult P_0 worms were transferred to fresh plates in an interval of 48 h (N2) or 72 h (*sams-1* mutants). Viable F_1 progenies were scored at the L4 stage. For each strain 10 individual worms were analyzed in two independent experiments.

2.15 Lipid extraction for phospholipid and triacylglycerol quantification via thin-layer chromatography

Hypochlorite treated worms were grown until they reached the fourth larval stage (N2 after 94 hr; *sams-1(t5669)* after 122 hr; *sams-1(ok3033)* after 140 hr) and the fifth day of adulthood (N2 after 216 hr; *sams-1(t5669)* after 260 hr; *sams-1(ok3033)* after 280 hr), respectively. Worms were washed three times with M9 buffer prior sample collection via COPAS Biosort flow cytometry. Samples comprised 3000 (N2) and 4000 (*sams-1* mutants) worms for lipid analysis at the L4 stage. For lipid analysis of five-day-old adult nematodes 1000 (N2) and 1500 (*sams-1* mutants) animals were collected. Samples were adjusted to a volume of 50 μ l and stored at -80°C until further processing. Lipids were extracted using methyl-tert-butyl ether (MTBE) extraction according to the protocol of Matyash et al. [125]. Briefly, 375 μ l MeOH were added to thawed samples. After homogenization with a bead-beating homogenizer (Precellys®24, Bertin Technologies, Montigny le Bretonneux, France; glass beads; 3 \times 30 sec, 6500 rpm), 1250 μ l MTBE were added and the mixture was incubated for 1 hr at room temperature on a rotator. Phase separation was induced by addition of 312 μ l distilled water, 10 min incubation on a rotator and centrifugation (10 min, 14.000 rpm, 4°C). A defined volume of the upper (organic) phase was splitted up into two equal portions, collected into tubes and dried by vacuum centrifugation. Dried lipids were dissolved in 20 μ l chloroform.

2.16 Separation and quantification of phospholipids and triacylglycerol using thin-layer chromatography

The protocol for thin-layer chromatography (TLC) was recently described by our group [126]. PL and TAG fractions were purified from the lipid extract by TLC. Samples and standards were loaded on Polygram silica gel G pre-coated TLC sheets

(Macherey-Nagel) in an equal volume of 5 μ l. For TAG purification, a trioleine standard (Sigma Aldrich®, Steinheim, Germany; concentrations: 4; 2; 1; 0.5; 0.25; 0.125; 0.0625 μ g trioleine/ μ l) was used. TLC sheets were run in a 20:20:1 n-hexane/diethyl ether/formic acid solvent mixture. To determine total PL content, a PL-mixture (Sigma Aldrich®, Steinheim, Germany; P3817; concentrations: 4; 2; 1; 0.5; 0.25; 0.125; 0.0625 μ g PL mixture/ μ l) and the TAG solvent mixture were used as standard and mobile phase, respectively. For separated PC and PE analysis, TLC plates were run in a 3:2:2:1 1-propanol/propionic acid/chloroform/water solvent system. Lipid spots were stained for 20 seconds in a dip solution (10 % copper(II) sulphate, 8 % phosphor acid, 5% methanol, according to Lee et al. [127]) and heated for 20 min at 150°C. Lipid spots were imaged with the Alphaimager HP at equal exposure times of 20 seconds and analyzed by the FluorChem-software. The spot denso tool was used to calculate the average pixel values of all standard and worm sample spots and its respective backgrounds. Next, average pixel values for TAG and PL standard spots were used to calculate a standard curve in GraphPad Prism 4 that enabled computation of TAG or PL content in *C. elegans* samples. For all measurements at least three biological replicates were analyzed.

2.17 BODIPY™ 493/503 staining and fluorescence imaging

To visualize fat storage in eggs, synchronized L4 larvae and five-day-old adults, vital BODIPY™ 493/503 (Invitrogen, Darmstadt, Germany) staining was performed as previously described [86]. Briefly, freshly harvested worms were washed three times with M9 buffer and incubated in 500 μ l BODIPY™ 493/503 solution (6.7 μ g/ μ l M9 buffer) for 20 min. After three M9 washing steps, worms were anesthetized in sodium azide (2 %) for 2 min on ice, washed again and used immediately for microscopy. A sufficient number of eggs for vital fat staining was derived from hypochlorite treatment of gravid adults. BODIPY™ 493/503 fluorescence was visualized using a Axio Imager.Z1 microscope equipped with a 38 HE filter (excitation: BP 470/40, beamsplitter: FT 495, emission: BP 525/50) and coupled with an apotome sectioning system (ApoTome.2, Zeiss). Single plane images of whole eggs as well as the anterior and the posterior intestine of worms were captured by a AxioCam MRm (Zeiss) at indicated magnification.

2.18 Colocalization experiments

sams-1(t5669) mutants were crossed with males of VS20 (hjls67), expressing an ATGL-1::GFP fusion protein [atgl-1p::atgl-1::GFP]. F₂ progenies showing the vacuole phenotype as well as GFP fluorescence were used for colocalization studies. Therefore, *sams-1(t5669);atgl-1p::atgl-1::gfp* worms were vitally stained with LipidToxRed (1:200; Invitrogene) analogously to vital BODIPY 493/505™ staining. GFP fluorescence was visualized using filter 38HE (excitation BP 470/40; beam splitter FT 495; emission BP 525/50). LipidToxRed fluorescence was visualized with a 43HE filter (excitation BP 550/25; beam splitter FT 570; emission BP605/70). Images were captured with an AxioObserver.D1 inverted microscope, equipped with an EC Plan-Neoluar 63×/1.25 oil objective and a AxioCam MRm Rev.2 camera.

2.19 Design of starvation experiments

For starvation experiments, hypochlorite synchronized worms were grown on NGM agar plates until the L4 stage, before they were harvested and washed three times with M9 buffer. As control group (0 hr starvation), one third of each population was immediately collected in 0.5 ml tubes in samples of 3000 worms by COPAS Biosort flow cytometry and stored at -80°C until further processing. For starvation, residual worms of each population were splitted up into two portions and cultivated in M9 buffer, supplemented with an antibiotic (dilution: 1:100, Cell Culture Guard, AppliChem), in 15 ml falcon tubes on a nutator mixer. After 24 hr and 48 hr, the respective starvation groups were collected analogously to control samples. Samples were used for colorimetric TAG and protein quantification (section 2.20). An aliquot of worms for each starvation condition (0 hr, 24 hr and 48 hr of starvation) was separated and used for fixative lipid staining to analyse number and size of lipid droplets (section 2.21).

2.20 Quantification of triacylglycerol and protein level using colorimetric assays

For worm lysis, samples were suspended in 100 µl NET buffer (50 mM Tris pH 7.5, 150 mM NaCl, 1 mM EDTA ph 8.0, 0.5 % CHAPS) and homogenized with the Precellys®24 (1.4 mm ceramic beads; 1×6500 rpm). By centrifugation (20 min; 14.000 rpm; 4°C) cell debris was pelleted. Supernatants were transferred to new

tubes and used for colorimetric assays. The TAG content was determined using an enzymatic assay kit (Analyticon diagnostic, Lichtenfels, Germany) with a separate TAG standard (BioCat, Heidelberg, Germany) according to manufactures instructions. A Bicinchoninic acid (BCA) assay kit (Pierce protein assay kit, Thermo Fisher Scientific Inc., Rockford, USA) and BSA as standard were used for protein quantification. Three biological replicates for each strain and each condition were analyzed as duplicate for TAG and protein determination, respectively.

2.21 Analysis of number and size of lipid droplets

To determine number and size of lipid droplets in response to starvation, a BODIPY™ 493/503 fixative staining of *ad libitum* and starved L4 larvae (see section 2.19 for experimental design) was performed as previously described [86]. Briefly, freshly harvested worms were washed with M9 and fixed in 4 % paraformaldehyde solution for 15 min. After three freeze/thaw cycles in liquid nitrogen worms were washed again to remove paraformaldehyde and were incubated in BODIPY™ 493/503 staining solution (1 µg/µl) for 1 hr, followed by three final washing steps. BODIPY™ 493/503 positive lipid droplets in the anterior and in the posterior intestine were imaged by 3D fluorescence microscopy using the Axio Imager.Z1 microscope and a plan-apochromat 40x/1.3 oil-immersion objective. The apotome sectioning system was used to collect z-stacks with a step size of 1 µm. Z-stacks comprised 10 to 25 plane images (format: 223×168 µm; 692×520 pixel) depending on strain and developmental stage. Images were captured using a AxioCam MRm (Zeiss). The ImageJ software (version 1.47h) and the 3D object counter plugin [128, 129] were used to analyze z-stacks. BODIPY™ 493/503 positive structures were automatically identified by adaptive thresholding and the volume of each droplet was evaluated by summing up the voxels per droplet. Further calculations of total lipid droplet number, mean lipid droplet size and total lipid droplet volume were performed using Microsoft Excel (version 2003). From three independent experiments at least 10 images per strain, region and developmental stage were analyzed.

2.22 Determination of surviving rates of worms exposed to arsenite and osmotic stress

Synchronized L4 worms were transferred to small NGM agar plates containing 4mM sodium arsenite (Sigma Aldrich®, Steinheim, Germany). Worms transferred to standard NGM agar plates were used as control. Each experiment comprised three stress and control plates, respectively. Per plate 10 worms were cultivated. To calculate the survival rate, worms were scored for viability after 24 h of sodium arsenite exposure. A worm was scored as dead when it did not respond to a mechanical stimulus. The experiment was performed three times. RNAi against *sams-1* and *gcs-1* was used as internal control. Therefore, N2 worms were fed individual *E. coli* strains expressing the respective target-gene dsRNA. RNAi *E. coli* strains were derived from the Ahringer RNAi library [130]. To induce gene knockdown in worms, RNAi bacteria were grown in LB media containing 50 µg/ml ampicillin and 5 µg/ml tetracycline and seeded on RNAi plates (NGM supplemented with 50 µg/ml ampicillin and 2.5 mM IPTG). Eggs were scattered on the RNAi plates and allowed to develop. At the L4 stage RNAi-construct fed worms were transferred to RNAi/+sodium arsenite and RNAi/-sodium arsenite plates and scored for viability analogously to RNAi-untreated worms.

For osmotic stress tests synchronized L4 larvae were placed on high-salt plates (500 mM NaCl). Worms placed on regular NGM plates (50 mM NaCl) were used as control. On each plate 10 animals were cultivated and analyzed. Nematodes were scored for viability and for reduction of body volume in a time dependent manner. Viability was assayed until the last worm died. Again, a worm was scored as dead when it did not respond to a mechanical stimulus. To determine body volume, individual worms were photographed after 0.5, 2 and 5 hr. Photography, image analysis and body volume calculation were performed as described in section 2.13. In three independent experiments stress and control plates were analyzed as triplicate. For both, oxidative and osmotic stress tests, plates were prepared with a palmitic acid ring (2 %, dissolved in absolute ethanol) to prevent worms escaping from the plates [131].

2.23 Total RNA isolation and whole genome gene expression analysis

1000 to 2000 synchronized L4 larvae and 2000 to 3500 five-day-old adult worms were harvested, washed three times with M9 buffer and resuspended in 350 μ l RLT buffer (RNeasy Mini Kit, QIAGEN, Hilden, Germany), respectively. Worm homogenization was performed with the Precellys@24 and by additional disruption using QIAshredder spin columns (QIAGEN, Hilden, Germany). The RNeasy Mini Kit was used for total RNA isolation, including on-column DNA digestion (RNase-free DNase Set; QIAGEN, Hilden, Germany) according to manufactures instructions. Quality and yield of the extracted RNA were assessed spectrophotometrically (BioPhotometer, Eppendorf, Hamburg, Germany). Labeling, hybridization and processing of cRNA was generated by Source BioScience (imaGenes, Berlin, Germany). A customized Agilent gene expression microarray, containing 61643 oligos, was used. After quantile normalization each data set contained gene expression values of 26843 genes. Gene expression data were derived from three biological replicates of L4 larvae and five-day-old adults, respectively. Fold changes of expression intensities were calculated from the average gene expression value of each gene and represent the mutant to wild type ratio. Significance analysis was performed using an unpaired t-test with unequal variance. P-values > 0.05 were considered as not significant.

2.24 Statistical analysis

Statistical analysis was performed with Microsoft Excel (2003) and GraphPad Prism (Version 4.0). Significances were calculated using unpaired two-tailed t-test. Welch`s correction was used if variances were different. Differences were considered statistically significant at $p < 0.05$ (*), $p < 0.01$ (**) and $p < 0.001$ (***) .

3 Results

3.1 Identification of the *sams-1(t5669)* mutant showing enlarged vacuoles in the embryo

From a collection of *C. elegans* mutants isolated from a temperature-sensitive embryonic lethal screen, we accidentally identified a mutant strain (*t5669*) showing enlarged vacuoles in the embryo (Figure 4A). Whole genome sequencing of the mutant combined with SNP mapping revealed a point mutation in the *S-adenosylmethionine synthetase 1* (*sams-1*) gene (Figure S1; table S1-S2). At position X: 11966380 cytosine is exchanged by thymine resulting in the amino acid change A105V in SAMS-1 (Figure 4B; 5A). Sanger sequencing and RFLP analysis of an amplified genomic PCR fragment confirmed the C→T transition in the *sams-1* gene (Figure 4C, figure S2).

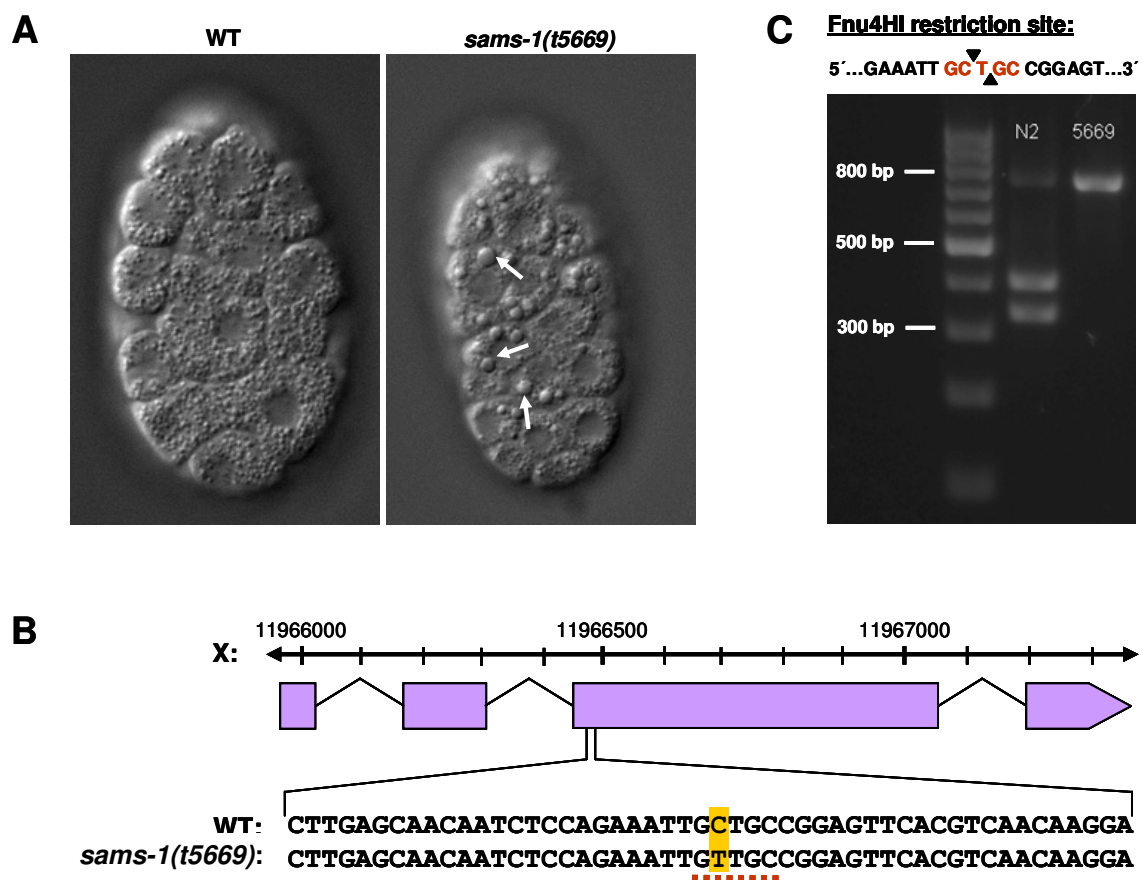


Figure 4: Identification of a putative loss-of-function mutation in *sams-1* in *C. elegans*. (A) Enlarged embryonic vacuoles in the *C. elegans* mutant

sams-1(t5669), isolated from an EMS mutagenesis screen. (B) Genomic structure of the *C. elegans sams-1* gene. Exons and introns are depicted as boxes and lines, respectively. WGS and SNP mapping revealed a cytosine to thymine transition in the third exon. 50 bp sequences harbouring the mutation site of wild type and *sams-1(t5669)* genomes are shown. Exchanged bases are highlighted with a yellow bar. (C) The C→T change was verified by RFLP analysis. C→T change alters Fnu4HI recognition site (red dotted line in B, red letters in (C) in *sams-1(t5669)*). The restriction site is marked by black triangles. Wild type and *sams-1(t5669)* restriction fragments are shown.

Next, the *sams-1(t5669)* mutant was crossed five times against wild type N2. The mutant was found to behave as simple Mendelian recessive. The embryonic enlarged vacuoles of the mutant segregated with the C→T mutation in *sams-1*. Hemizygous *sams-1(t5669)* mutant males also showed enlarged vacuoles. Based on the vacuolar phenotype, complementation testing between the *sams-1(t5669)* allele and a 480 bp deletion allele of *sams-1 (ok3033)* revealed no intragenic complementation. Thus, we conclude that the C→T transition in the *sams-1* gene is the phenotype causing mutation and impairs the function of SAMS-1.

3.2 *In silico* analysis predicts an impairment of protein function due to A105V substitution in SAMS-1

Database search revealed that SAMS-1 is evolutionary conserved and contains three protein domains. The conserved alanine, at position 105, lies between the N-terminal domain and the central domain of SAMS-1 (Figure 5A). Algorithms based on sequence alignments predicted that A105V substitution in SAMS-1 causes an impairment of the enzyme function (Figure 5B). Algorithms based on physiochemical properties of exchanged amino acids or structural and functional protein features predicted no or moderate impact of A105V substitution on SAMS-1 function (Figure 5B). By use of the online prediction tool HOPE, a 3D structure model of SAMS-1 was built on the basis of structure homology to the α -subunit of human methionine adenosyltransferase MAT2 (PDB entry 2P02) [132]. This structure model shows that the substitution site lies within an α -helix (Figure 5C). Since the substituted amino acid valine does not prefer helices as secondary structure, this model indicates reduced SAMS-1 activity due to local instability [133].

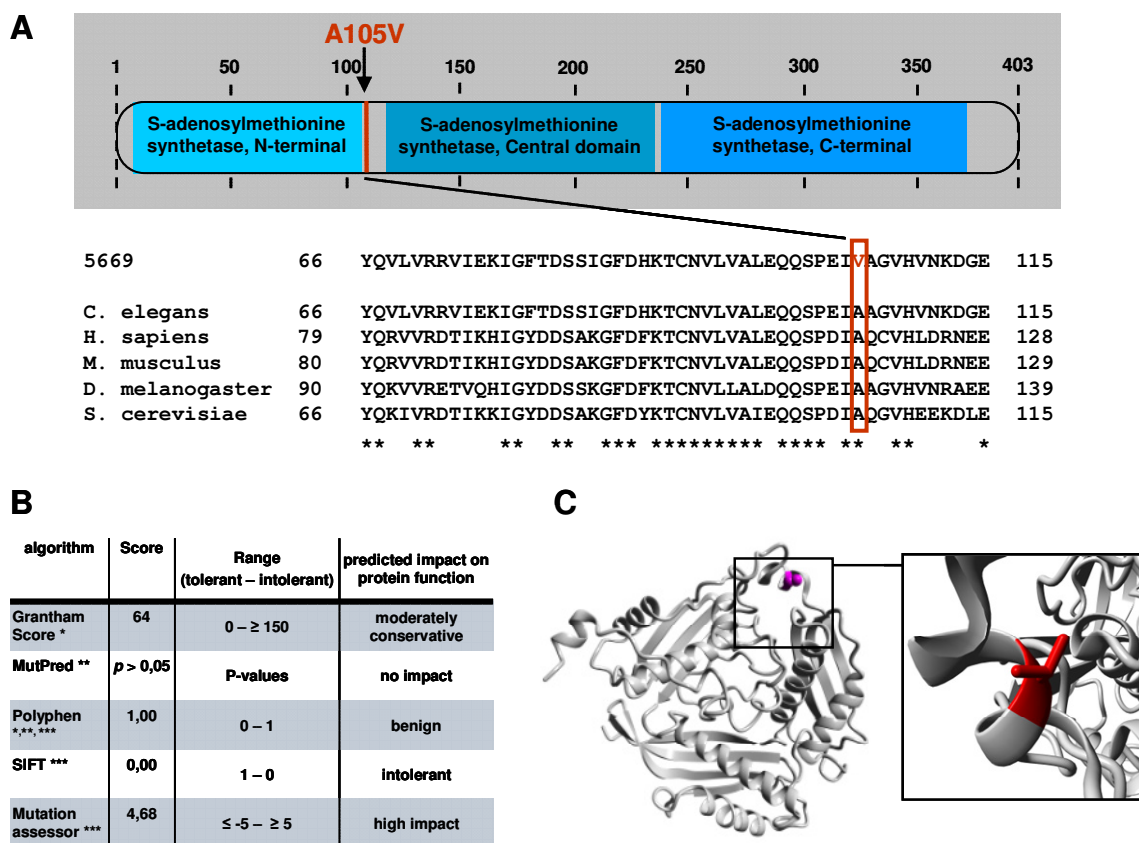


Figure 5: *In silico* analysis of SAMS-1. (A) Structure of the *C. elegans* SAMS-1 protein. The A105V substitution, found in the *sams-1(t5669)* mutant, is depicted. The three functional domains of SAMS-1 are marked by blue boxes. Multiple sequence alignment of distinct SAMS-1 species is shown. (B) Different web based tools were used to predict the impact of A105V substitution on function and structure of SAMS-1. Predictions based on: *physicochemical properties of exchanged amino acids; **probability of impairment of structural and functional protein features; ***evolutionary conservation. (C) Model of SAMS-1 crystal structure, prepared by HOPE. The A105V substitution site is shown in magenta in the total view and in red in the detailed view.

3.3 Vulnerability to arsenite, a glutathione-depleting agent, is similar in *sams-1(t5669)* mutants, *sams-1(RNAi)* worms and *sams-1(ok3033)* mutants

To provide further evidence for impaired protein activity due to the A105V substitution in SAMS-1, we performed arsenite-treatment experiments. Arsenite is a GSH-depleting agent. To detoxify inorganic arsenicals, GSH is used to form stable GSH-arsenic conjugates, which can be discarded from the organism [134]. In this way, clearance of arsenite also depletes GSH level, if GSH synthesis is disturbed. SAM synthesis is linked to GSH formation by the transsulfuration pathway, which converts homocysteine, the product of SAM-dependent transmethylation reactions, to

cysteine, the limiting substrate in GSH synthesis. (Figure S3). It has been shown that in liver ~50 % of cysteine used for GSH formation derives from homocysteine [135-137]. Thus, defective SAM synthesis can lead to reduced amounts of homocysteine and consequentially to a diminished GSH-forming capacity. Consequently, we supposed that increased vulnerability to arsenite would indicate reduced SAM synthesis and therefore impaired SAMS-1 function. To test this, we measured mortality of *sams-1(t5669)* mutants in response to arsenite treatment. *gcs-1(RNAi)* worms were used as positive control. *gcs-1* encodes γ -glutamylcysteine synthetase, the key enzyme in GSH-formation. As expected, due to reduced GSH synthesis, *gcs-1(RNAi)* worms were highly vulnerable to arsenite. They showed a survival rate of only ~5 %. In contrast, wild type worms were only slightly affected by arsenite treatment. Remarkably, only 5 % of the *sams-1(t5669)* mutants survived upon arsenite exposure (Figure 6A). The impaired resistance of the *sams-1(t5669)* mutant to arsenite stress seems to be rather specific because mutant worms showed neither increased mortality nor impaired recovery of normal body volume under high osmotic conditions (Figure 6B-C). Thus, these data indicate a reduced capacity to form GSH in the *sams-1(t5669)* mutant.

To test if high vulnerability of the *sams-1(t5669)* mutant was indeed due to impaired SAM synthesis and therefore due to impaired SAMS-1 function, we also determined mortality of *sams-1(RNAi)* worms and *sams-1(ok3033)* mutants. The latter harbours a 480 bp deletion in the *sams-1* gene. Indeed, also *sams-1(RNAi)* worms and *sams-1(ok3033)* mutants showed increased vulnerability to arsenite. They exhibited a survival rate of about 40 % and 10 %, respectively (Figure 6A). Thus, mortality of the *sams-1(t5669)* mutant was comparable to that of *gcs-1(RNAi)* worms, and more importantly, similar to that of *sams-1(RNAi)* worms and *sams-1(ok3033)* mutants. Therefore, we supposed that the A105V substitution indeed impairs SAMS-1 function in the *sams-1(t5669)* mutant. For further analysis, we have used the identified *sams-1(t5669)* allele as well as the deletion allele *sams-1(ok3033)*.

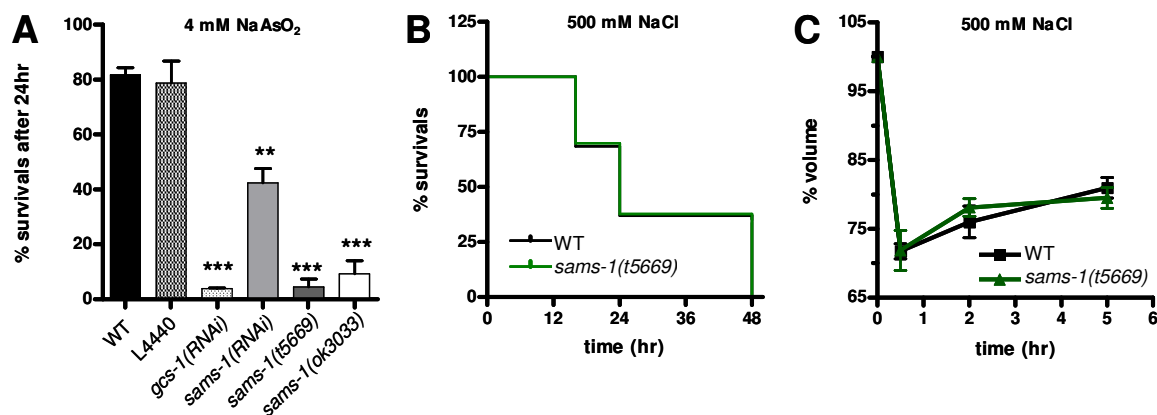


Figure 6: Vulnerability of *sams-1* mutants to arsenite and NaCl. (A) Survival rate (% survivals) of wild type and *sams-1* larvae cultured on 4mM sodium arsenite NGM plates for 24 hr. Worms fed a *gcs-1* RNAi construct were used as positive controls. Survival rate (B) and time dependent changes in body volume (C) of wild type worms and *sams-1*(t5669) mutants that were transferred to high salt NGM plates (500mM NaCl) at the L4 stage. Bars (A) and data points (B-C) represent mean \pm SEM of three independent experiments, each comprising 30 worms per strain. Significant differences compared with wild types are indicated by asterisks and were calculated by unpaired t-test (** $p < 0.01$, *** $p < 0.001$).

3.4 *sams-1* adults but not *sams-1* larvae show a reduced proportion of phosphatidylcholine and an elevated triacylglycerol proportion

SAMS-1 catalyzes the formation of SAM, a major methyl donor required for many biochemical reactions [138-141]. From a quantitative point of view, the synthesis of PC consumes substantial amounts of SAM [142]. Therefore, we expected that the synthesis of PC is impaired in *sams-1* mutants. In *C. elegans*, PC is synthesized via two pathways. The Kennedy pathway comprises the phosphorylation of choline to phosphocholine, which is converted to PC via CDP-choline. An alternative route is represented by the PEAMT pathway and involves the stepwise SAM-dependent methylation of phosphoethanolamine to phosphocholine, which then enters the Kennedy-route (Figure 2). It is also important to mention that diacylglycerol (DAG) is a precursor for the synthesis of PC, PE and TAG. Thus, the syntheses of PC, PE and TAG are interconnected. Thin layer chromatography based analysis of lipid extracts revealed that the amount of PC, PE and TAG per worm is more than 2 fold reduced in *sams-1* L4 larvae compared to wild type larvae, respectively (Figure 7A). *sams-1* adults exhibited up to 6 fold reduced amounts of PC. *sams-1* PE and TAG amounts were reduced 4.4 fold and 2 fold at the 5d ad stage, respectively (Figure 7B). Next, the relative distribution of this three lipid classes was calculated. At the L4 stage, the

relative proportions of TAG (~60 %), PC (~20 %) and PE (~20 %) were similar between *sams-1* mutants and wild type worms (Figure 7C). In adult wild type worms, the proportions of these lipids were not changed. In contrast, *sams-1* adults exhibited a reduced PC fraction of about 8 % and an elevated TAG fraction of about 76 %. The PE fraction was not substantially altered in *sams-1* adults compared to wild type (Figure 7D). Collectively, these data indicate a reduced level of PC and an accumulation of TAG in *sams-1* mutants.

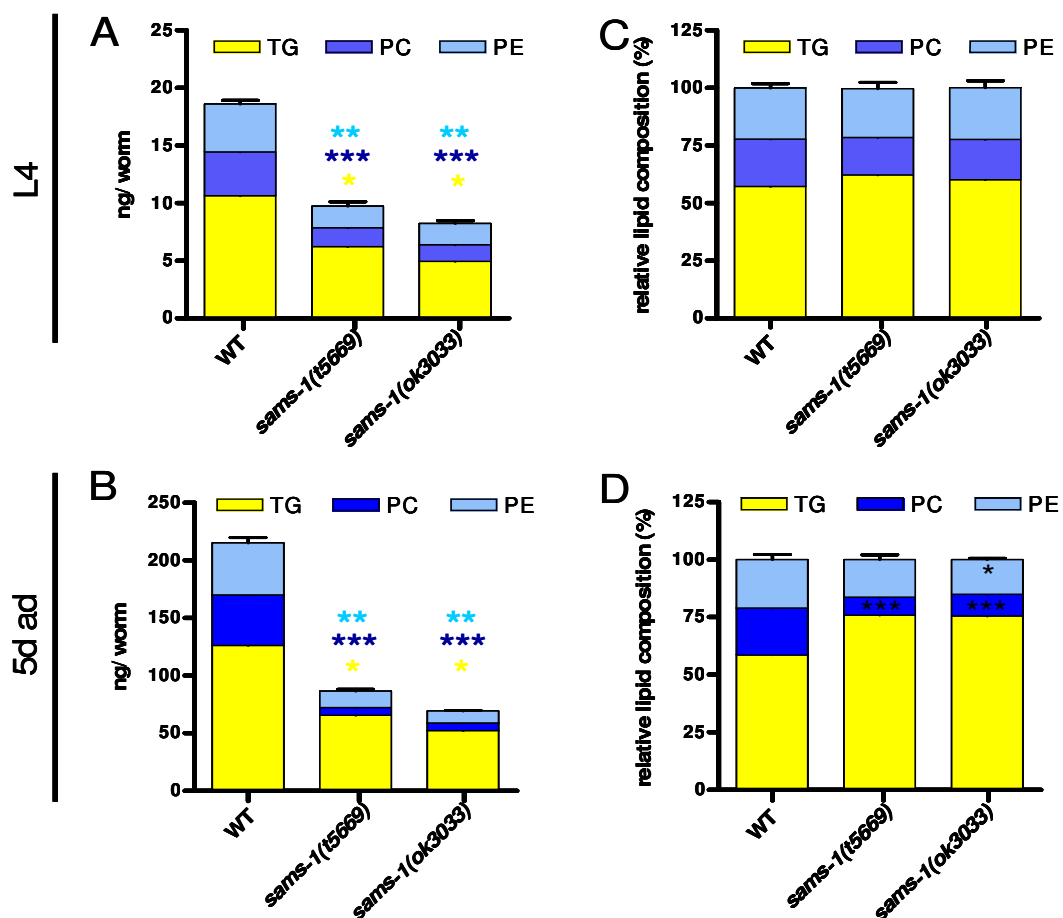


Figure 7: TLC analysis of TAG, PC and PE fractions of wild type worms and *sams-1* mutants. TAG, PC and PE levels were determined by total lipid extraction from 2000 (WT) to 4000 (*sams-1* mutants) worms and lipid separation by thin layer chromatography. Amounts of TAG, PC and PE per worm (A, B) and their relative proportions (C, D) in wild type worms and *sams-1* mutants at fourth larval stage (A, C) and when worm reached fifth day of adulthood (B, D). Bars represent mean \pm SEM of 3 to 5 independent experiments. Significant differences were analyzed between wild types and the respective *sams-1* mutant using unpaired t-test (* $p < 0.05$, ** $p < 0.01$, *** $p < 0.001$).

3.5 *sams-1* adults but not *sams-1* larvae show higher expression of genes involved in the synthesis of both phosphatidylcholine and triacylglycerol

To test whether a faulty lipid metabolism is coupled to altered gene expression, we compared mRNA steady-state levels of genes involved in metabolic pathways of PL and TAG synthesis from wild types and *sams-1* mutants. *sams-1* larvae showed essentially no altered expression of genes involved in PC synthesis (Figure 8A; Table 2). In contrast, *sams-1* adults showed higher expression of genes contributing to both, the Kennedy pathway and the PEAMT route (Figure 8B; Table 2). In *sams-1* adults, *pmt-1* and *pmt-2*, SAM-dependent PEAMTs, were up-regulated more than 2 fold compared with wild type adults. *sams-1* adults also exhibited 2 fold and 4 fold elevated expression of *cka-2* and *ckb-2*, respectively. These genes encode choline kinases, which catalyze the formation of phosphocholine. Conversion of phosphocholine to CDP-choline is catalyzed by CCT, the key enzyme in PC formation encoded by *pcyt-1*. Adult *sams-1* nematodes showed 2 fold higher expression of *pcyt-1*. Finally, *sams-1* adults also showed an ~4 fold up-regulation of *cept-1*, which encodes CPT. CPT catalyzes the final step in PC synthesis. Thus, higher expression of genes involved in PC synthesis may indicate a compensatory response to reduced PC level in adult *sams-1* mutants.

Analysis of gene expression data further revealed an up-regulation of several lipogenic genes (Figure 8C; Table 2). *sams-1* larvae as well as *sams-1* adults showed elevated expression of *pod-2* and *fasn-1* encoding an acetyl-CoA carboxylase (ACC) and a fatty acid synthase (FASN), respectively. ACC catalyzes the first step in *de novo* FA synthesis, providing malonyl CoA. Malonyl CoA is subsequently stepwise elongated by FASN to form FA of distinct length. FA are modified by desaturases and elongases that produce diverse unsaturated FA. Remarkably, L4 larvae and adults of *sams-1* mutants exhibited higher expression of all seven *fat* genes encoding desaturases in *C. elegans*. By contrast, in most cases increased expression of elongase encoding genes (*elo*) was restricted to adult *sams-1* nematodes. *sams-1* adults but not *sams-1* larvae exhibited a 4 fold up-regulation of *dgat-2*. *dgat-2* encodes a diacylglycerol acyltransferase (DGAT2), a key enzyme in TAG synthesis. Recently, ACS-22, an acyl-CoA synthetase, has been found to form a protein complex with DGAT2 to facilitate TAG formation [18]. Interestingly, *acs-22* was also up-regulated (2.76 fold) in *sams-1* adults

(Figure 8B, C). Overall, gene expression data revealed increased expression of several genes that contribute to FA and TAG synthesis, which indicates increased lipogenesis in *sams-1* mutants.

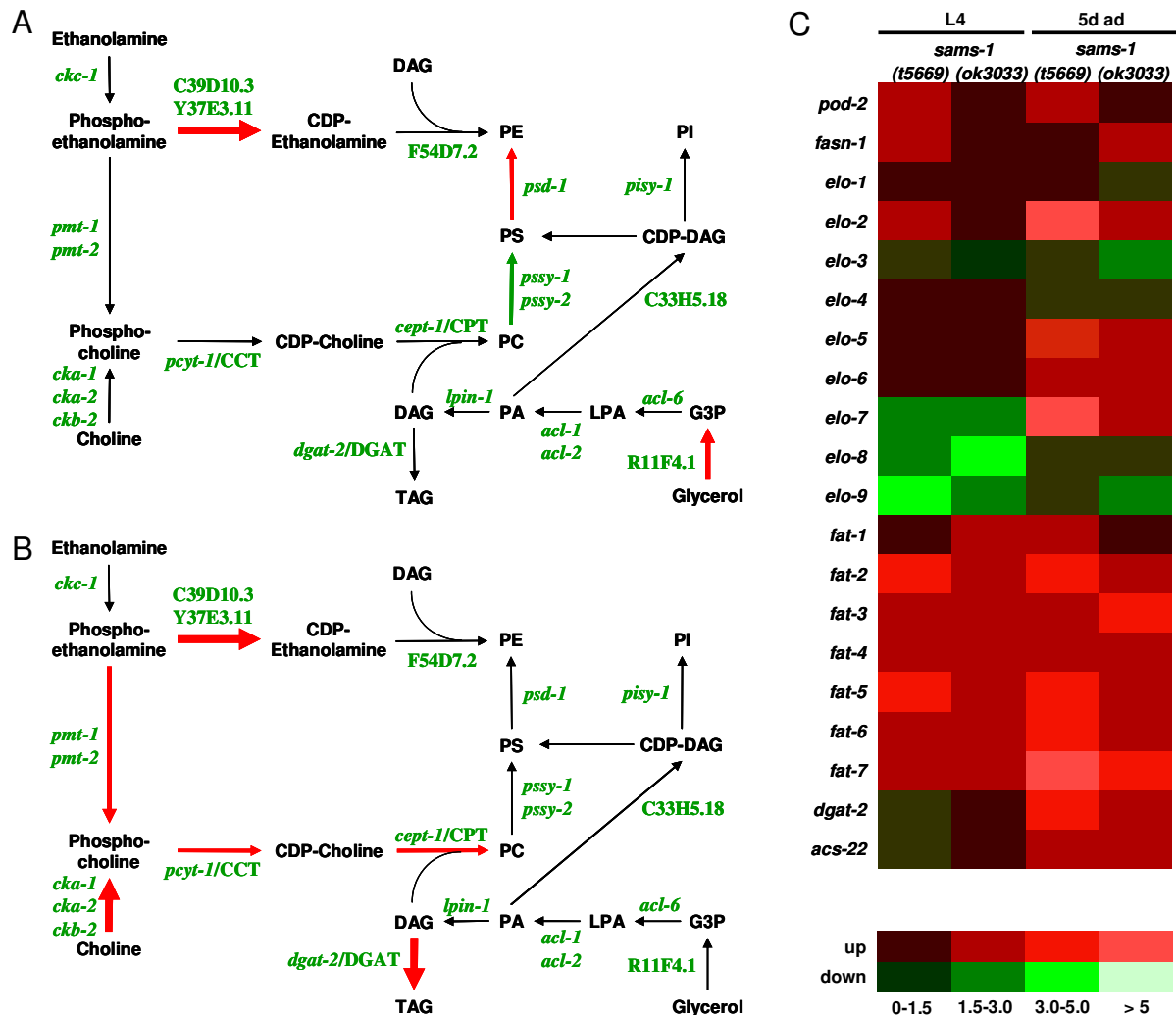


Figure 8: Genes involved in PC synthesis and lipogenesis are differentially expressed in wild types and *sams-1* mutants. (A-B) Interconnected metabolic pathways of PL and TAG synthesis and its respective genes. Differences in gene expression between wild types and *sams-1* mutants are represented by colour and width of arrows. Red arrows represent an increased expression of respective genes in *sams-1* mutants compared with wild type worms: \rightarrow 1.5-2 fold; \rightarrow 2-3 fold; \rightarrow >3 fold increased expression. Gene expression levels are compared at the L4 stage (A) and at the 5d ad stage (B), respectively. (C) Expression level of lipogenic genes are compared between wild type worms and *sams-1* mutants at the L4 stage and at the 5d ad stage. Genes, up-regulated in *sams-1* mutants are shown in red, down-regulated genes are shown in green. Fold changes of expression intensities were calculated from the average gene expression value of each gene and represent the mutant to wild type ratio. Gene expression data were derived from three biological replicates of L4 larvae and five-day-old adults of wild type worms and *sams-1* mutants, respectively.

Table 2: Expression level of genes involved in PL synthesis and lipogenesis compared in wild type worms and *sams-1* mutants.^a

		Fold change of regulation ^a			
Gene name	Gene ID	L4		5d	
		<i>sams-1(t5669)</i> vs. N2	<i>sams-1(ok3033)</i> vs. N2	<i>sams-1(t5669)</i> vs. N2	<i>sams-1(ok3033)</i> vs. N2
<u>FA synthesis</u>					
<i>pod-2</i>	W09B6.1	2.53	1.41	2.14*	1.27
<i>fasn-1</i>	F32H2.5	2.88*	1.37	1.38*	1.87
<u>FA elongation</u>					
<i>elo-1</i>	F56H11.4	1.31*	1.04*	1.36*	-1.05*
<i>elo-2</i>	F11E6.5	1.79	1.42*	5.16	2.34
<i>elo-3</i>	D2024.3	-1.27*	-1.02*	-1.15*	-1.96
<i>elo-4</i>	C40H1.4	1.17*	1.11*	-1.33*	-1.35
<i>elo-5</i>	F41H10.7	1.20*	1.07*	4.29	2.19
<i>elo-6</i>	F41H10.8	1.29*	1.11*	2.49	1.56
<i>elo-7</i>	F56H11.3	-2.22	-1.69	5.46	2.67
<i>elo-8</i>	Y47D3A.30	-2.44*	-3.85	-1.23*	-1.11*
<i>elo-9</i>	Y53F4B.2	-3.70*	-2.50*	-1.41*	-1.52*
<u>FA desaturation</u>					
<i>fat-1</i>	Y67H2A.8	1.39	1.61	1.58	1.47
<i>fat-2</i>	W02A2.1	3.12	2.67	3.48	2.74
<i>fat-3</i>	W08D2.4	1.59	2.16	2.36*	3.24
<i>fat-4</i>	T13F2.1	2.15	2.03	1.61*	1.6
<i>fat-5</i>	W06D12.3	3.86	2.39*	4.55*	1.79
<i>fat-6</i>	VZK822L.1	1.94*	1.55*	3.22*	1.95
<i>fat-7</i>	F10D2.9	2.54*	2.53	12.44	3.24
<u>TAG synthesis</u>					
	R11F4.1.1	2.08*	2.94	-1.15	2.41
	R11F4.1.2	2.09*	2.59	-1.39	1.76
<i>acl-6</i>	F08F3.2a.1	-1.19*	-1.54*	-1.02*	-1.45*
	F08F3.2a.2	-1.20	-1.45	-1.08*	-1.54
<i>acl-1</i>	F59F4.4	1.01*	1.15*	1.62*	-1.15*
<i>acl-2</i>	T06E8.1.1	1.32*	1.19*	-1.01	-1.28
	T06E8.1.2	1.18	1.09*	-1.11	-1.47
<i>lpin-1</i>	H37A05.1	2.57	1.46	1.92	1.39
<i>dgat-2</i>	F59A1.10	-1.03*	1.29*	4.09	1.98
<i>acs-22</i>	D1009.1	-1.10*	1.28	1.88	2.76

Continued table 2

PE synthesis

<i>ckc-1</i>	T27A10.3	-1.37	-1.25	-1.15*	-1.43
	C39D10.3	-1.08	1.12*	-1.09*	1.20
<i>psd-1</i>	Y37E3.11	1.30	12.23	1.06	5.84
	F54D7.2	1.20*	-1.08*	-1.01*	-1.14*
	B0361.5	2.12	1.49	1.60	1.27

PC synthesis

<i>cka-1</i>	C28D4.2	1.14*	-1.10*	1.18	-1.19
<i>cka-2</i>	C52B9.1	1.23*	1.48*	1.48	2.17
<i>ckb-2</i>	B0285.9	1.00*	1.15*	4.03	2.39
<i>pmt-1</i>	ZK622.3	1.51	1.03*	2.84*	2.34
<i>pmt-2</i>	F54D11.1	1.26*	-1.06*	3.17	1.74
<i>pcyt-1</i>	F08C6.2	1.45	-1.03*	2.01	1.44
<i>cept-1</i>	F22E10.5	1.47	-1.02*	4.39	1.10

Synthesis of other PLs

<i>pssy-1</i>	ZC506.3	1.14*	1.12*	1.43*	1.44
<i>pssy-2</i>	T27E9.5	-1.47	-2.04	-1.22	-1.85
	C33H5.18	-1.14*	-1.20*	-1.22	-1.79
<i>pisyl-1</i>	Y46G5A.5	1.22	1.00*	-1.15*	-1.37

Polyamine synthesis

<i>odc-1</i>	K11C4.4	-1.82	-1.32	1.51*	4.99
<i>smd-1</i>	F47G4.7	1.37*	-1.64	1.1*	-1.49
<i>spds-1</i>	Y46G5A.19	-1.79	-1.52	1.68	1.88

^a Gene expression is compared between wild type worms and *sams-1* mutants at the L4 stage and at the 5d ad stage. Fold-changes are understood between the respective mutant and the wild type. A positive value indicates higher expression in the mutant. A negative value indicates lower gene expression in the mutant. In this case fold change was calculated as 1/ratio and a minus was added to the quotient. Significance was determined using an unpaired t-test with unequal variance. P-values > 0.05 were considered as not significant and marked by an asterisk.

3.6 *sams-1* mutants exhibit a small body size and a reduced number of progenies

Because PC is a major component of membranes and is therefore necessary for growth and reproduction, we wanted to know, whether body size and fertility of *sams-1* mutants is reduced. Indeed, *sams-1* mutants showed a significantly reduced body size (Figure 9; figure S5). Microscopic analysis revealed that both, *sams-1* L4 larvae and 5-day-old adults, showed a 1.5 fold reduction in body length compared

with wild type worms (Figure 9A-B). Body width was also reduced 1.5 fold in *sams-1* L4 larvae and 5-day-old adults, respectively (Figure 9C-D). Moreover, *sams-1* mutants exhibited only 25 % of wild type volume at the L4 stage and the 5d ad stage, respectively (Figure 9E-F). While nearly all wild type embryos hatched, *sams-1* mutants actually exhibited a hatching rate of only ~75 % (Figure 9G). More drastically, *sams-1* nematodes produced only ~50 progenies whereas the number of progenies in wild type worms was about 300 (Figure 9H). Together, body size and number of progenies were markedly reduced in *sams-1* mutants.

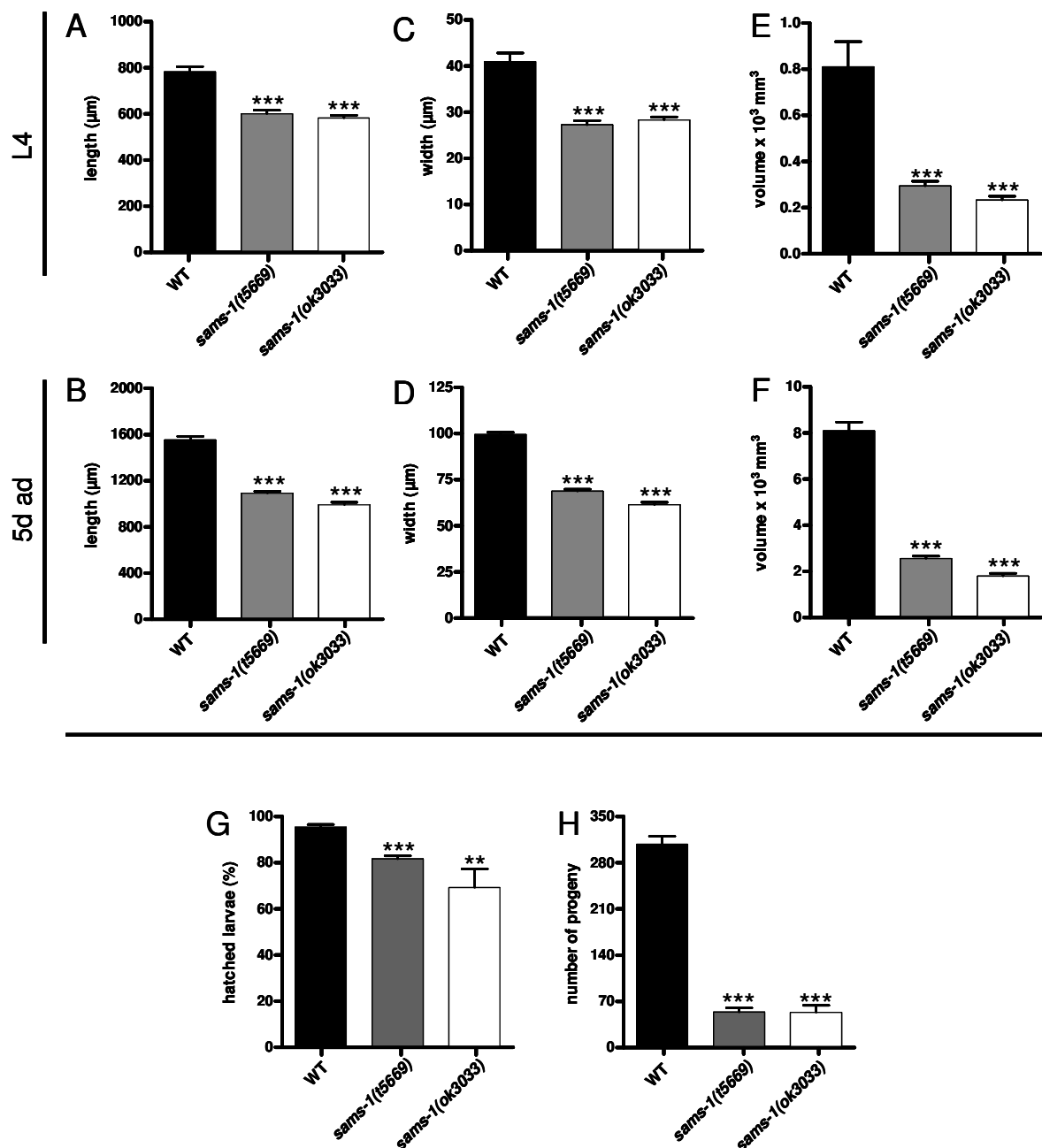


Figure 9: Body size, hatching rate and number of progenies of wild type worms and *sams-1* mutants. Body length (A-B), body width (C-D) and body volume (E-F) of stage synchronized L4 (A, C, E) and 5-day-old adult (B, D, F) wild type worms and

sams-1 mutants. Data were derived from analysis of bright-field microscopy images. Images of 10 worms per strain and experiment were analyzed. (G) Hatching rates represent the proportion of larvae that hatched from a defined number of laid eggs. At least 30 freshly laid eggs per worm were analyzed for hatching. 10 worms per strain and experiment were analyzed, respectively. (H) Counting viable L4 progenies during entire reproductive phase revealed number of progenies per worm. 5 worms per strain and experiment were analyzed, respectively. Each bar represents mean \pm SEM of 2 independent experiments. Significance asterisks refer to differences between wild type worms and the respective *sams-1* mutant and were determined by an unpaired t-test (** $p < 0.001$, ** $p < 0.01$).

3.7 *sams-1* mutants exhibit enlarged lipid droplets in embryos as well as in the anterior and posterior intestine of L4 larvae and adults

TAG is stored in LDs, which are surrounded by a PL monolayer. PC and PE are the most prominent PLs in LD membranes [7, 143, 144]. We supposed LD expansion in *sams-1* mutants because they are characterized by large embryonic vacuoles, reduced levels of PC and elevated levels of TAG. To test this hypothesis, LDs were visualized using 3D fluorescence imaging combined with our BODIPY™ 493/503 based vital fat staining method [86]. Large vacuoles present in *sams-1* embryos were indeed identified as LDs. Compared to wild type, *in utero* as well as *ex utero* embryos of *sams-1* mutants showed markedly increased LDs (Figure 10). Wild type L4 larvae displayed fine dispersed small-sized LDs in the anterior and posterior intestine, respectively (Figure 11A). In contrast, larvae of *sams-1* mutants contained large-sized LDs in both parts of the intestine (Figure 11B-C). At the 5d adult stage, *sams-1* nematodes formed enlarged intestinal LDs that dramatically differ from wild type (Figure 12). The authenticity of LDs was confirmed by localization of ATGL-1::GFP, a lipase-GFP fusion protein to mark LDs in *C. elegans* [98], to the surface of LipidToxRed stained LDs in *sams-1(t5669);atgl-1p::atgl-1::gfp* animals (Figure S6). Together, in *sams-1* mutants, we found enlarged LDs in embryos as well as in anterior and posterior intestine of L4 larvae and adults. Moreover, LD enlargement is in agreement with elevated expression of lipogenic genes and the increased TAG proportion found in *sams-1* mutants. Thus, these observations indicate SAMS-1 as contributor to LD size and fat storage.

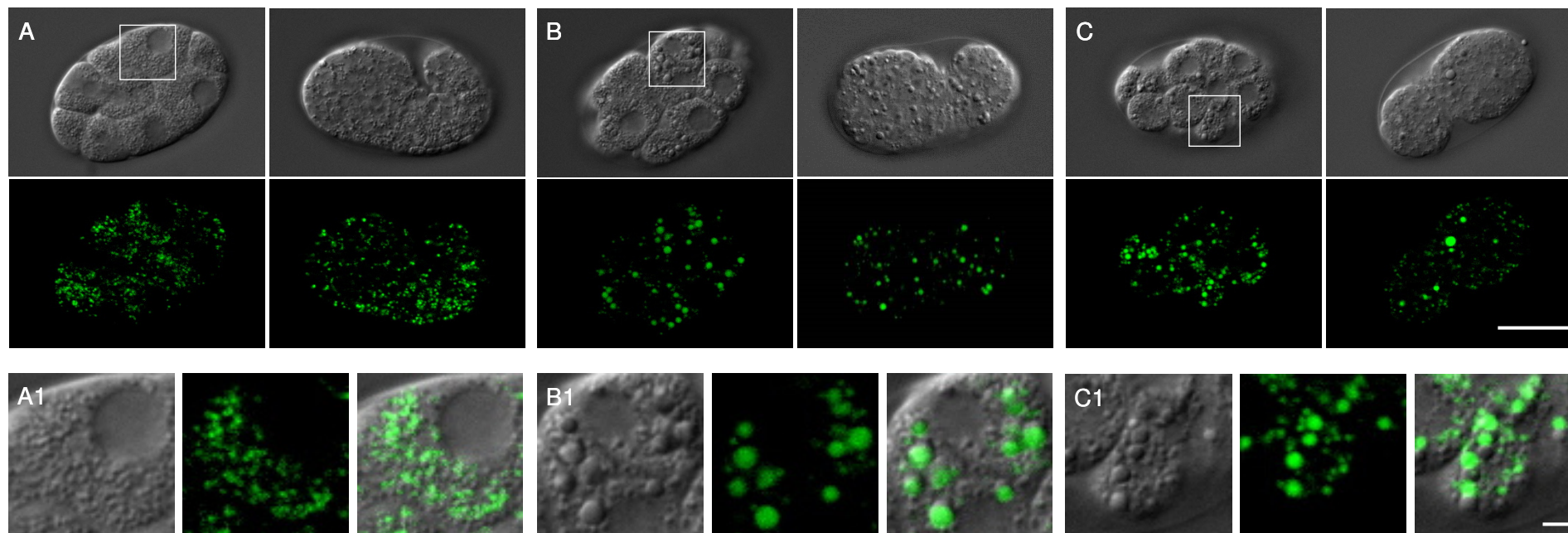


Figure 10: Lipid droplets in wild type and *sams-1* embryos. Lipid droplets were visualized by vital BODIPY™ 493/503 staining. (A-C) DIC images (upper panel) and BODIPY images (lower panel) of 12-cell embryos (left panel) and comma stage embryos (right panel) of wild type worms (A) and the mutants *sams-1(t5669)* (B) and *sams-1(ok3033)* are shown. (A1-C1) For each strain a detailed view of lipid droplets is shown in DIC optic (left panel), as BODIPY image (middle panel) and as merge (right panel). Scale bar represents 20 μm in full view images (A-C) and 2 μm in the detailed view (A1-C1).

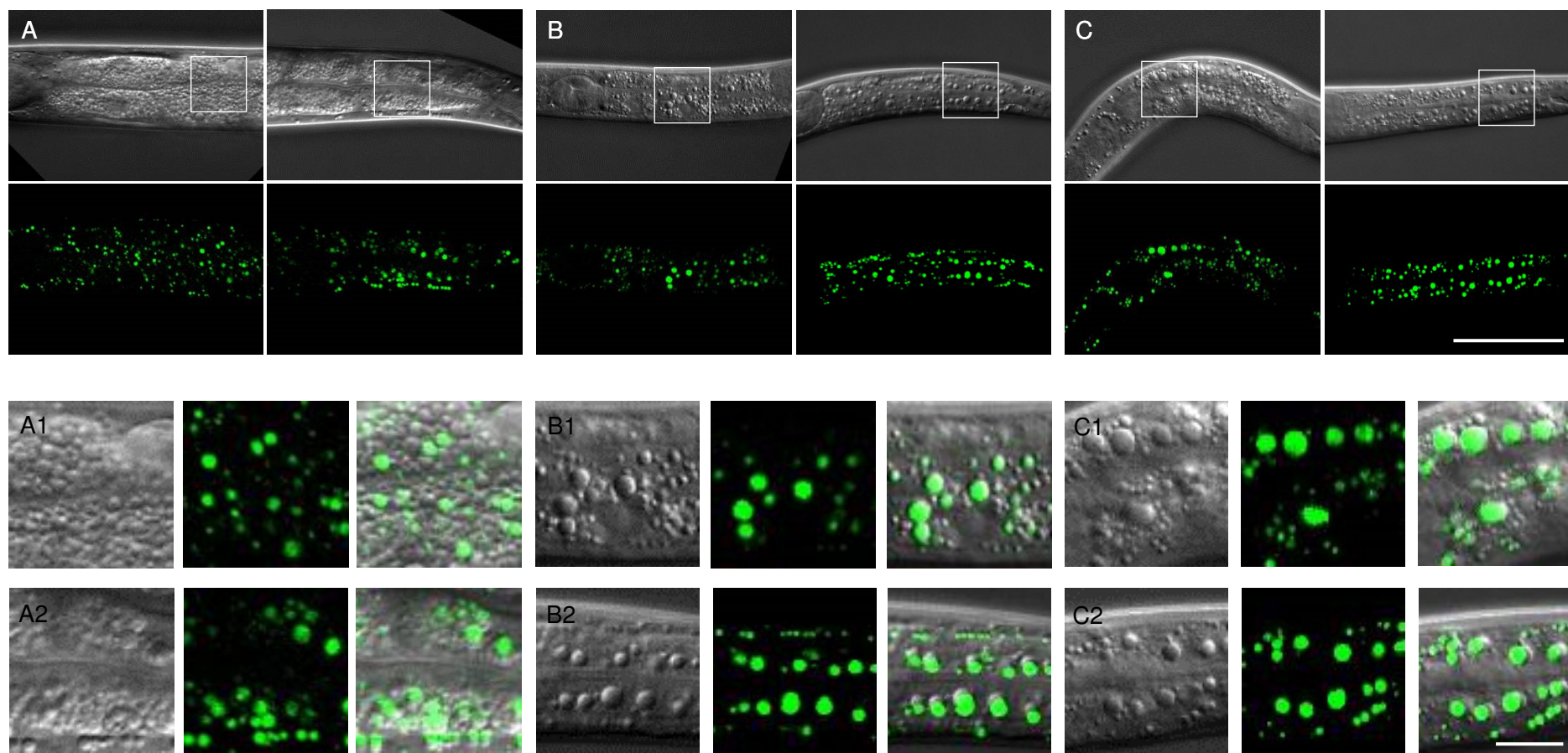


Figure 11: Lipid droplets in wild type and *sams-1* L4 larvae. Lipid droplets were visualized by vital BODIPY™ 493/503 staining. (A-C) DIC images (upper panel) and BODIPY images (lower panel) of the anterior intestine (left panel) and the posterior intestine (right panel) of wild type L4s (A) and larvae of the mutants *sams-1(t5669)* (B) and *sams-1(ok3033)* are shown. For each strain a detailed view of lipid droplets in the anterior intestine (A1-C1) and in the posterior intestine (A2-C2) is shown in DIC optic (left panel), as BODIPY image (middle panel) and as merge (right panel). Scale bar represents 50 μm in full view images (A-C) and 10 μm in the detailed view (A1-C1; A2-C2).

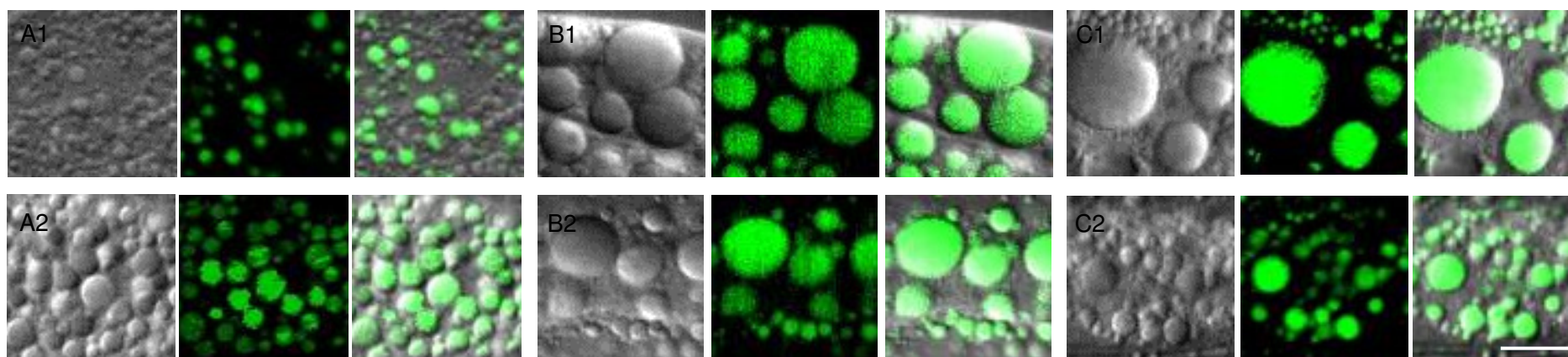
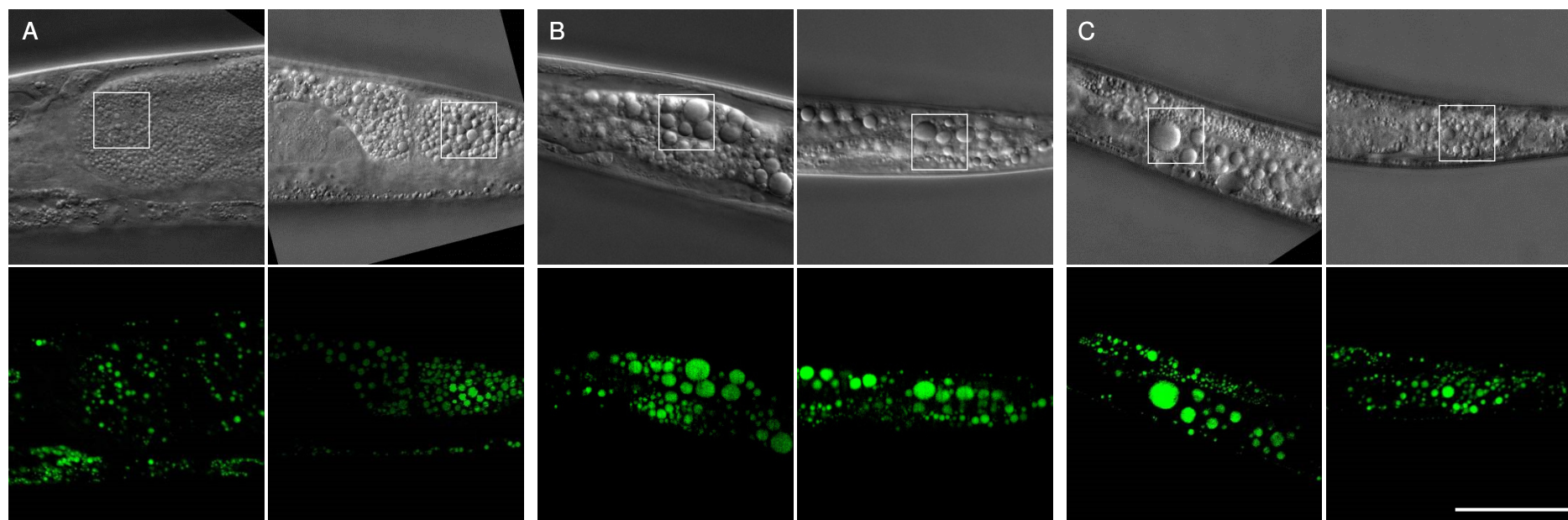


Figure 12: Lipid droplets in 5-day-old wild type worms and *sams-1* mutants. Lipid droplets were visualized by vital BODIPY™ 493/503 staining. (A-C) DIC images (upper panel) and BODIPY images (lower panel) of the anterior intestine (left panel) and the posterior intestine (right panel) of 5-day-old adult wild type worms (A) and the mutants *sams-1(t5669)* (B) and *sams-1(ok3033)* (C) are shown. For each strain a detailed view of lipid droplets in the anterior intestine (A1-C1) and in the posterior intestine (A2-C2) is shown in DIC optic (left panel), as BODIPY image (middle panel) and as merge (right panel). Scale bar represents 50 μm in full view images (A-C) and 10 μm in the detailed view (A1-C1; A2-C2).

3.8 *sams-1* larvae show a 2 fold enrichment of LDs that are $\geq 5 \mu\text{m}^3$ in size and are located in the anterior and the posterior intestine

3D fluorescence imaging of fixative fat stained wild type and *sams-1* larvae was used to quantify size and number of LDs. Compared to wild type larvae, *sams-1* larvae displayed a reduced number of LDs in the anterior intestine (Figure 13A). The number of LDs in the posterior intestine was similar between wild type and mutant larvae (Figure 13B). The mean LD volume in both regions of intestine was about 2 fold higher in *sams-1* larvae compared with wild type larvae (Figure 13C-D). Next, proportions of LDs that were $0-2 \mu\text{m}^3$, $2-5 \mu\text{m}^3$, $5-10 \mu\text{m}^3$, $10-30 \mu\text{m}^3$ and $>30 \mu\text{m}^3$ in volume were calculated. Independent of the respective region of the intestine, tiny-sized LDs ($<2 \mu\text{m}^3$) represented the largest fraction of all LDs in wild type as well as in *sams-1* larvae. Nevertheless, we found clear differences in the proportion of large LDs ($> 5 \mu\text{m}^3$) between wild type worms and *sams-1* mutants. In wild type L4 larvae, we found that 11 % of anterior and posterior intestinal LDs are $\geq 5 \mu\text{m}^3$ in size, respectively (Figure 13E-F). In *sams-1* L4 larvae, more than 20 % and 25 % of all anterior and posterior intestinal LDs are $\geq 5 \mu\text{m}^3$ in size, respectively (Figure 13E-F). Thus, compared to wild type larvae, *sams-1* larvae showed a more than 2 fold enrichment of large LDs ($\geq 5 \mu\text{m}^3$) in both, the anterior and the posterior intestine. These data may indicate an increased fat storage capacity in *sams-1* mutants.

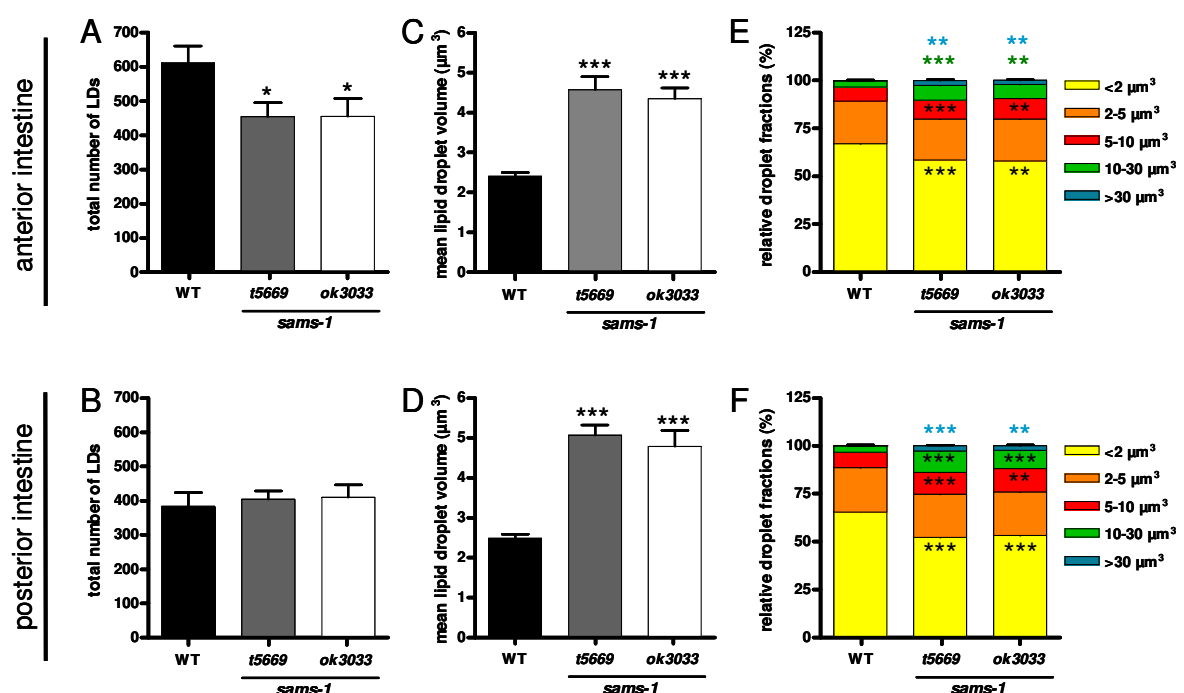


Figure 13: Total number and mean volume of lipid droplets in wild type and *sams-1* L4 larvae. LDs were visualized by fixative BODIPY™ 493/503 fat staining. The 3D object counter plugin of the ImageJ software was used to analyze total number of LDs (A-B) and mean volume of all LDs (C-D) in the anterior intestine (upper panel) and in the posterior intestine (lower panel) of wild type and *sams-1* larvae. LDs were clustered in different size classes and the relative proportion of each size class was calculated for the anterior intestine (E) and for the posterior intestine (F), respectively. Bars represent mean \pm SEM of at least 10 individual worms from three independent experiments. Statistically significant differences between wild type and each *sams-1* mutant were determined by unpaired t-test (** $p < 0.01$, *** $p < 0.001$).

3.9 In response to starvation, *sams-1* larvae show diminished depletion of triacylglycerol stores

C. elegans actively consumes TAG stored in LDs in response to starvation [37, 85, 145]. To test whether lipid mobilization from LDs is affected in *sams-1* mutants, we monitored LD breakdown in L4 larvae, which were starved for 24 hr and 48 hr, respectively. For this purpose, LDs of fixative fat stained worms were examined using 3D fluorescence microscopy (Figure S7) [86]. We measured starvation-induced alterations in the LD number, the mean volume of LDs and the total LD volume (LD number multiplied by mean LD volume). In 48 hr starved wild types, LD number was reduced to ~26 % and 40 % in the anterior and posterior intestine, respectively (Figure 14A-B). In contrast, *sams-1* larvae retained up to 88 % of their initial LD number in response to 48 hr starvation (Figure 14A-B). The mean LD volume was not substantially altered under starvation in wild type worms as well as in *sams-1* larvae (Figure 14C-D). Next, total volume of all LDs was calculated and was used as an approximate value for TAG storage. After 48 hr of starvation, wild type larvae retained 20 % of their initial total LD volume in the anterior intestine (Figure 14E). In contrast, 48 hr starved *sams-1* larvae retained up to 70 % of their initial total LD volume in that region (Figure 14E). In the posterior intestine, starved wild type and *sams-1* larvae retained 40 % and 60 % of their initial total LD volume, respectively (Figure 14F). Taken together, starvation-induced reduction of LD number and LD size is decreased in *sams-1* larvae compared with wild type worms (Figure S8).

It has been postulated that larger LDs are more lipolysis resistant than smaller ones [98]. To test this hypothesis, changes of the relative distribution of small-, medium- and large-sized LDs were determined before and after starvation of wild type and

sams-1 larvae. In the anterior intestine, wild type larvae showed a preferred reduction of medium- and large size LDs in response to starvation (Figure 15; Table S3). Such a preference was not found in *sams-1* larvae. Rather, starved *sams-1* larvae were able to conserve large-sized LDs in the anterior intestine. In the posterior intestine, wild type as well as *sams-1* larvae showed no size-dependent breakdown of LDs in response to starvation (Figure 15; Table S3). Together, these data indicate an impaired starvation-induced breakdown of LDs in *sams-1* mutants. Moreover, especially breakdown of large-sized LDs seems to be diminished in *sams-1* larvae.

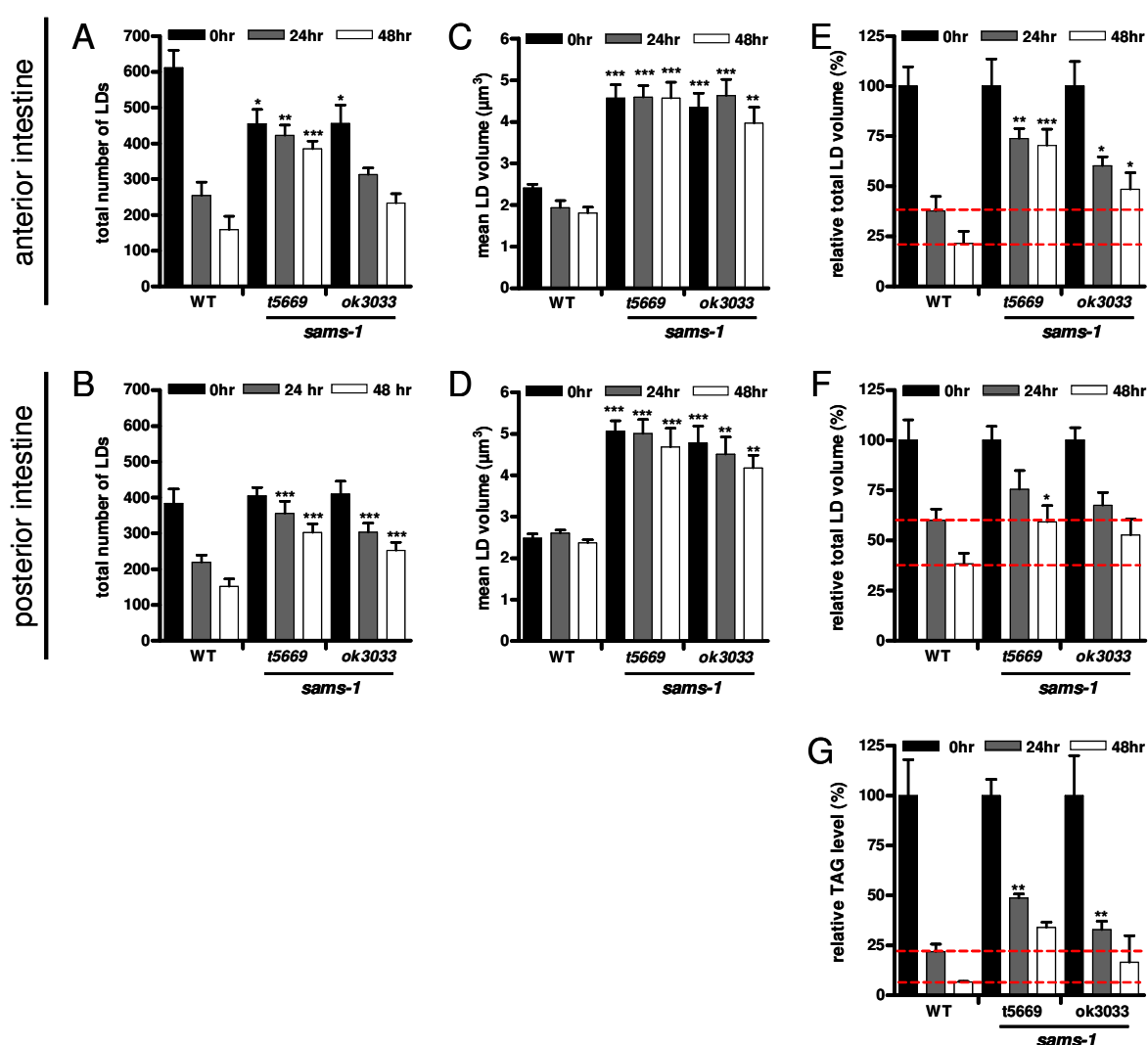


Figure 14: Starvation-induced LD breakdown and TAG consumption in wild type worms and *sams-1* mutants. Analysis of fluorescence images of fixative BODIPYTM 493/503 stained nematodes revealed total LD number (A-B), mean LD volume (C-D) and total LD volume (E-F) of wild type and *sams-1* L4 larvae. Worms have been fed *ad libitum* until the L4 stage (0 hr) before they have been starved for 24 hr and 48 hr. Parameters were determined for the anterior intestine (A, C, E) and for the posterior intestine (B, D, F) separately. Starvation-induced changes in total LD volume (LD number multiplied by mean LD volume) are shown as relative proportion

referred to the respective control (0 hr starvation). Bars represent mean \pm SEM of at least 10 individual worms from three independent experiments. (G) Enzymatically determined TAG levels of wild type and *sams-1* L4 larvae fed *ad libitum* (0 hr) and starved for 24 hr and 48 hr. Bars represent mean \pm SEM of 3-5 independent experiments. Each experiment comprised ~2000 (wild type) to ~4000 (*sams-1* mutants) worms. For each parameter significance asterisks refer to differences between wild type worms and the respective *sams-1* mutant at the respective time point and were determined by unpaired t-test with Welch-correction (* $p < 0.05$, ** $p < 0.01$ *** $p < 0.001$).

To confirm reduced release of lipids from LDs in *sams-1* mutants we biochemically determined alterations of TAG amount in response to starvation. As expected, TAG amount was drastically reduced in starved wild types. In response to 24 hr and 48 hr of starvation, wild type larvae retained only 25 % and 10 % of their initial TAG stores, respectively (Figure 14G). In contrast, starved *sams-1* larvae retained up to 50 % and 30 % of their initial TAG stores in response to 24 hr and 48 hr of starvation, respectively (Figure 14G). Reduced consumption of TAG is in good agreement with diminished starvation-induced LD breakdown, shown by reduced decrease of total LD volume in *sams-1* mutants (Figure 14E-F). Together, these data imply a diminished depletion of TAG stores in response to starvation in *sams-1* mutants and indicate that SAMS-1 is necessary for starvation-induced lipolysis.

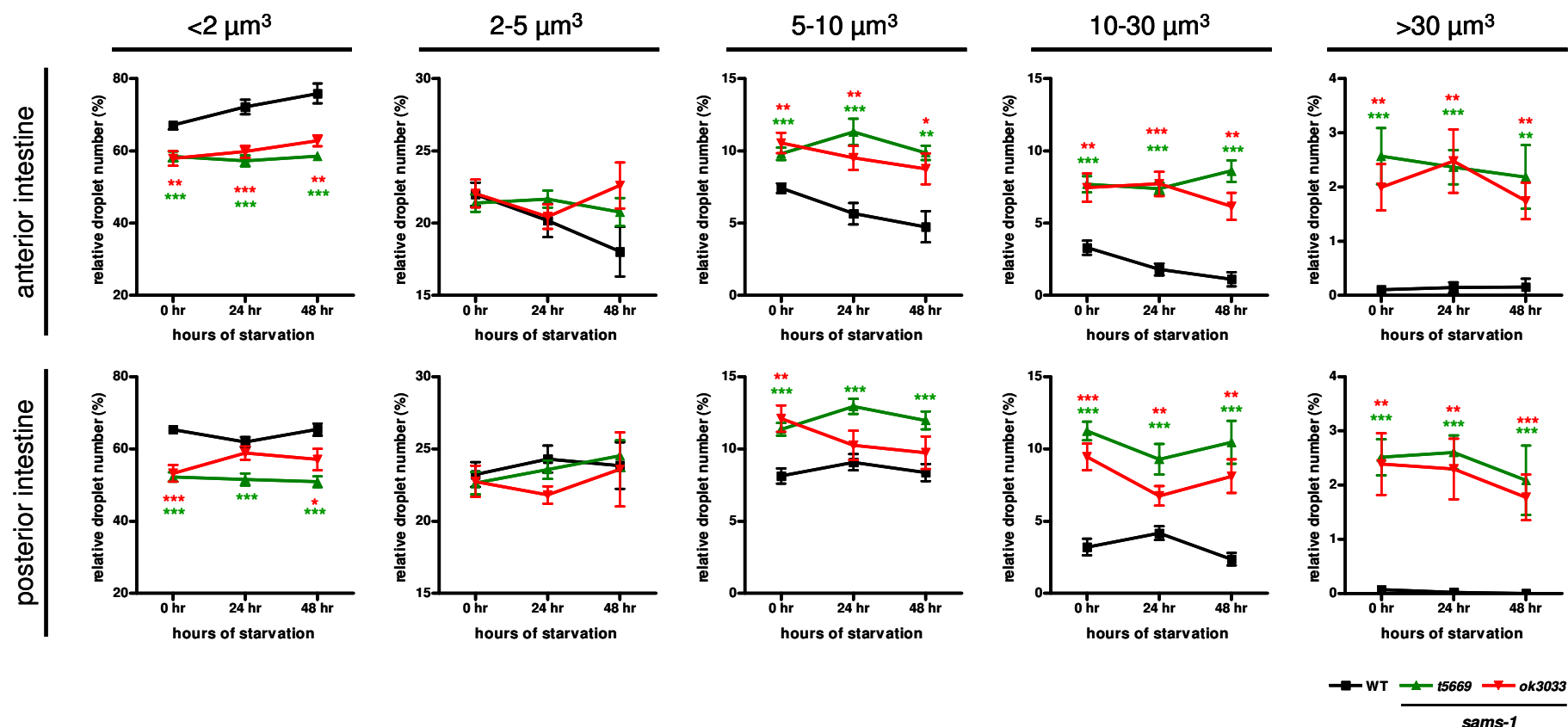


Figure 15: Size classification of LDs from *ad libitum* fed and starved wild type and *sams-1* larvae. Volumes of all BODIPYTM 493/503 positive LDs in the anterior (upper panel) and in the posterior intestine (lower panel) were determined by 3D fluorescence microscopy and image analysis using the 3D object counter plugin of the imageJ software. The relative number of LDs that are $<2 \mu\text{m}^3$, $2-5 \mu\text{m}^3$, $5-10 \mu\text{m}^3$, $10-30 \mu\text{m}^3$ and $>30 \mu\text{m}^3$ are shown for *ad libitum* fed larvae (0 hr) as well as for 24 hr and 48 hr starved wild type and *sams-1* larvae. Data points represent mean \pm SEM of at least 10 individual worms from three independent experiments. Significance asterisks refer to differences between wild type worms and the respective *sams-1* mutant at the respective time point and were determined by an unpaired t-test with Welch correction (* $p < 0.05$, ** $p < 0.01$, *** $p < 0.001$).

4 Discussion

4.1 A missense mutation in *sams-1* most likely impairs protein function

The S-adenosylmethionine synthetase 1 (SAMS-1) of *C. elegans* belongs to a family of evolutionary conserved enzymes, which catalyze the only known route of SAM synthesis [146-148]. As the major methyl group donor, SAM is used for a broad range of transmethylation reactions, like DNA methylation or PL synthesis [146]. Moreover, SAM serves as a precursor for glutathione, a major cellular antioxidant, and is necessary for the synthesis of polyamines [135, 138, 149, 150]. Thus, an impaired synthesis of SAM should affect central biological functions. In the present study, a point mutation (C→T) in *sams-1* was identified. *In silico* analysis of the resulting A105V substitution in SAMS-1 predicts an impairment of the protein function. The *sams-1(t5669)* mutant shows an increased arsenite-induced mortality, a delayed development, an impaired growth, a reduced reproductive capability and several alterations in lipid metabolism. These phenotypes are consistent with those observed in the mutant strain RB2240 harbouring a 480 bp deletion allele (*ok3033*) of *sams-1*. Complementation testing between the *sams-1(t5669)* allele and the *sams-1(ok3033)* allele revealed no intragenic complementation. All of these findings provide strong evidence that the *sams-1(t5669)* mutant allele most likely impairs protein function.

4.2 SAMS-1 deficiency lowers phosphatidylcholine level - SAM-dependent synthesis of phosphatidylcholine may be of quantitative importance for growth and fertility

In *C. elegans*, PC can be formed either by *de novo* synthesis via the Kennedy-route or by the PEAMT-pathway [60, 151]. The Kennedy-route involves the phosphorylation of free choline to phosphocholine, which is converted to CDP-choline and finally to PC. Within the PEAMT-pathway successive methylations of phosphoethanolamine give rise to phosphocholine, which then enters the Kennedy-route. Methylations are catalyzed by the phosphoethanolamine methyltransferases PMT-1 and PMT-2 [69, 70]. Both enzymes use SAM as methyl donor. In the present study it was shown that *sams-1(t5669)* and *sams-1(ok3033)*

mutants show a significantly reduced level of PC compared to wild type animals. The amount of PC per worm is reduced up to ~6 fold in *sams-1* adults. Most likely, this *sams-1* mutant phenotype is caused by a reduced synthesis of PC via the PEAMT-pathway. Thus, the PEAMT pathway is of quantitative importance for the synthesis of PC in *C. elegans*. In accordance, depletion of *pmt-1* reduces PC level as well [101]. In mammals, the analogous PEMT-pathway accounts for about 30 % of hepatic PC synthesis [152-154].

A reduced body size as well as a reduced number of progenies was observed in *sams-1* mutants. PC is a major PL of eukaryotic membranes [50, 57, 155, 156], which are necessary for growth and proliferation. *C. elegans* displays an age-related increase in body size and grows continuously until late adulthood [157, 158]. Previous studies in *pmt-1*, *pmt-2* or *sams-1* deficient worms have already shown a link between impaired PC synthesis and reduced number of progenies [69, 70, 159]. Thus, it is conceivable that SAMS-1 deficiency restricts growth and number of progenies due to the reduced PC level. However, it cannot be excluded that other factors than impaired membrane formation due to reduced PC synthesis contribute to reduced reproductive capability in *sams-1* mutants. As mentioned above, SAM is also necessary for polyamine synthesis and polyamines have been shown to be essential for oogenesis, egg fertilization and embryogenesis [160, 161]. In this context, increased expression of genes involved in polyamine synthesis, namely *odc-1* (ornithine decarboxylase, up to 4.9 fold) and *spds-1* (spermidine synthase, up to 1.9 fold), may represent a compensatory mechanism in *sams-1* adults.

Taken together, our data indicate that SAMS-1 is necessary for proper PC synthesis, since its product SAM serves as an essential methyl donor within the PEAMT-pathway. We further suggest that PC synthesis via SAMS-1 is necessary for proper growth and production of progenies in *C. elegans*.

4.3 SAMS-1 deficiency lowers phosphatidylcholine level – this phenotype may be coupled to increased synthesis of triacylglycerol in order to reduce toxic effects of free fatty acids

Although PLs and TAG have distinct functions, they share common substrates and metabolic routes. DAG, FA and phosphatidic acid are lipid intermediates used for

both, PL and TAG synthesis. Moreover, both pathways are regulated by common transcription factors. For instance, the sterol regulatory element binding protein SREBP-1 up-regulates the expression of the mitochondrial glycerol-3-phosphate transferase (GPAT) as well as the expression of the CTP:phosphocholine cytidyltransferase (CCT). These enzymes are involved in TAG and PC synthesis, respectively [162-164]. It is well known that TAG stored in LDs serves as a reservoir for PL precursors. More recently, it has been shown that PC is also an quantitatively important source for TAG intermediates and that DAG and FA derived from PL hydrolysis are directly incorporated into TAG [165-167]. These findings indicate a close relationship between PC and TAG synthesis. Thus, conditions, which perturb one of both pathways, also affect the other one. Accordingly, this study shows that a reduced proportion of PC is accompanied by an elevated proportion of TAG in *sams-1* adults. Interestingly, mice fed a methionine-choline-deficient diet have a markedly reduced PC level and develop steatohepatitis, which is characterized by excessive fat storage in the liver [168, 169]. Similar results have been found in humans ingesting a choline-deficient diet [170, 171]. Moreover, it has been shown in *C. elegans*, mice or cell culture that deficiency of CCT, SAMS or enzymes of the PEMT/PEAMT pathway lead to elevated TAG level [73, 100, 101, 172]. Taken together, these data indicate that SAMS-1 deficiency reduces PC synthesis and simultaneously promotes fat storage.

In accordance with the elevated TAG content, this study revealed an increased expression of genes involved in FA synthesis and TAG formation in *sams-1* mutants. Up-regulated genes encode, for instance, the acetyl-CoA carboxylase POD-2, the fatty acid synthase FASN-1, several FA elongases (i.e. ELO-2; -5; -6; -7) and desaturases (i.e. FAT-1 - FAT-7), the diacylglycerol acyltransferase DGAT-2 and the acyl-CoA synthetase ACS-22. DGAT-2 and ACS-22 form a protein complex to promote TAG formation [18]. In agreement to our study, it has been shown that *sams-1* depletion by RNAi increases expression of *pod-2* and *fat-7* [101]. Furthermore, Walker *et al.* found *fat-5*, *fat-6*, *fat-7* and *fat-2* as well as *elo-2* and *elo-6* to be up-regulated in *sams-1(RNAi)* and *sams-1(lof)* worms. They have also found increased hepatic expression of *Scd1*, the mouse ortholog of *fat-6* and *fat-7*, in CCT-deficient mice [100]. Increased enzyme activities of GPAT, the glycerol-3-phosphat acyltransferase, and DGAT have been found in CCT-deficient

Chinese hamster ovary (CHO) cells [173]. In rat hepatocytes, CDP-choline depletion causes accumulation of DAG due to defective PC synthesis [174]. It has been shown that DGAT exhibits its maximal activity in response to DAG accumulation, thereby providing full TAG formation capacity [174]. Thus, accumulating DAG is dissipated by TAG synthesis [175, 176]. Overall, these data indicate that SAM and/or PC depletion, as observed in SAMS-1 deficient mutants, increases TAG formation via induced expression of lipogenic genes.

It has been postulated that increased expression of lipogenic genes is caused by decreased PC levels [100]. Interestingly, most of the lipogenic genes found to be up-regulated in *sams-1* mutants are targets of the nutrient responding transcription factor SBP-1. SBP-1 is the worm ortholog of mammalian SREBP-1 and has been shown to mediate fat accumulation in *C. elegans* [83, 100, 145, 177]. SREBP proteins are resident at the ER as inactive precursors. After proteolytic cleavage by SREBP-activating proteases, which are located at the Golgi, SREBP becomes activated and transits to the nucleus to activate gene expression [178]. Walker *et al.* suggested a post-transcriptional activation of SBP-1 in response to low PC level, because RNAi depletion of *sams-1* caused an increased nuclear accumulation of SBP-1 [100]. It has been further suggested that limiting the amount of membrane PC alters the membrane function of the Golgi, which leads to augmented release of the SBP-activating proteases and, consequently, to an increased SBP-1 activation [100].

All together, due to common intermediates (FA, DAG), shared biosynthetic routes and mutual gene regulatory mechanisms (SREBP proteins), metabolisms of PC and TAG are intimately linked to each other. In *sams-1* mutants, a reduced PC level is accompanied by an increased level of TAG and higher expression of lipogenic genes indicating increased lipogenesis in these mutants. This is in accordance to the current hypothesis that dropping PC levels directly affect SBP-1 activation and that SBP-1 dependent transcription of lipogenic genes induces TAG synthesis. In turn, increased TAG synthesis under SAMS-1 deficiency might be mechanism to protect cells from toxicity of accumulating DAG and FA.

4.4 SAMS-1 deficiency enlarges lipid droplets – a possible adaption to economize phosphatidylcholine

sams-1(t5669) and *sams-1(ok3033)* mutants displayed LD expansion in embryos, larvae and adults. The extent of LD expansion was positively correlated to an increased PC demand of *sams-1* adults compared with *sams-1* larvae. PC levels of *sams-1* mutants were reduced ~2 fold at the L4 stage, but up to ~6 fold at fifth day of adulthood. Moreover, *sams-1* adults, but not *sams-1* larvae, showed elevated expression of genes involved in PC formation (i.e. *cka-2*, *ckb-2*, *pmt-1*, *pmt-2*, *pcyt-1*, *cept-1*), which may indicate a compensatory response in order to increase PC synthesis. Indeed, worms passing the transition from late L4 to adulthood undergo dramatic germ cell proliferation, intense extension of gonadal arms and gametogenesis, all processes that consume a huge amount of PC [179]. Subsequently, LD enlargement intensified from larval stage to adulthood. Interestingly, LD enlargement was also observed in *sams-1* embryos. Because *sams-1* shows no zygotic expression [159], the *sams-1* mutant phenotype may rise from the maternal provision of the mutated *sams-1* transcript. However, LD expansion has been observed very early in embryogenesis, hence, the actual embryonic LD size may reflect maternal PC deficiency.

A connection between LD size and PC demand has been reported in several other studies, which revealed LD enlargement upon inhibition of PC synthesis [16, 71, 100, 101, 180]. In principle, LD expansion is mediated either by incorporation of neutral lipids or by fusion of existing, adjacent LDs [15, 24, 181]. LD expansion due to increased uptake of neutral lipids, particularly during lipid loading, is a well accepted and intensively studied process [17, 24, 182]. In contrast, LD fusion, as a process of LD enlargement, is debated to be a rare event, which solely occurs in mutant cells and under extreme conditions [72, 181, 183, 184]. Interestingly, LD fusion has been previously found to be a consequence of impaired PC synthesis [16, 71]. Thus, it was proposed that that LD enlargement is, at least in part, mediated via coalescence in *sams-1* mutants.

It has been suggested that LD expansion requires huge amounts of additional PC to cover the growing surface [16]. However, another study showed that even upon FA treatment less than 10 % of newly synthesized PC is incorporated in the expanding

LD membrane, which indicates that LD enlargement is not an expensive PC-consuming process [185]. Quite the contrary, while fusing LDs maintain their initial volume, the overall surface area decreases. A decreased surface-to-volume ratio indicates that LD fusion enables rapid removal of excess membrane components, including PC [186]. Therefore, LD expansion in SAMS-1 deficient mutants may represent a process to economize PC, necessary for membrane formation during cell growth and reproduction.

4.5 SAMS-1 deficiency reduces lipolysis efficiency under starvation conditions – an indication of inefficient liberation of lipid droplet-derived fatty acids

The most important function of LDs is to store lipids and to release FA in times of increased energy demand. Hydrolysis of neutral lipids is catalyzed by lipases and needs to be tightly regulated [187]. LD size was supposed to be an important determinant in regulating lipolysis efficiency. For instance, deletion of FSP27 (Fat-specific protein of 27 kDa) enhances lipolysis by promoting the formation of smaller LDs [12]. In contrast, factors promoting LD enlargement have been shown to inhibit lipolysis. In *C. elegans*, defective peroxisomal β -oxidation results in enlarged intestinal LDs that are more resistant to lipase-triggered lipolysis during fasting [98]. A similar effect has been shown for LDs, which were enlarged due to defective PC synthesis [16, 71]. Examination of starvation-induced lipolysis revealed that TAG hydrolysis is diminished in *sams-1* mutants. In particular, lipolysis has been shown to be more diminished in large LDs compared with small LDs. These data suggest that maintenance of small LDs is necessary for efficient lipolysis. A simple explanation may be that clusters of small LDs provide enough surface area for lipases, while the reduced surface area of a few large LDs limits the accessibility of TAG hydrolyzing lipases. However, *C. elegans acbp-1* mutants also exhibit enlarged LDs, which are effectively reduced in number and size in response to starvation [93]. This indicates the existence of further determinants affecting lipolysis efficiency.

Astonishingly, this study revealed body region-specific differences in starvation-induced LD breakdown. In wild type larvae, the total LD volume was reduced by 80 % in the anterior intestine, but only by 60 % in the posterior intestine.

There are few reports providing functional evidence for distinct LD subclasses. Beller *et al.* analyzed the proteome of LDs isolated from fat body of *D. melanogaster* [188]. They found that different subsets of LDs can be distinguished on the basis of LD-associated proteins [188]. It has been also reported that LDs within one cell incorporate TAG at very different rates [24]. This effect was independent of LD size, but was ascribed to differences in the protein coat, since DGAT2 associated with some but not all LDs [24]. Differences in the assembly of LD-associated proteins have been supposed to reflect the metabolic state and/ or functional differences of individual LDs [188]. In this context, body region-specific LD breakdown, which has been seen in wild type *C. elegans*, may also represent functionally distinct LD classes differing in their susceptibility to lipolysis, e.g. to build long-term and short-term energy stores, respectively.

In contrast to wild type worms, *sams-1* mutants did not show significant differences in body region-specific LD breakdown. Thus, loss-of-function mutation of *sams-1* may alter not only LD size but also the specific protein coat of LDs and thereby their functional identity, which leads to altered regulation of lipolysis. To date, it is not fully understood how differential recruitment of proteins is managed by LDs, however recent findings highlight an important role of the PL composition of LD membranes [189]. Yeast *cds1* and *ino2Δ* mutant cells produce supersized LDs. Analysis of the PL composition has revealed a higher proportion of PC in *cds1* and a lower proportion of PC in *ino2Δ* LDs compared with wild type ones. Interestingly, both mutants exhibited significantly reduced level of known LD-resident proteins, including neutral lipid hydrolases. Accordingly, mobilization of neutral lipids was impaired in both strains [189]. These data demonstrate that both reduced and elevated relative amounts of PC in the LD membrane mediate altered protein recruitment, which subsequently impairs release of neutral lipids. Since PC levels are reduced in *sams-1* mutants, their reduced capability for LD breakdown in response to starvation may be mediated by altered PL composition of LD membranes. All together, these findings indicate that SAMS-1 is necessary for an efficient lipolysis.

Efficient lipolysis is not only essential under food limiting conditions. Several studies have shown that FA released from stored TAG are preferentially used for different physiological functions over FA derived from exogenous sources or *de novo*

synthesized FA. In humans, free FA taken up by resting muscles are not oxidized directly, but incorporated into intramuscular TAG stores, before they are released for β -oxidation [190, 191]. Studies in hepatocytes have shown that LD-derived lipids are preferentially used for very low-density lipoprotein (VLDL) production [192]. In *S. cerevisiae* and *D. melanogaster*, lipolysis-derived FA seem to be essential for cellular growth, since deletion of Tgl4 and Brummer, the respective ATGL homologs in yeast and fly, caused a delay in cell-cycle entry and embryonic lethality, respectively [35, 36]. Considering this, inefficient supply of LD-derived lipids may contribute to reduced growth and reproduction of *sams-1* mutants.

Taken together, LD enlargement and an altered PL composition of the LD membrane due to SAMS-1 deficiency are supposed to diminish lipolysis efficiency. While LD enlargement reduces surface area and therefore access of lipases, alterations in the relative abundance of PC may modify recruitment of neutral lipid hydrolases to the LD surface. In consideration of its impact on LD size and PC synthesis, SAMS-1 is suggested to regulate liberation of LD-derived lipids for fundamental physiological functions like growth and reproduction.

4.6 SAMS-1 deficiency reflects symptoms of non-alcoholic steatohepatitis

In humans, the majority of SAM is synthesized in the liver, where it is also mainly consumed [193, 194]. Hepatic lipid accumulation and LD enlargement are early steps in the development of non-alcoholic fatty liver disease (NAFLD) [195]. Major risk factors for NAFLD are obesity, diabetes and the metabolic syndrome [196]. However, impaired SAM synthesis also contributes to NAFLD and its progressive form, non-alcoholic steatohepatitis (NASH) [73, 197-199]. For instance, mice, depleted for MAT1A, the mammalian ortholog of SAMS-1, are animal models of NASH [200]. Next to SAMS-1 deficiency, also a diminished PC synthesis is associated with the progression of NAFLD. For instance, NASH patients exhibit a reduced PC to PE ratio within the liver [201]. Moreover, PEMT-depleted mice fed a choline-deficient diet also develop steatohepatitis [142, 201]. Hepatic lipid accumulation is supposed to be mediated by SREBP [100, 195, 202]. Together, diminished synthesis of SAM and PC as well as SREBP-mediated lipogenesis have been shown to contribute to NAFLD/ NASH, a metabolic disorder characterized by excessive hepatic lipid storage and abnormal LD morphology. Interestingly, these phenotypes have been also

observed in *sams-1* mutants highlighting the conserved function of SAMS-1 in maintaining lipid homeostasis.

4.7 SAMS-1 deficiency mimics a dietary restriction state - a possible role of SAM-levels as gauge for nutrient availability

Dietary restriction (DR) is an environmental intervention that is characterized by a reduced food intake without inducing malnutrition [203]. In *C. elegans*, among a variety of phenotypes, DR reduces body size and fertility, enlarges LDs in larvae and adults and protects against proteotoxicity due to reduced age-related paralysis [126, 204-211]. Interestingly, all of these phenotypes have been also observed in SAMS-1 deficient worms, as shown here and in other studies [100, 101, 159, 211]. Life span extension has been observed in a wide range of species in response to DR [212-218]. Interestingly, inhibition of *sams-1* increases life span, too [205, 219]. The longevity effect of DR is mediated, at least in part, by the nutrient sensing target of rapamycin (TOR) pathway [220-222]. *sams-1* mRNA level were reduced after inhibition of *let-363*, the worm homolog of mammalian TOR as well as in the *eat-2(ad1116)* mutant, a genetic model of DR [205, 219, 223]. In the *eat-2* mutant, *sams-1* RNAi does not further extend lifespan [205]. Additionally, *sams-1* inhibition down-regulates *drr-2*, a DR-responsive gene necessary for DR-mediated longevity [219]. These findings indicate that *sams-1* is necessary for DR-mediated effects and that *sams-1* is down-regulated in response to DR. Thus, DR may reduce the activity of SAMS-1 and the subsequent production of SAM [205]. Accordingly, restricted intake of methionine reduces SAM production and prolongs lifespan in rodents as well [224-227]. Methionine is the crucial precursor for SAM synthesis and is recycled within the one-carbon-cycle. Nutrients as folic acid and vitamin B12 are involved in the re-synthesis of methionine from SAH, the product of SAM-dependent methylation reactions. It is therefore conceivable that restriction of these nutrients also impairs SAM synthesis. Thus, SAM levels may represent a gauge for nutrient availability.

Taken together SAMS-1 deficiency leads to a broad range of phenotypes that are usually associated with DR. Moreover, *sams-1* expression is reduced by DR regimes (*eat-2*) and DR signalling pathways (TOR). In turn, reduced expression of *sams-1*

down-regulates *drr-2*, a gene also down-regulated by DR. Therefore, inhibition of SAMS-1 and subsequent reduction of SAM-level may mimic a DR condition.

4.8 Conclusion

The present study shows that SAMS-1 deficiency in *C. elegans* reduces the PC to TAG ratio, elevates expression of lipogenic genes, enlarges LDs, reduces lipolysis efficiency under starvation conditions and reduces body size and number of progenies as well. It is proposed that SAMS-1 deficiency reduces synthesis of PC via reduction of the SAM-dependent PEAMT pathway. A reduced level of PC increases SBP-1 dependent transcription of lipogenic genes contributing to an elevated proportion of TAG. In turn, the decreased PC to TAG ratio may compels LD enlargement by LD fusion, thereby reducing the surface-to volume ratio of LDs. This reduced surface area as well as a reduced portion of PC within the LD membrane may contribute to reduced lipolysis efficiency. Both, a reduced PC availability and an inefficient liberation of FA from LDs may explain reduced growth and reproduction of *sams-1* deficient mutants. Storage of lipids in enlarged LDs and increased lipogenesis, as observed in *sams-1* mutants, seems to be important to protect from lipotoxicity and to economize PC. Given the importance of PC for membrane formation, these adaptations may reflect strategies to ensure survival in times of growth, reproduction and reduced food availability (Figure 16). In conclusion, SAMS-1 seems to be crucial in regulating homeostasis of lipid metabolism. In particular, because SAMS-1 deficiency mediates increased fat storage through impaired PC synthesis, LD expansion, increased lipogenesis and reduced lipolysis efficiency, it is proposed that synthesis of the methyl group donor SAM is necessary to limit fat storage.

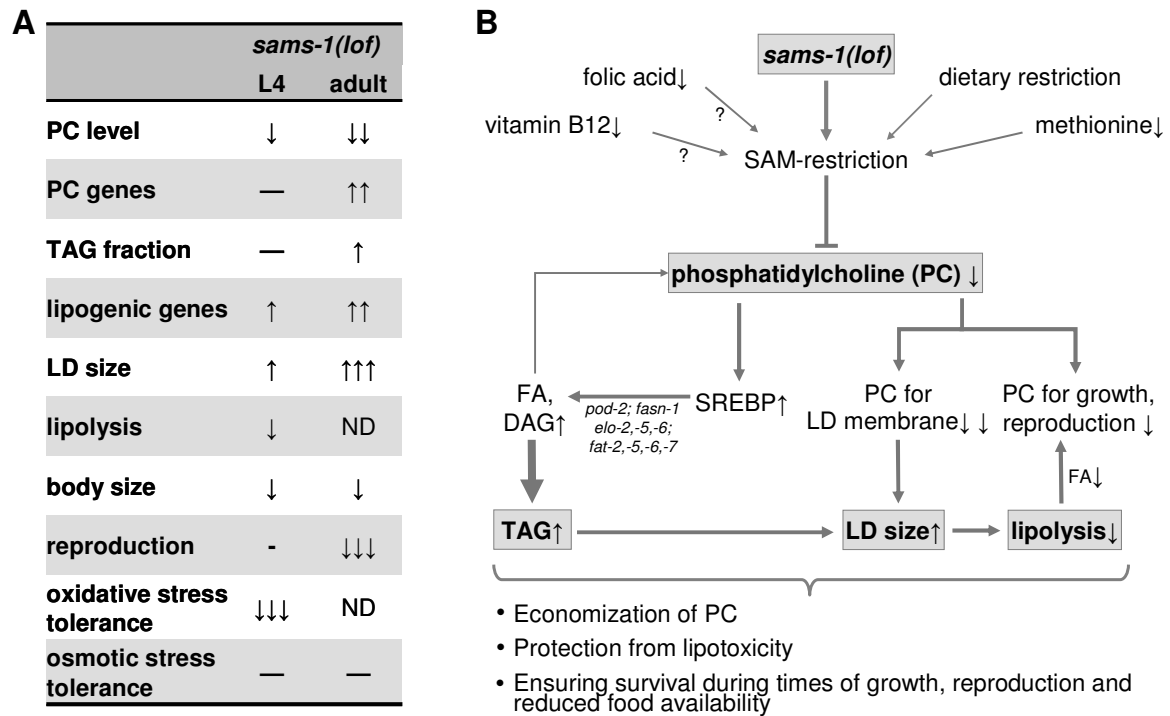


Figure 16: Physiological consequences of *sams-1* inhibition. (A) Phenotypes observed in *sams-1* mutants. Arrows indicate direction and degree of modification compared with wild type worms. "—" means no significant difference to wild type worms. (B) A working model for *sams-1* as operator in fat storage. SAM deficiency promotes fat storage by increased lipogenesis, LD enlargement and reduced lipolysis. Reduced SAM-dependent synthesis of PC is central in mediating these processes. Increased fat storage is supposed to represent an adaptation to the imbalance of lipid metabolism.

5 References

1. Alvarez HM, Steinbuchel A: **Triacylglycerols in prokaryotic microorganisms.** *Applied microbiology and biotechnology* 2002, **60**(4):367-376.
2. Wolinski H, Kohlwein SD: **Microscopic analysis of lipid droplet metabolism and dynamics in yeast.** *Methods Mol Biol* 2008, **457**:151-163.
3. James CN, Horn PJ, Case CR, Gidda SK, Zhang D, Mullen RT, Dyer JM, Anderson RG, Chapman KD: **Disruption of the Arabidopsis CGI-58 homologue produces Chanarin-Dorfman-like lipid droplet accumulation in plants.** *Proceedings of the National Academy of Sciences of the United States of America* 2010, **107**(41):17833-17838.
4. Chien CH, Chen WW, Wu JT, Chang TC: **Investigation of lipid homeostasis in living Drosophila by coherent anti-Stokes Raman scattering microscopy.** *Journal of biomedical optics* 2012, **17**(12):126001.
5. Hellerer T, Axang C, Brackmann C, Hillertz P, Pilon M, Enejder A: **Monitoring of lipid storage in Caenorhabditis elegans using coherent anti-Stokes Raman scattering (CARS) microscopy.** *Proceedings of the National Academy of Sciences of the United States of America* 2007, **104**(37):14658-14663.
6. Zweytick D, Athenstaedt K, Daum G: **Intracellular lipid particles of eukaryotic cells.** *Biochimica et biophysica acta* 2000, **1469**(2):101-120.
7. Bartz R, Li WH, Venables B, Zehmer JK, Roth MR, Welti R, Anderson RG, Liu P, Chapman KD: **Lipidomics reveals that adiposomes store ether lipids and mediate phospholipid traffic.** *Journal of lipid research* 2007, **48**(4):837-847.
8. Murphy DJ, Vance J: **Mechanisms of lipid-body formation.** *Trends in biochemical sciences* 1999, **24**(3):109-115.
9. Tauchi-Sato K, Ozeki S, Houjou T, Taguchi R, Fujimoto T: **The surface of lipid droplets is a phospholipid monolayer with a unique Fatty Acid composition.** *The Journal of biological chemistry* 2002, **277**(46):44507-44512.
10. Brasaemle DL: **Thematic review series: adipocyte biology. The perilipin family of structural lipid droplet proteins: stabilization of lipid droplets and control of lipolysis.** *Journal of lipid research* 2007, **48**(12):2547-2559.
11. Bickel PE, Tansey JT, Welte MA: **PAT proteins, an ancient family of lipid droplet proteins that regulate cellular lipid stores.** *Biochimica et biophysica acta* 2009, **1791**(6):419-440.
12. Nishino N, Tamori Y, Tateya S, Kawaguchi T, Shibakusa T, Mizunoya W, Inoue K, Kitazawa R, Kitazawa S, Matsuki Y *et al*: **FSP27 contributes to efficient energy storage in murine white adipocytes by promoting the formation of unilocular lipid droplets.** *The Journal of clinical investigation* 2008, **118**(8):2808-2821.
13. Zhou L, Xu L, Ye J, Li D, Wang W, Li X, Wu L, Wang H, Guan F, Li P: **Cidea promotes hepatic steatosis by sensing dietary fatty acids.** *Hepatology* 2012, **56**(1):95-107.
14. Gong J, Sun Z, Li P: **CIDE proteins and metabolic disorders.** *Current opinion in lipidology* 2009, **20**(2):121-126.
15. Bostrom P, Andersson L, Rutberg M, Perman J, Lidberg U, Johansson BR, Fernandez-Rodriguez J, Ericson J, Nilsson T, Boren J *et al*: **SNARE proteins mediate fusion between cytosolic lipid droplets and are implicated in insulin sensitivity.** *Nature cell biology* 2007, **9**(11):1286-1293.
16. Krahmer N, Guo Y, Wilfling F, Hilger M, Lingrell S, Heger K, Newman HW, Schmidt-Supprian M, Vance DE, Mann M *et al*: **Phosphatidylcholine synthesis for lipid droplet expansion is mediated by localized activation of CTP:phosphocholine cytidyltransferase.** *Cell metabolism* 2011, **14**(4):504-515.
17. McFie PJ, Banman SL, Kary S, Stone SJ: **Murine diacylglycerol acyltransferase-2 (DGAT2) can catalyze triacylglycerol synthesis and promote lipid droplet**

- formation independent of its localization to the endoplasmic reticulum. *The Journal of biological chemistry* 2011, **286**(32):28235-28246.
18. Xu N, Zhang SO, Cole RA, McKinney SA, Guo F, Haas JT, Bobba S, Farese RV, Jr., Mak HY: **The FATP1-DGAT2 complex facilitates lipid droplet expansion at the ER-lipid droplet interface.** *The Journal of cell biology* 2012, **198**(5):895-911.
 19. Fujimoto Y, Itabe H, Sakai J, Makita M, Noda J, Mori M, Higashi Y, Kojima S, Takano T: **Identification of major proteins in the lipid droplet-enriched fraction isolated from the human hepatocyte cell line HuH7.** *Biochimica et biophysica acta* 2004, **1644**(1):47-59.
 20. Farese RV, Jr., Walther TC: **Lipid droplets finally get a little R-E-S-P-E-C-T.** *Cell* 2009, **139**(5):855-860.
 21. Martin S, Parton RG: **Lipid droplets: a unified view of a dynamic organelle.** *Nature reviews Molecular cell biology* 2006, **7**(5):373-378.
 22. Brasaemle DL, Wolins NE: **Packaging of fat: an evolving model of lipid droplet assembly and expansion.** *The Journal of biological chemistry* 2012, **287**(4):2273-2279.
 23. Listenberger LL, Han X, Lewis SE, Cases S, Farese RV, Jr., Ory DS, Schaffer JE: **Triglyceride accumulation protects against fatty acid-induced lipotoxicity.** *Proceedings of the National Academy of Sciences of the United States of America* 2003, **100**(6):3077-3082.
 24. Kuerschner L, Moessinger C, Thiele C: **Imaging of lipid biosynthesis: how a neutral lipid enters lipid droplets.** *Traffic* 2008, **9**(3):338-352.
 25. Zechner R, Kienesberger PC, Haemmerle G, Zimmermann R, Lass A: **Adipose triglyceride lipase and the lipolytic catabolism of cellular fat stores.** *Journal of lipid research* 2009, **50**(1):3-21.
 26. Fujimoto T, Parton RG: **Not just fat: the structure and function of the lipid droplet.** *Cold Spring Harbor perspectives in biology* 2011, **3**(3).
 27. Walther TC, Farese RV, Jr.: **Lipid droplets and cellular lipid metabolism.** *Annual review of biochemistry* 2012, **81**:687-714.
 28. Zimmermann R, Strauss JG, Haemmerle G, Schoiswohl G, Birner-Gruenberger R, Riederer M, Lass A, Neuberger G, Eisenhaber F, Hermetter A *et al*: **Fat mobilization in adipose tissue is promoted by adipose triglyceride lipase.** *Science* 2004, **306**(5700):1383-1386.
 29. Villena JA, Roy S, Sarkadi-Nagy E, Kim KH, Sul HS: **Desnutrin, an adipocyte gene encoding a novel patatin domain-containing protein, is induced by fasting and glucocorticoids: ectopic expression of desnutrin increases triglyceride hydrolysis.** *The Journal of biological chemistry* 2004, **279**(45):47066-47075.
 30. Jenkins CM, Mancuso DJ, Yan W, Sims HF, Gibson B, Gross RW: **Identification, cloning, expression, and purification of three novel human calcium-independent phospholipase A2 family members possessing triacylglycerol lipase and acylglycerol transacylase activities.** *The Journal of biological chemistry* 2004, **279**(47):48968-48975.
 31. Greenberg AS, Egan JJ, Wek SA, Garty NB, Blanchette-Mackie EJ, Londos C: **Perilipin, a major hormonally regulated adipocyte-specific phosphoprotein associated with the periphery of lipid storage droplets.** *The Journal of biological chemistry* 1991, **266**(17):11341-11346.
 32. Miyoshi H, Perfield JW, 2nd, Souza SC, Shen WJ, Zhang HH, Stancheva ZS, Kraemer FB, Obin MS, Greenberg AS: **Control of adipose triglyceride lipase action by serine 517 of perilipin A globally regulates protein kinase A-stimulated lipolysis in adipocytes.** *The Journal of biological chemistry* 2007, **282**(2):996-1002.
 33. Miyoshi H, Souza SC, Zhang HH, Strissel KJ, Christoffolete MA, Kovsan J, Rudich A, Kraemer FB, Bianco AC, Obin MS *et al*: **Perilipin promotes hormone-sensitive lipase-mediated adipocyte lipolysis via phosphorylation-dependent and -independent mechanisms.** *The Journal of biological chemistry* 2006, **281**(23):15837-15844.

34. Wu JW, Wang SP, Casavant S, Moreau A, Yang GS, Mitchell GA: **Fasting energy homeostasis in mice with adipose deficiency of desnutrin/adipose triglyceride lipase.** *Endocrinology* 2012, **153**(5):2198-2207.
35. Kurat CF, Wolinski H, Petschnigg J, Kaluarachchi S, Andrews B, Natter K, Kohlwein SD: **Cdk1/Cdc28-dependent activation of the major triacylglycerol lipase Tgl4 in yeast links lipolysis to cell-cycle progression.** *Molecular cell* 2009, **33**(1):53-63.
36. Gronke S, Mildner A, Fellert S, Tennagels N, Petry S, Muller G, Jackle H, Kuhnlein RP: **Brummer lipase is an evolutionary conserved fat storage regulator in Drosophila.** *Cell metabolism* 2005, **1**(5):323-330.
37. Jo H, Shim J, Lee JH, Lee J, Kim JB: **IRE-1 and HSP-4 contribute to energy homeostasis via fasting-induced lipases in C. elegans.** *Cell metabolism* 2009, **9**(5):440-448.
38. Suzuki M, Shinohara Y, Ohsaki Y, Fujimoto T: **Lipid droplets: size matters.** *Journal of electron microscopy* 2011, **60 Suppl 1**:S101-116.
39. Cocchiari JL, Kumar Y, Fischer ER, Hackstadt T, Valdivia RH: **Cytoplasmic lipid droplets are translocated into the lumen of the Chlamydia trachomatis parasitophorous vacuole.** *Proceedings of the National Academy of Sciences of the United States of America* 2008, **105**(27):9379-9384.
40. Herker E, Ott M: **Unique ties between hepatitis C virus replication and intracellular lipids.** *Trends in endocrinology and metabolism: TEM* 2011, **22**(6):241-248.
41. Camus G, Herker E, Modi AA, Haas JT, Ramage HR, Farese RV, Jr., Ott M: **Diacylglycerol glycerol acyltransferase-1 localizes hepatitis C virus NS5A protein to lipid droplets and enhances NS5A interaction with the viral capsid core.** *The Journal of biological chemistry* 2013.
42. Samsa MM, Mondotte JA, Iglesias NG, Assuncao-Miranda I, Barbosa-Lima G, Da Poian AT, Bozza PT, Gamarnik AV: **Dengue virus capsid protein usurps lipid droplets for viral particle formation.** *PLoS pathogens* 2009, **5**(10):e1000632.
43. Carvalho FA, Carneiro FA, Martins IC, Assuncao-Miranda I, Faustino AF, Pereira RM, Bozza PT, Castanho MA, Mohana-Borges R, Da Poian AT *et al*: **Dengue virus capsid protein binding to hepatic lipid droplets (LD) is potassium ion dependent and is mediated by LD surface proteins.** *Journal of virology* 2012, **86**(4):2096-2108.
44. Martins IC, Gomes-Neto F, Faustino AF, Carvalho FA, Carneiro FA, Bozza PT, Mohana-Borges R, Castanho MA, Almeida FC, Santos NC *et al*: **The disordered N-terminal region of dengue virus capsid protein contains a lipid-droplet-binding motif.** *The Biochemical journal* 2012, **444**(3):405-415.
45. Cole NB, Murphy DD, Grider T, Rueter S, Brasaemle D, Nussbaum RL: **Lipid droplet binding and oligomerization properties of the Parkinson's disease protein alpha-synuclein.** *The Journal of biological chemistry* 2002, **277**(8):6344-6352.
46. Ohsaki Y, Cheng J, Fujita A, Tokumoto T, Fujimoto T: **Cytoplasmic lipid droplets are sites of convergence of proteasomal and autophagic degradation of apolipoprotein B.** *Molecular biology of the cell* 2006, **17**(6):2674-2683.
47. Ohsaki Y, Cheng J, Suzuki M, Fujita A, Fujimoto T: **Lipid droplets are arrested in the ER membrane by tight binding of lipidated apolipoprotein B-100.** *Journal of cell science* 2008, **121**(Pt 14):2415-2422.
48. Li Z, Thiel K, Thul PJ, Beller M, Kuhnlein RP, Welte MA: **Lipid droplets control the maternal histone supply of Drosophila embryos.** *Current biology : CB* 2012, **22**(22):2104-2113.
49. Anand P, Cermelli S, Li Z, Kassan A, Bosch M, Sigua R, Huang L, Ouellette AJ, Pol A, Welte MA *et al*: **A novel role for lipid droplets in the organismal antibacterial response.** *eLife* 2012, **1**:e000003.
50. Kent C: **Eukaryotic phospholipid biosynthesis.** *Annual review of biochemistry* 1995, **64**:315-343.

51. Aoyama C, Nakashima K, Ishidate K: **Molecular cloning of mouse choline kinase and choline/ethanolamine kinase: their sequence comparison to the respective rat homologs.** *Biochimica et biophysica acta* 1998, **1393**(1):179-185.
52. Kalmar GB, Kay RJ, Lachance A, Aebersold R, Cornell RB: **Cloning and expression of rat liver CTP: phosphocholine cytidyltransferase: an amphipathic protein that controls phosphatidylcholine synthesis.** *Proceedings of the National Academy of Sciences of the United States of America* 1990, **87**(16):6029-6033.
53. Henneberry AL, Wistow G, McMaster CR: **Cloning, genomic organization, and characterization of a human cholinephosphotransferase.** *The Journal of biological chemistry* 2000, **275**(38):29808-29815.
54. Hjelmstad RH, Bell RM: **Mutants of *Saccharomyces cerevisiae* defective in sn-1,2-diacylglycerol cholinephosphotransferase. Isolation, characterization, and cloning of the CPT1 gene.** *The Journal of biological chemistry* 1987, **262**(8):3909-3917.
55. Tsukagoshi Y, Nikawa J, Yamashita S: **Molecular cloning and characterization of the gene encoding cholinephosphate cytidyltransferase in *Saccharomyces cerevisiae*.** *European journal of biochemistry / FEBS* 1987, **169**(3):477-486.
56. Hosaka K, Kodaki T, Yamashita S: **Cloning and characterization of the yeast CKI gene encoding choline kinase and its expression in *Escherichia coli*.** *The Journal of biological chemistry* 1989, **264**(4):2053-2059.
57. Sohlenkamp C, Lopez-Lara IM, Geiger O: **Biosynthesis of phosphatidylcholine in bacteria.** *Progress in lipid research* 2003, **42**(2):115-162.
58. Dewey RE, Wilson RF, Novitzky WP, Goode JH: **The AAPT1 gene of soybean complements a cholinephosphotransferase-deficient mutant of yeast.** *The Plant cell* 1994, **6**(10):1495-1507.
59. Nishida I, Swinhoe R, Slabas AR, Murata N: **Cloning of *Brassica napus* CTP: phosphocholine cytidyltransferase cDNAs by complementation in a yeast cct mutant.** *Plant molecular biology* 1996, **31**(2):205-211.
60. Lochnit G, Geyer R: **Evidence for the presence of the Kennedy and Bremer-Greenberg pathways in *Caenorhabditis elegans*.** *Acta biochimica Polonica* 2003, **50**(4):1239-1243.
61. Kennedy EP, Weiss SB: **The function of cytidine coenzymes in the biosynthesis of phospholipides.** *The Journal of biological chemistry* 1956, **222**(1):193-214.
62. Weiss SB, Smith SW, Kennedy EP: **The enzymatic formation of lecithin from cytidine diphosphate choline and D-1,2-diglyceride.** *The Journal of biological chemistry* 1958, **231**(1):53-64.
63. Bremer J, Greenberg DM: **Mono- and dimethylethanolamine isolated from rat-liver phospholipids.** *Biochimica et biophysica acta* 1959, **35**:287-288.
64. Vance DE, Ridgway ND: **The methylation of phosphatidylethanolamine.** *Progress in lipid research* 1988, **27**(1):61-79.
65. Kanipes MI, Henry SA: **The phospholipid methyltransferases in yeast.** *Biochimica et biophysica acta* 1997, **1348**(1-2):134-141.
66. Vance DE, Walkey CJ, Cui Z: **Phosphatidylethanolamine N-methyltransferase from liver.** *Biochimica et biophysica acta* 1997, **1348**(1-2):142-150.
67. Nuccio ML, Ziemak MJ, Henry SA, Weretilnyk EA, Hanson AD: **cDNA cloning of phosphoethanolamine N-methyltransferase from spinach by complementation in *Schizosaccharomyces pombe* and characterization of the recombinant enzyme.** *The Journal of biological chemistry* 2000, **275**(19):14095-14101.
68. Charron JB, Breton G, Danyluk J, Muzac I, Ibrahim RK, Sarhan F: **Molecular and biochemical characterization of a cold-regulated phosphoethanolamine N-methyltransferase from wheat.** *Plant physiology* 2002, **129**(1):363-373.
69. Brendza KM, Haakenson W, Cahoon RE, Hicks LM, Palavalli LH, Chiapelli BJ, McLaird M, McCarter JP, Williams DJ, Hresko MC *et al*: **Phosphoethanolamine N-methyltransferase (PMT-1) catalyses the first reaction of a new pathway for phosphocholine biosynthesis in *Caenorhabditis elegans*.** *The Biochemical journal* 2007, **404**(3):439-448.

70. Palavalli LH, Brendza KM, Haakenson W, Cahoon RE, McLaird M, Hicks LM, McCarter JP, Williams DJ, Hresko MC, Jez JM: **Defining the role of phosphomethylethanolamine N-methyltransferase from *Caenorhabditis elegans* in phosphocholine biosynthesis by biochemical and kinetic analysis.** *Biochemistry* 2006, **45**(19):6056-6065.
71. Guo Y, Walther TC, Rao M, Stuurman N, Goshima G, Terayama K, Wong JS, Vale RD, Walter P, Farese RV: **Functional genomic screen reveals genes involved in lipid-droplet formation and utilization.** *Nature* 2008, **453**(7195):657-661.
72. Fei W, Shui G, Zhang Y, Krahmer N, Ferguson C, Kapterian TS, Lin RC, Dawes IW, Brown AJ, Li P *et al*: **A role for phosphatidic acid in the formation of "supersized" lipid droplets.** *PLoS genetics* 2011, **7**(7):e1002201.
73. Lu SC, Alvarez L, Huang ZZ, Chen L, An W, Corrales FJ, Avila MA, Kanel G, Mato JM: **Methionine adenosyltransferase 1A knockout mice are predisposed to liver injury and exhibit increased expression of genes involved in proliferation.** *Proceedings of the National Academy of Sciences of the United States of America* 2001, **98**(10):5560-5565.
74. Ashrafi K, Chang FY, Watts JL, Fraser AG, Kamath RS, Ahringer J, Ruvkun G: **Genome-wide RNAi analysis of *Caenorhabditis elegans* fat regulatory genes.** *Nature* 2003, **421**(6920):268-272.
75. Mak HY, Nelson LS, Basson M, Johnson CD, Ruvkun G: **Polygenic control of *Caenorhabditis elegans* fat storage.** *Nature genetics* 2006, **38**(3):363-368.
76. Jones KT, Ashrafi K: ***Caenorhabditis elegans* as an emerging model for studying the basic biology of obesity.** *Disease models & mechanisms* 2009, **2**(5-6):224-229.
77. Sze JY, Victor M, Loer C, Shi Y, Ruvkun G: **Food and metabolic signalling defects in a *Caenorhabditis elegans* serotonin-synthesis mutant.** *Nature* 2000, **403**(6769):560-564.
78. Srinivasan S, Sadegh L, Elle IC, Christensen AG, Faergeman NJ, Ashrafi K: **Serotonin regulates *C. elegans* fat and feeding through independent molecular mechanisms.** *Cell metabolism* 2008, **7**(6):533-544.
79. Kimura KD, Tissenbaum HA, Liu Y, Ruvkun G: ***daf-2*, an insulin receptor-like gene that regulates longevity and diapause in *Caenorhabditis elegans*.** *Science* 1997, **277**(5328):942-946.
80. Greer ER, Perez CL, Van Gilst MR, Lee BH, Ashrafi K: **Neural and molecular dissection of a *C. elegans* sensory circuit that regulates fat and feeding.** *Cell metabolism* 2008, **8**(2):118-131.
81. Soukas AA, Kane EA, Carr CE, Melo JA, Ruvkun G: **Rictor/TORC2 regulates fat metabolism, feeding, growth, and life span in *Caenorhabditis elegans*.** *Genes & development* 2009, **23**(4):496-511.
82. Jones KT, Greer ER, Pearce D, Ashrafi K: **Rictor/TORC2 regulates *Caenorhabditis elegans* fat storage, body size, and development through *sgk-1*.** *PLoS biology* 2009, **7**(3):e60.
83. Yang F, Vought BW, Satterlee JS, Walker AK, Jim Sun ZY, Watts JL, DeBeaumont R, Saito RM, Hyberts SG, Yang S *et al*: **An ARC/Mediator subunit required for SREBP control of cholesterol and lipid homeostasis.** *Nature* 2006, **442**(7103):700-704.
84. Van Gilst MR, Hadjivassiliou H, Jolly A, Yamamoto KR: **Nuclear hormone receptor NHR-49 controls fat consumption and fatty acid composition in *C. elegans*.** *PLoS biology* 2005, **3**(2):e53.
85. Van Gilst MR, Hadjivassiliou H, Yamamoto KR: **A *Caenorhabditis elegans* nutrient response system partially dependent on nuclear receptor NHR-49.** *Proceedings of the National Academy of Sciences of the United States of America* 2005, **102**(38):13496-13501.
86. Klapper M, Ehmke M, Palgunow D, Bohme M, Matthaus C, Bergner G, Dietzek B, Popp J, Doring F: **Fluorescence-based fixative and vital staining of lipid droplets in *Caenorhabditis elegans* reveal fat stores using microscopy and flow cytometry approaches.** *Journal of lipid research* 2011, **52**(6):1281-1293.

87. Le TT, Duren HM, Slipchenko MN, Hu CD, Cheng JX: **Label-free quantitative analysis of lipid metabolism in living *Caenorhabditis elegans***. *Journal of lipid research* 2010, **51**(3):672-677.
88. Yen K, Le TT, Bansal A, Narasimhan SD, Cheng JX, Tissenbaum HA: **A comparative study of fat storage quantitation in nematode *Caenorhabditis elegans* using label and label-free methods**. *PloS one* 2010, **5**(9).
89. Wang MC, Min W, Freudiger CW, Ruvkun G, Xie XS: **RNAi screening for fat regulatory genes with SRS microscopy**. *Nature methods* 2011, **8**(2):135-138.
90. Spanier B, Lasch K, Marsch S, Benner J, Liao W, Hu H, Kienberger H, Eisenreich W, Daniel H: **How the intestinal peptide transporter PEPT-1 contributes to an obesity phenotype in *Caenorhabditis elegans***. *PloS one* 2009, **4**(7):e6279.
91. Benner J, Daniel H, Spanier B: **A glutathione peroxidase, intracellular peptidases and the TOR complexes regulate peptide transporter PEPT-1 in *C. elegans***. *PloS one* 2011, **6**(9):e25624.
92. Mullaney BC, Blind RD, Lemieux GA, Perez CL, Elle IC, Faergeman NJ, Van Gilst MR, Ingraham HA, Ashrafi K: **Regulation of *C. elegans* fat uptake and storage by acyl-CoA synthase-3 is dependent on NR5A family nuclear hormone receptor *nhr-25***. *Cell metabolism* 2010, **12**(4):398-410.
93. Elle IC, Simonsen KT, Olsen LC, Birck PK, Ehmsen S, Tuck S, Le TT, Faergeman NJ: **Tissue- and paralogue-specific functions of acyl-CoA-binding proteins in lipid metabolism in *Caenorhabditis elegans***. *The Biochemical journal* 2011, **437**(2):231-241.
94. Xu M, Joo HJ, Paik YK: **Novel functions of lipid-binding protein 5 in *Caenorhabditis elegans* fat metabolism**. *The Journal of biological chemistry* 2011, **286**(32):28111-28118.
95. Zhang J, Yang C, Brey C, Rodriguez M, Oksov Y, Gaugler R, Dickstein E, Huang CH, Hashmi S: **Mutation in *Caenorhabditis elegans* Kruppel-like factor, KLF-3 results in fat accumulation and alters fatty acid composition**. *Experimental cell research* 2009, **315**(15):2568-2580.
96. Zhang J, Bakheet R, Parhar RS, Huang CH, Hussain MM, Pan X, Siddiqui SS, Hashmi S: **Regulation of fat storage and reproduction by Kruppel-like transcription factor KLF3 and fat-associated genes in *Caenorhabditis elegans***. *Journal of molecular biology* 2011, **411**(3):537-553.
97. Hashmi S, Zhang J, Siddiqui SS, Parhar RS, Bakheet R, Al-Mohanna F: **Partner in fat metabolism: role of KLFs in fat burning and reproductive behavior**. *3 Biotech* 2011, **1**(2):59-72.
98. Zhang SO, Box AC, Xu N, Le Men J, Yu J, Guo F, Trimble R, Mak HY: **Genetic and dietary regulation of lipid droplet expansion in *Caenorhabditis elegans***. *Proceedings of the National Academy of Sciences of the United States of America* 2010, **107**(10):4640-4645.
99. Joo HJ, Yim YH, Jeong PY, Jin YX, Lee JE, Kim H, Jeong SK, Chitwood DJ, Paik YK: ***Caenorhabditis elegans* utilizes dauer pheromone biosynthesis to dispose of toxic peroxisomal fatty acids for cellular homeostasis**. *The Biochemical journal* 2009, **422**(1):61-71.
100. Walker AK, Jacobs RL, Watts JL, Rottiers V, Jiang K, Finnegan DM, Shioda T, Hansen M, Yang F, Niebergall LJ *et al*: **A conserved SREBP-1/phosphatidylcholine feedback circuit regulates lipogenesis in metazoans**. *Cell* 2011, **147**(4):840-852.
101. Li Y, Na K, Lee HJ, Lee EY, Paik YK: **Contribution of *sams-1* and *pmt-1* to lipid homeostasis in adult *Caenorhabditis elegans***. *Journal of biochemistry* 2011, **149**(5):529-538.
102. Zhang Y, Zou X, Ding Y, Wang H, Wu X, Liang B: **Comparative genomics and functional study of lipid metabolic genes in *Caenorhabditis elegans***. *BMC genomics* 2013, **14**:164.
103. Lee HC, Inoue T, Imae R, Kono N, Shirae S, Matsuda S, Gengyo-Ando K, Mitani S, Arai H: ***Caenorhabditis elegans mboa-7*, a member of the MBOAT family, is**

- required for selective incorporation of polyunsaturated fatty acids into phosphatidylinositol. *Molecular biology of the cell* 2008, **19**(3):1174-1184.
104. Wollam J, Magner DB, Magomedova L, Rass E, Shen Y, Rottiers V, Habermann B, Cummins CL, Antebi A: **A novel 3-hydroxysteroid dehydrogenase that regulates reproductive development and longevity.** *PLoS biology* 2012, **10**(4):e1001305.
105. Entchev EV, Schwudke D, Zagorij V, Matyash V, Bogdanova A, Habermann B, Zhu L, Shevchenko A, Kurzchalia TV: **LET-767 is required for the production of branched chain and long chain fatty acids in *Caenorhabditis elegans*.** *The Journal of biological chemistry* 2008, **283**(25):17550-17560.
106. Lykidis A: **Comparative genomics and evolution of eukaryotic phospholipid biosynthesis.** *Progress in lipid research* 2007, **46**(3-4):171-199.
107. Golden A, Liu J, Cohen-Fix O: **Inactivation of the *C. elegans* lipin homolog leads to ER disorganization and to defects in the breakdown and reassembly of the nuclear envelope.** *Journal of cell science* 2009, **122**(Pt 12):1970-1978.
108. Gorjanacz M, Mattaj IW: **Lipin is required for efficient breakdown of the nuclear envelope in *Caenorhabditis elegans*.** *Journal of cell science* 2009, **122**(Pt 12):1963-1969.
109. Deng X, Yin X, Allan R, Lu DD, Maurer CW, Haimovitz-Friedman A, Fuks Z, Shaham S, Kolesnick R: **Ceramide biogenesis is required for radiation-induced apoptosis in the germ line of *C. elegans*.** *Science* 2008, **322**(5898):110-115.
110. Kniazeva M, Shen H, Euler T, Wang C, Han M: **Regulation of maternal phospholipid composition and IP(3)-dependent embryonic membrane dynamics by a specific fatty acid metabolic event in *C. elegans*.** *Genes & development* 2012, **26**(6):554-566.
111. Watts JL, Browse J: **Genetic dissection of polyunsaturated fatty acid synthesis in *Caenorhabditis elegans*.** *Proceedings of the National Academy of Sciences of the United States of America* 2002, **99**(9):5854-5859.
112. Watts JL, Browse J: **A palmitoyl-CoA-specific delta9 fatty acid desaturase from *Caenorhabditis elegans*.** *Biochemical and biophysical research communications* 2000, **272**(1):263-269.
113. Brock TJ, Browse J, Watts JL: **Genetic regulation of unsaturated fatty acid composition in *C. elegans*.** *PLoS genetics* 2006, **2**(7):e108.
114. Brock TJ, Browse J, Watts JL: **Fatty acid desaturation and the regulation of adiposity in *Caenorhabditis elegans*.** *Genetics* 2007, **176**(2):865-875.
115. Brenner S: **The genetics of *Caenorhabditis elegans*.** *Genetics* 1974, **77**(1):71-94.
116. Stienagle T: **Maintenance of *C. elegans*.** In: *C elegans A Practical Approach*. Edited by Hope IA. New York, USA: Oxford University Press; 2005: 51-67.
117. Jorgensen EM, Mango SE: **The art and design of genetic screens: *caenorhabditis elegans*.** *Nature reviews Genetics* 2002, **3**(5):356-369.
118. Stienagle T: **Maintenance of *C. elegans*.** In: *C elegans A Practical Approach*. Edited by Hope IA. New York, USA: Oxford University Press; 2005: 59-60.
119. Doitsidou M, Poole RJ, Sarin S, Bigelow H, Hobert O: ***C. elegans* mutant identification with a one-step whole-genome-sequencing and SNP mapping strategy.** *PLoS one* 2010, **5**(11):e15435.
120. Minevich G, Park DS, Blankenberg D, Poole RJ, Hobert O: **CloudMap: a cloud-based pipeline for analysis of mutant genome sequences.** *Genetics* 2012, **192**(4):1249-1269.
121. Davis MW, Hammarlund M, Harrach T, Hullett P, Olsen S, Jorgensen EM: **Rapid single nucleotide polymorphism mapping in *C. elegans*.** *BMC genomics* 2005, **6**:118.
122. Wicks SR, Yeh RT, Gish WR, Waterston RH, Plasterk RH: **Rapid gene mapping in *Caenorhabditis elegans* using a high density polymorphism map.** *Nature genetics* 2001, **28**(2):160-164.
123. Knight CG, Patel MN, Azevedo RB, Leroi AM: **A novel mode of ecdysozoan growth in *Caenorhabditis elegans*.** *Evolution & development* 2002, **4**(1):16-27.

124. Salomon MP, Ostrow D, Phillips N, Blanton D, Bour W, Keller TE, Levy L, Sylvestre T, Upadhyay A, Baer CF: **Comparing mutational and standing genetic variability for fitness and size in *Caenorhabditis briggsae* and *C. elegans*.** *Genetics* 2009, **183**(2):685-692, 681SI-619SI.
125. Matyash V, Liebisch G, Kurzchalia TV, Shevchenko A, Schwudke D: **Lipid extraction by methyl-tert-butyl ether for high-throughput lipidomics.** *Journal of lipid research* 2008, **49**(5):1137-1146.
126. Palgunow D, Klapper M, Doring F: **Dietary restriction during development enlarges intestinal and hypodermal lipid droplets in *Caenorhabditis elegans*.** *PloS one* 2012, **7**(11):e46198.
127. Lee EY, Jeong PY, Kim SY, Shim YH, Chitwood DJ, Paik YK: **Effects of sterols on the development and aging of *Caenorhabditis elegans*.** *Methods Mol Biol* 2009, **462**:167-179.
128. Bolte S, Cordelieres FP: **A guided tour into subcellular colocalization analysis in light microscopy.** *Journal of microscopy* 2006, **224**(Pt 3):213-232.
129. Schneider CA, Rasband WS, Eliceiri KW: **NIH Image to ImageJ: 25 years of image analysis.** *Nature methods* 2012, **9**(7):671-675.
130. Kamath RS, Ahringer J: **Genome-wide RNAi screening in *Caenorhabditis elegans*.** *Methods* 2003, **30**(4):313-321.
131. Miller DL, Roth MB: ***C. elegans* are protected from lethal hypoxia by an embryonic diapause.** *Current biology : CB* 2009, **19**(14):1233-1237.
132. Venselaar H, Te Beek TA, Kuipers RK, Hekkelman ML, Vriend G: **Protein structure analysis of mutations causing inheritable diseases. An e-Science approach with life scientist friendly interfaces.** *BMC bioinformatics* 2010, **11**:548.
133. Lyu PC, Sherman JC, Chen A, Kallenbach NR: **Alpha-helix stabilization by natural and unnatural amino acids with alkyl side chains.** *Proceedings of the National Academy of Sciences of the United States of America* 1991, **88**(12):5317-5320.
134. Watanabe T, Hirano S: **Metabolism of arsenic and its toxicological relevance.** *Archives of toxicology* 2012.
135. Beatty PW, Reed DJ: **Involvement of the cystathionine pathway in the biosynthesis of glutathione by isolated rat hepatocytes.** *Archives of biochemistry and biophysics* 1980, **204**(1):80-87.
136. Mosharov E, Cranford MR, Banerjee R: **The quantitatively important relationship between homocysteine metabolism and glutathione synthesis by the transsulfuration pathway and its regulation by redox changes.** *Biochemistry* 2000, **39**(42):13005-13011.
137. Vitvitsky V, Dayal S, Stabler S, Zhou Y, Wang H, Lentz SR, Banerjee R: **Perturbations in homocysteine-linked redox homeostasis in a murine model for hyperhomocysteinemia.** *American journal of physiology Regulatory, integrative and comparative physiology* 2004, **287**(1):R39-46.
138. Chiang PK, Gordon RK, Tal J, Zeng GC, Doctor BP, Pardhasaradhi K, McCann PP: **S-Adenosylmethionine and methylation.** *FASEB journal : official publication of the Federation of American Societies for Experimental Biology* 1996, **10**(4):471-480.
139. Fontecave M, Atta M, Mulliez E: **S-adenosylmethionine: nothing goes to waste.** *Trends in biochemical sciences* 2004, **29**(5):243-249.
140. Grillo MA, Colombatto S: **S-adenosylmethionine and its products.** *Amino acids* 2008, **34**(2):187-193.
141. Roje S: **S-Adenosyl-L-methionine: beyond the universal methyl group donor.** *Phytochemistry* 2006, **67**(15):1686-1698.
142. Vance DE, Li Z, Jacobs RL: **Hepatic phosphatidylethanolamine N-methyltransferase, unexpected roles in animal biochemistry and physiology.** *The Journal of biological chemistry* 2007, **282**(46):33237-33241.
143. Leber R, Zinser E, Zellnig G, Paltauf F, Daum G: **Characterization of lipid particles of the yeast, *Saccharomyces cerevisiae*.** *Yeast* 1994, **10**(11):1421-1428.
144. Chitraju C, Trotschmuller M, Hartler J, Wolinski H, Thallinger GG, Lass A, Zechner R, Zimmermann R, Kofeler HC, Spener F: **Lipidomic analysis of lipid droplets from**

- murine hepatocytes reveals distinct signatures for nutritional stress.** *Journal of lipid research* 2012, **53**(10):2141-2152.
145. McKay RM, McKay JP, Avery L, Graff JM: **C elegans: a model for exploring the genetics of fat storage.** *Developmental cell* 2003, **4**(1):131-142.
146. Cantoni GL: **Biological methylation: selected aspects.** *Annual review of biochemistry* 1975, **44**:435-451.
147. Kotb M, Geller AM: **Methionine adenosyltransferase: structure and function.** *Pharmacology & therapeutics* 1993, **59**(2):125-143.
148. Mato JM, Alvarez L, Ortiz P, Pajares MA: **S-adenosylmethionine synthesis: molecular mechanisms and clinical implications.** *Pharmacology & therapeutics* 1997, **73**(3):265-280.
149. Bowman WH, Tabor CW, Tabor H: **Spermidine biosynthesis. Purification and properties of propylamine transferase from Escherichia coli.** *The Journal of biological chemistry* 1973, **248**(7):2480-2486.
150. Tabor CW, Tabor H: **Polyamines.** *Annual review of biochemistry* 1984, **53**:749-790.
151. Lochnit G, Bongaarts R, Geyer R: **Searching new targets for anthelmintic strategies: Interference with glycosphingolipid biosynthesis and phosphorylcholine metabolism affects development of Caenorhabditis elegans.** *International journal for parasitology* 2005, **35**(8):911-923.
152. Sundler R, Akesson B: **Regulation of phospholipid biosynthesis in isolated rat hepatocytes. Effect of different substrates.** *The Journal of biological chemistry* 1975, **250**(9):3359-3367.
153. DeLong CJ, Shen YJ, Thomas MJ, Cui Z: **Molecular distinction of phosphatidylcholine synthesis between the CDP-choline pathway and phosphatidylethanolamine methylation pathway.** *The Journal of biological chemistry* 1999, **274**(42):29683-29688.
154. Reo NV, Adinehzadeh M, Foy BD: **Kinetic analyses of liver phosphatidylcholine and phosphatidylethanolamine biosynthesis using (13)C NMR spectroscopy.** *Biochimica et biophysica acta* 2002, **1580**(2-3):171-188.
155. Carman GM, Henry SA: **Phospholipid biosynthesis in yeast.** *Annual review of biochemistry* 1989, **58**:635-669.
156. Lykidis A, Jackowski S: **Regulation of mammalian cell membrane biosynthesis.** *Progress in nucleic acid research and molecular biology* 2001, **65**:361-393.
157. Croll NA, Smith JM, Zuckerman BM: **The aging process of the nematode Caenorhabditis elegans in bacterial and axenic culture.** *Experimental aging research* 1977, **3**(3):175-189.
158. Bolanowski MA, Russell RL, Jacobson LA: **Quantitative measures of aging in the nematode Caenorhabditis elegans. I. Population and longitudinal studies of two behavioral parameters.** *Mechanisms of ageing and development* 1981, **15**(3):279-295.
159. Tamiya H, Hirota K, Takahashi Y, Daitoku H, Kaneko Y, Sakuta G, Iizuka K, Watanabe S, Ishii N, Fukamizu A: **Conserved SAMS function in regulating egg-laying in C. elegans.** *Journal of receptor and signal transduction research* 2013, **33**(1):56-62.
160. Bauer MA, Carmona-Gutierrez D, Ruckenstuhl C, Reisenbichler A, Megalou EV, Eisenberg T, Magnes C, Jungwirth H, Sinner FM, Pieber TR *et al*: **Spermidine promotes mating and fertilization efficiency in model organisms.** *Cell Cycle* 2013, **12**(2):346-352.
161. MacRae M, Kramer DL, Coffino P: **Developmental effect of polyamine depletion in Caenorhabditis elegans.** *The Biochemical journal* 1998, **333** (Pt 2):309-315.
162. Ericsson J, Jackson SM, Kim JB, Spiegelman BM, Edwards PA: **Identification of glycerol-3-phosphate acyltransferase as an adipocyte determination and differentiation factor 1- and sterol regulatory element-binding protein-responsive gene.** *The Journal of biological chemistry* 1997, **272**(11):7298-7305.
163. Lagace TA, Storey MK, Ridgway ND: **Regulation of phosphatidylcholine metabolism in Chinese hamster ovary cells by the sterol regulatory element-**

- binding protein (SREBP)/SREBP cleavage-activating protein pathway. *The Journal of biological chemistry* 2000, **275**(19):14367-14374.
164. Kast HR, Nguyen CM, Anisfeld AM, Ericsson J, Edwards PA: **CTP:phosphocholine cytidyltransferase, a new sterol- and SREBP-responsive gene.** *Journal of lipid research* 2001, **42**(8):1266-1272.
165. van der Veen JN, Lingrell S, Vance DE: **The membrane lipid phosphatidylcholine is an unexpected source of triacylglycerol in the liver.** *The Journal of biological chemistry* 2012, **287**(28):23418-23426.
166. Igal RA, Caviglia JM, de Gomez Dumm IN, Coleman RA: **Diacylglycerol generated in CHO cell plasma membrane by phospholipase C is used for triacylglycerol synthesis.** *Journal of lipid research* 2001, **42**(1):88-95.
167. Bagnato C, Igal RA: **Overexpression of diacylglycerol acyltransferase-1 reduces phospholipid synthesis, proliferation, and invasiveness in simian virus 40-transformed human lung fibroblasts.** *The Journal of biological chemistry* 2003, **278**(52):52203-52211.
168. Rinella ME, Green RM: **The methionine-choline deficient dietary model of steatohepatitis does not exhibit insulin resistance.** *Journal of hepatology* 2004, **40**(1):47-51.
169. Rinella ME, Elias MS, Smolak RR, Fu T, Borensztajn J, Green RM: **Mechanisms of hepatic steatosis in mice fed a lipogenic methionine choline-deficient diet.** *Journal of lipid research* 2008, **49**(5):1068-1076.
170. Zeisel SH, Da Costa KA, Franklin PD, Alexander EA, Lamont JT, Sheard NF, Beiser A: **Choline, an essential nutrient for humans.** *FASEB journal : official publication of the Federation of American Societies for Experimental Biology* 1991, **5**(7):2093-2098.
171. Buchman AL, Dubin MD, Moukarzel AA, Jenden DJ, Roch M, Rice KM, Gornbein J, Ament ME: **Choline deficiency: a cause of hepatic steatosis during parenteral nutrition that can be reversed with intravenous choline supplementation.** *Hepatology* 1995, **22**(5):1399-1403.
172. Jacobs RL, Devlin C, Tabas I, Vance DE: **Targeted deletion of hepatic CTP:phosphocholine cytidyltransferase alpha in mice decreases plasma high density and very low density lipoproteins.** *The Journal of biological chemistry* 2004, **279**(45):47402-47410.
173. Caviglia JM, De Gomez Dumm IN, Coleman RA, Igal RA: **Phosphatidylcholine deficiency upregulates enzymes of triacylglycerol metabolism in CHO cells.** *Journal of lipid research* 2004, **45**(8):1500-1509.
174. Stals HK, Mannaerts GP, Declercq PE: **Factors influencing triacylglycerol synthesis in permeabilized rat hepatocytes.** *The Biochemical journal* 1992, **283** (Pt 3):719-725.
175. Waite KA, Vance DE: **Why expression of phosphatidylethanolamine N-methyltransferase does not rescue Chinese hamster ovary cells that have an impaired CDP-choline pathway.** *The Journal of biological chemistry* 2000, **275**(28):21197-21202.
176. Jackowski S, Wang J, Baburina I: **Activity of the phosphatidylcholine biosynthetic pathway modulates the distribution of fatty acids into glycerolipids in proliferating cells.** *Biochimica et biophysica acta* 2000, **1483**(3):301-315.
177. Nomura T, Horikawa M, Shimamura S, Hashimoto T, Sakamoto K: **Fat accumulation in *Caenorhabditis elegans* is mediated by SREBP homolog SBP-1.** *Genes & nutrition* 2010, **5**(1):17-27.
178. Osborne TF, Espenshade PJ: **Evolutionary conservation and adaptation in the mechanism that regulates SREBP action: what a long, strange tRIP it's been.** *Genes & development* 2009, **23**(22):2578-2591.
179. Hubbard EJAG, D.: **Introduction to the germ line.** In: *WormBook*. Edited by Community TCeR; 2005.
180. Moessinger C, Kuerschner L, Spandl J, Shevchenko A, Thiele C: **Human lysophosphatidylcholine acyltransferases 1 and 2 are located in lipid droplets**

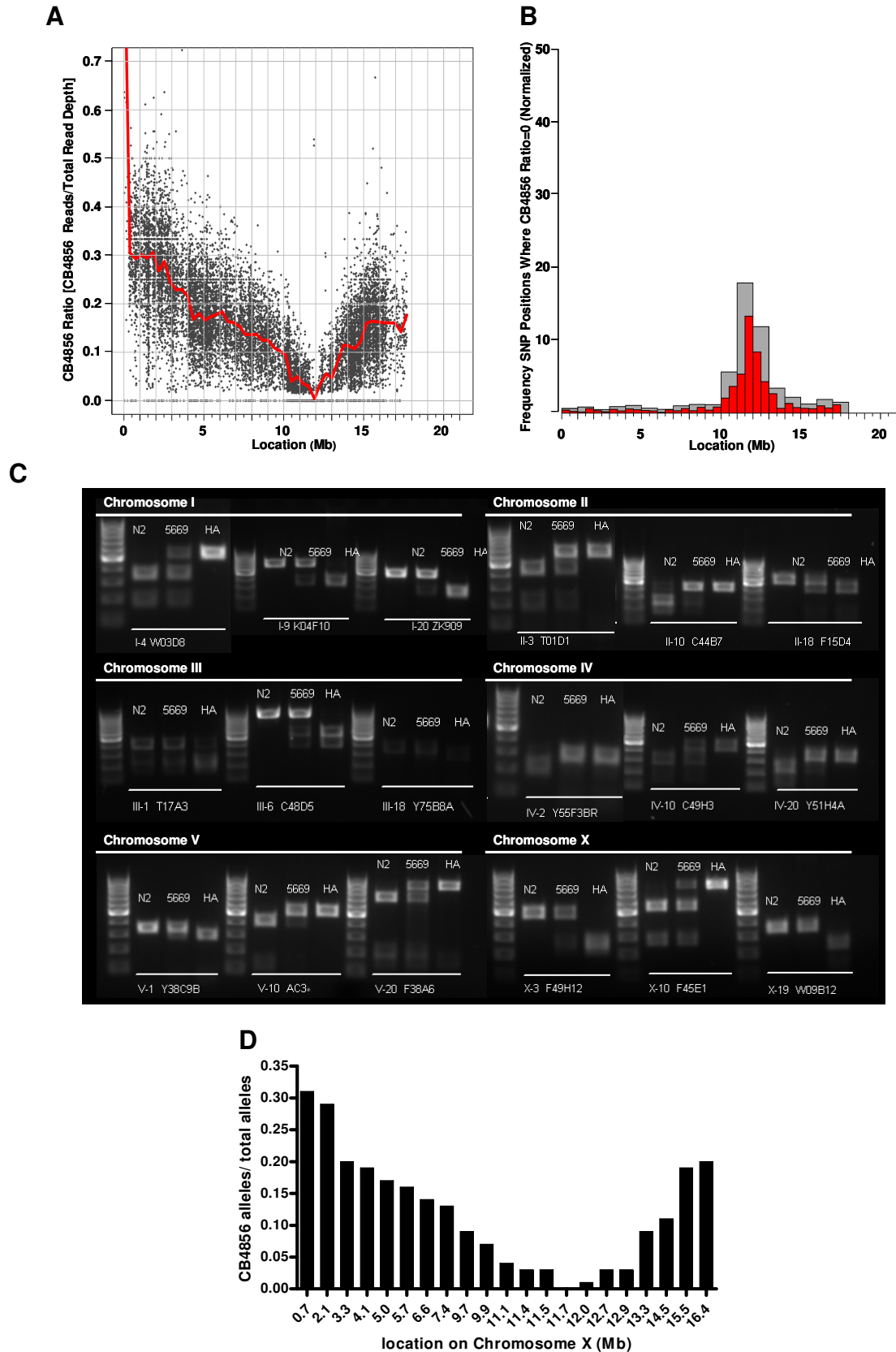
- where they catalyze the formation of phosphatidylcholine. *The Journal of biological chemistry* 2011, **286**(24):21330-21339.
181. Bostrom P, Rutberg M, Ericsson J, Holmdahl P, Andersson L, Frohman MA, Boren J, Olofsson SO: **Cytosolic lipid droplets increase in size by microtubule-dependent complex formation.** *Arteriosclerosis, thrombosis, and vascular biology* 2005, **25**(9):1945-1951.
182. Stone SJ, Levin MC, Zhou P, Han J, Walther TC, Farese RV, Jr.: **The endoplasmic reticulum enzyme DGAT2 is found in mitochondria-associated membranes and has a mitochondrial targeting signal that promotes its association with mitochondria.** *The Journal of biological chemistry* 2009, **284**(8):5352-5361.
183. Fei W, Shui G, Gaeta B, Du X, Kuerschner L, Li P, Brown AJ, Wenk MR, Parton RG, Yang H: **Fld1p, a functional homologue of human seipin, regulates the size of lipid droplets in yeast.** *The Journal of cell biology* 2008, **180**(3):473-482.
184. Gong J, Sun Z, Wu L, Xu W, Schieber N, Xu D, Shui G, Yang H, Parton RG, Li P: **Fsp27 promotes lipid droplet growth by lipid exchange and transfer at lipid droplet contact sites.** *The Journal of cell biology* 2011, **195**(6):953-963.
185. Penno A, Hackenbroich G, Thiele C: **Phospholipids and lipid droplets.** *Biochimica et biophysica acta* 2013, **1831**(3):589-594.
186. Murphy S, Martin S, Parton RG: **Quantitative analysis of lipid droplet fusion: inefficient steady state fusion but rapid stimulation by chemical fusogens.** *PLoS one* 2010, **5**(12):e15030.
187. Zechner R, Zimmermann R, Eichmann TO, Kohlwein SD, Haemmerle G, Lass A, Madeo F: **FAT SIGNALS--lipases and lipolysis in lipid metabolism and signaling.** *Cell metabolism* 2012, **15**(3):279-291.
188. Beller M, Riedel D, Jansch L, Dieterich G, Wehland J, Jackle H, Kuhnlein RP: **Characterization of the Drosophila lipid droplet subproteome.** *Molecular & cellular proteomics : MCP* 2006, **5**(6):1082-1094.
189. Fei W, Zhong L, Ta MT, Shui G, Wenk MR, Yang H: **The size and phospholipid composition of lipid droplets can influence their proteome.** *Biochemical and biophysical research communications* 2011, **415**(3):455-462.
190. Dagenais GR, Tancredi RG, Zierler KL: **Free fatty acid oxidation by forearm muscle at rest, and evidence for an intramuscular lipid pool in the human forearm.** *The Journal of clinical investigation* 1976, **58**(2):421-431.
191. Kanaley JA, Shadid S, Sheehan MT, Guo Z, Jensen MD: **Relationship between plasma free fatty acid, intramyocellular triglycerides and long-chain acylcarnitines in resting humans.** *The Journal of physiology* 2009, **587**(Pt 24):5939-5950.
192. Gibbons GF, Islam K, Pease RJ: **Mobilisation of triacylglycerol stores.** *Biochimica et biophysica acta* 2000, **1483**(1):37-57.
193. Mudd SH, Ebert MH, Scriver CR: **Labile methyl group balances in the human: the role of sarcosine.** *Metabolism: clinical and experimental* 1980, **29**(8):707-720.
194. Mudd SH, Poole JR: **Labile methyl balances for normal humans on various dietary regimens.** *Metabolism: clinical and experimental* 1975, **24**(6):721-735.
195. Browning JD, Horton JD: **Molecular mediators of hepatic steatosis and liver injury.** *The Journal of clinical investigation* 2004, **114**(2):147-152.
196. Farrell GC, Larter CZ: **Nonalcoholic fatty liver disease: from steatosis to cirrhosis.** *Hepatology* 2006, **43**(2 Suppl 1):S99-S112.
197. Martinez-Chantar ML, Corrales FJ, Martinez-Cruz LA, Garcia-Trevijano ER, Huang ZZ, Chen L, Kanel G, Avila MA, Mato JM, Lu SC: **Spontaneous oxidative stress and liver tumors in mice lacking methionine adenosyltransferase 1A.** *FASEB journal : official publication of the Federation of American Societies for Experimental Biology* 2002, **16**(10):1292-1294.
198. Cano A, Buque X, Martinez-Una M, Aurrekoetxea I, Menor A, Garcia-Rodriguez JL, Lu SC, Martinez-Chantar ML, Mato JM, Ochoa B *et al*: **Methionine adenosyltransferase 1A gene deletion disrupts hepatic very low-density lipoprotein assembly in mice.** *Hepatology* 2011, **54**(6):1975-1986.

199. Mato JM, Martinez-Chantar ML, Lu SC: **Methionine metabolism and liver disease.** *Annual review of nutrition* 2008, **28**:273-293.
200. Larter CZ, Yeh MM: **Animal models of NASH: getting both pathology and metabolic context right.** *Journal of gastroenterology and hepatology* 2008, **23**(11):1635-1648.
201. Li Z, Agellon LB, Allen TM, Umeda M, Jewell L, Mason A, Vance DE: **The ratio of phosphatidylcholine to phosphatidylethanolamine influences membrane integrity and steatohepatitis.** *Cell metabolism* 2006, **3**(5):321-331.
202. Ferre P, Fougere F: **Hepatic steatosis: a role for de novo lipogenesis and the transcription factor SREBP-1c.** *Diabetes, obesity & metabolism* 2010, **12** Suppl 2:83-92.
203. Masoro EJ: **Overview of caloric restriction and ageing.** *Mechanisms of ageing and development* 2005, **126**(9):913-922.
204. Tain LS, Lozano E, Saez AG, Leroi AM: **Dietary regulation of hypodermal polyploidization in *C. elegans*.** *BMC developmental biology* 2008, **8**:28.
205. Hansen M, Hsu AL, Dillin A, Kenyon C: **New genes tied to endocrine, metabolic, and dietary regulation of lifespan from a *Caenorhabditis elegans* genomic RNAi screen.** *PLoS genetics* 2005, **1**(1):119-128.
206. Mair W, Panowski SH, Shaw RJ, Dillin A: **Optimizing dietary restriction for genetic epistasis analysis and gene discovery in *C. elegans*.** *PloS one* 2009, **4**(2):e4535.
207. Park SK, Link CD, Johnson TE: **Life-span extension by dietary restriction is mediated by NLP-7 signaling and coelomocyte endocytosis in *C. elegans*.** *FASEB journal : official publication of the Federation of American Societies for Experimental Biology* 2010, **24**(2):383-392.
208. Castelein N, Hoogewijs D, De Vreese A, Braeckman BP, Vanfleteren JR: **Dietary restriction by growth in axenic medium induces discrete changes in the transcriptional output of genes involved in energy metabolism in *Caenorhabditis elegans*.** *Biotechnology journal* 2008, **3**(6):803-812.
209. Klass MR: **Aging in the nematode *Caenorhabditis elegans*: major biological and environmental factors influencing life span.** *Mechanisms of ageing and development* 1977, **6**(6):413-429.
210. Szewczyk NJ, Udranszky IA, Kozak E, Sunga J, Kim SK, Jacobson LA, Conley CA: **Delayed development and lifespan extension as features of metabolic lifestyle alteration in *C. elegans* under dietary restriction.** *The Journal of experimental biology* 2006, **209**(Pt 20):4129-4139.
211. Steinkraus KA, Smith ED, Davis C, Carr D, Pendergrass WR, Sutphin GL, Kennedy BK, Kaeberlein M: **Dietary restriction suppresses proteotoxicity and enhances longevity by an hsf-1-dependent mechanism in *Caenorhabditis elegans*.** *Ageing cell* 2008, **7**(3):394-404.
212. Lakowski B, Hekimi S: **The genetics of caloric restriction in *Caenorhabditis elegans*.** *Proceedings of the National Academy of Sciences of the United States of America* 1998, **95**(22):13091-13096.
213. Houthoofd K, Braeckman BP, Lenaerts I, Brys K, De Vreese A, Van Eygen S, Vanfleteren JR: **Axenic growth up-regulates mass-specific metabolic rate, stress resistance, and extends life span in *Caenorhabditis elegans*.** *Experimental gerontology* 2002, **37**(12):1371-1378.
214. Hosono R, Nishimoto S, Kuno S: **Alterations of life span in the nematode *Caenorhabditis elegans* under monoxenic culture conditions.** *Experimental gerontology* 1989, **24**(3):251-264.
215. Jiang JC, Jaruga E, Repnevskaya MV, Jazwinski SM: **An intervention resembling caloric restriction prolongs life span and retards aging in yeast.** *FASEB journal : official publication of the Federation of American Societies for Experimental Biology* 2000, **14**(14):2135-2137.
216. Austad SN: **Life extension by dietary restriction in the bowl and doily spider, *Frontinella pyramitela*.** *Experimental gerontology* 1989, **24**(1):83-92.

-
217. Stuchlikova E, Juricova-Horakova M, Deyl Z: **New aspects of the dietary effect of life prolongation in rodents. What is the role of obesity in aging?** *Experimental gerontology* 1975, **10**(2):141-144.
218. Kealy RD, Lawler DF, Ballam JM, Mantz SL, Biery DN, Greeley EH, Lust G, Segre M, Smith GK, Stowe HD: **Effects of diet restriction on life span and age-related changes in dogs.** *Journal of the American Veterinary Medical Association* 2002, **220**(9):1315-1320.
219. Ching TT, Paal AB, Mehta A, Zhong L, Hsu AL: **drr-2 encodes an eIF4H that acts downstream of TOR in diet-restriction-induced longevity of C. elegans.** *Aging cell* 2010, **9**(4):545-557.
220. Vellai T, Takacs-Vellai K, Zhang Y, Kovacs AL, Orosz L, Muller F: **Genetics: influence of TOR kinase on lifespan in C. elegans.** *Nature* 2003, **426**(6967):620.
221. Kapahi P, Zid BM, Harper T, Koslover D, Sapin V, Benzer S: **Regulation of lifespan in Drosophila by modulation of genes in the TOR signaling pathway.** *Current biology : CB* 2004, **14**(10):885-890.
222. Kaerberlein M, Powers RW, 3rd, Steffen KK, Westman EA, Hu D, Dang N, Kerr EO, Kirkland KT, Fields S, Kennedy BK: **Regulation of yeast replicative life span by TOR and Sch9 in response to nutrients.** *Science* 2005, **310**(5751):1193-1196.
223. Long X, Spycher C, Han ZS, Rose AM, Muller F, Avruch J: **TOR deficiency in C. elegans causes developmental arrest and intestinal atrophy by inhibition of mRNA translation.** *Current biology : CB* 2002, **12**(17):1448-1461.
224. Orentreich N, Matias JR, DeFelice A, Zimmerman JA: **Low methionine ingestion by rats extends life span.** *The Journal of nutrition* 1993, **123**(2):269-274.
225. Zimmerman JA, Malloy V, Krajcik R, Orentreich N: **Nutritional control of aging.** *Experimental gerontology* 2003, **38**(1-2):47-52.
226. Richie JP, Jr., Komninou D, Leutzinger Y, Kleinman W, Orentreich N, Malloy V, Zimmerman JA: **Tissue glutathione and cysteine levels in methionine-restricted rats.** *Nutrition* 2004, **20**(9):800-805.
227. Miller RA, Buehner G, Chang Y, Harper JM, Sigler R, Smith-Wheelock M: **Methionine-deficient diet extends mouse lifespan, slows immune and lens aging, alters glucose, T4, IGF-I and insulin levels, and increases hepatocyte MIF levels and stress resistance.** *Aging cell* 2005, **4**(3):119-125.

6 Supporting Information

Supporting information figure S1: Presentation of WGS/ SNP mapping data and SNP mapping data.



Presentation of data revealed by WGS/ SNP mapping and SNP mapping.

(A-B) The WGS/ SNP data are shown for chromosome X. (A) SNP loci are depicted as XY scatter plot, where the ratio of CB4856 sequence over the total number of reads for each SNP is represented. A regression line was plotted through the dots to achieve higher accuracy of the linked region. The dip represents the region that is most N2 and the thus most linked to the vacuole phenotype causing mutation. (B) A frequency plot corresponding to the dot plot (A). The frequency plot represents the frequency of SNP loci, where the ratio of Hawaiian reads over the total number of reads is equal to 0. Grey bars are 1 Mb bins, red bars are 5 Mb bins. Both bins are separately normalized for the actual frequency of Hawaiian SNP density. The peak corresponds to the dip in the regression line [119]. WGS/ SNP mapping was performed by the Oliver Hobert laboratory (Department of Biochemistry & Molecular Biophysics, Columbia University, New York, USA). (C) Agarose gels representing results for SNP chromosome mapping. For each chromosome, 3 SNPs were analyzed ranging from the left to the right arm of the respective chromosome. For each SNP, N2 sequence is represented by the left band, recombinant *t5669* sequence is shown in the middle and CB4856 sequence is represented by the right band. (D) For interval mapping, 45 F2 recombinants were analyzed for 21 snip-SNPs along the entire X chromosome. The ratio of CB4856 alleles over the total number of alleles is shown. Interval mapping is in accordance with WGS/ SNP mapping.

Supporting information table S1: *t5669* variants within the linked region derived from the WGS/ SNP method.

Position	Ref.	<i>t5669</i>	Change type	Homo-zygous	Quality	Coverage	Gene ID	Gene name	Bio type	Transcript	Exon_ID	Effect	AA exchange	Codon exchange	Codon number	CDS size
X_11654833	*	-T	DEL	Hom	35.4	3	T04F8.2	T04F8.2	pc	T04F8.2.2		intron				
X_11654833	*	-T	DEL	Hom	35.4	3	T04F8.2	T04F8.2	pc	T04F8.2.1		intron				
X_11966380	C	T	SNP	Hom	222	41	C49F5.1	sams-1	pc	C49F5.1.2	X_11966320_11967112	ns_coding	A/V	gCt/gTt	105	1212
X_11966380	C	T	SNP	Hom	222	41	C49F5.1	sams-1	pc	C49F5.1.3	X_11966320_11967112	ns_coding	A/V	gCt/gTt	105	1212
X_11966380	C	T	SNP	Hom	222	41	C49F5.1	sams-1	pc	C49F5.1.1	X_11966320_11967112	ns_coding	A/V	gCt/gTt	105	1212
X_11989437	C	T	SNP	Hom	222	55	C49F5.6	C49F5.6	pc	C49F5.6		ns_coding	A/V	gCt/gTt	315	2355
X_12142716	C	T	SNP	Hom	174	26	M153.6	M153.6	nc RNA	M153.6		transcript M153.6				
X_12722771	A	T	SNP	Hom	79.2	15	F16H9.2	nhr-27	pc	F16H9.2b		intron				
X_12722771	A	T	SNP	Hom	79.2	15	F16H9.2	nhr-27	pc	F16H9.2a		intron				
X_12722771	A	T	SNP	Hom	79.2	15	F16H9.1	rgs-2	pc	F16H9.1c		intron				
X_12722771	A	T	SNP	Hom	79.2	15	F16H9.1	rgs-2	pc	F16H9.1b.1		intron				
X_12722771	A	T	SNP	Hom	79.2	15	F16H9.1	rgs-2	pc	F16H9.1b.2		intron				
X_12722771	A	T	SNP	Hom	79.2	15	F16H9.1	rgs-2	pc	F16H9.1a		intron				

Subset of variants, which were identified by the WGS/ SNP method [119]. The filtering criteria for this subset were the following: firstly, homozygous and heterozygous N2 variants were subtracted from *t5669* homozygous variants. Residual *t5669* variants were then filtered for variants in the mapped region. Finally only variants within coding regions (non-upstream/downstream and non-intergenic variants) were selected. The variation in the *sams-1* gene is highlighted in grey. pc=protein coding; ns=non-synonymous.

Supporting information table S2: List of primers used for chromosome and interval mapping.

Chr	Cosmid ID	genomic location of the cosmid	SNP location on the cosmid	5' primer	3' primer	N2 digest	CB4856 digest	enzyme used
<u>Chromosome mapping</u>								
I	W03D8	2.8 Mb	34384 bp	CGAACTTTTATCCGTCACCG	CACCCCAATTAATCTGTGCG	333+175 bp	-	DraI
I	K04F10	6.3 Mb	19618 bp	ATCATTCTCCAGGCCACGTTAC	CTGAACTAGTCGAACAAACCCC	-	300+300bp	NdeI
I	ZK909	14.9 Mb	10906 bp	CACAAGTGGTTTGGAGTACCG	CAACAAAGGGATAGATCACGGG	-	237+213bp	HindIII
II	T01D1	0.16 Mb	14052 bp	AAGAGGTGTTCTTCTGCAGC	ACCATCCACGCAGTTCATTC	215+406bp	-	DraI
II	C44B7	6.9 Mb	31922 bp	TACAAATCGAAGAACAAGTGGC	TTTTCCAGAATGCTTTCTCGG	160+233bp	-	SphI
II	F15D4	13.2 Mb	22810 bp	TTCCCATTTTCTCCCG	TCAAAAACCCAGACACTGG	-	400+120bp	DraI
III	T17A3	0.13 Mb	23338 bp	AGCAAGAATGAGCCGATTG	GTCGGCCGTTTTCAAATAACTG	150+230bp	150+30+195bp	TaqI
III	C48D5	3.6 Mb	33058 bp	CTTCATTGCGCTCACTTCTG	TACGCACATGCCTACAAAGG	-	376+510	BglII
III	Y75B8A	12.1 Mb	232973 bp	AAACAGCATTGTGACGAGC	AGCCTAAGCCCAAGCTTTAG	-	256+71bp	HindIII
IV	Y55F3BR	0.8 Mb	49546 bp	CCAAGCTGAAAACGGATATAAC	ATTGGGTTCACTGAGAGCTTC	264+49bp	-	DraI
IV	C49H3	7.9 Mb	3770 bp	TTGCAGTTCGGAGTGTCTTATG	TGGCTCGGTGCAAGTCTATTG	280+140bp	-	DraI
IV	Y51H4A	16.5 Mb	235180 bp	AATTCACCGATAGAAGTTTCCC	GCTTTGTCATAGGGAGTGTCCG	113+214	-	EcoRI
V	Y38C9B	50 kb	3742 bp	CCGCACTTCCTCAGAAATG	TGTAGGGCGAGTAACCAAGC	-	270+50bp	BamHI
V	AC3	10.4 Mb	3025 bp	CTCTTAGATACCCTTTCTGCGC	TTCAGCGTTTGGTCTGACGTAG	385+106bp	-	DraI
V	F38A6	20.7 Mb	14347 bp	TTTATCCGCAGGGACTTGAC	TCTCCTCTCCCTCATGGTTAAC	184+677+128bp	128+855bp	DraI
X	F49H12	2.1 Mb	8894 bp	ATGTGAGTTTACCATCACTGGG	TTTCGTAAAACCTACCGAGCAC	-	216+252bp	DraI
X	F45E1	7.9 Mb	9628 bp	TTTCTTGACACCTCCGGTAG	CTCACTCTGGTCTTTTTCCG	512+258bp	-	EcoRI
X	W09B12	16.4 Mb	8860 bp	CCTCAGGATTTACCAGTGACAC	TTAGTCTTGCGCCCCTAGAG	-	217+112bp	BglII
<u>Interval mapping</u>								
X	F02G3	0.7 Mb	5645 bp	CTGAAATCGTGTGCGAAGTC	TCTTCAGTTGGTTAAGGTCTC	293+289bp	-	BamHI

Continued table S2

X	F49H12	2.1 Mb	8894 bp	ATGTGAGTTTACCATCACTGGG	TTTCGTAAAACCTACCGAGCAC	-	216+252bp	DraI
X	F11D5	3.3 Mb	27263 bp	TCGTGGCACCATAAAAAGTG	GATTCAGATCAAACAGAGGTGG	-	116+130bp	DraI
X	ZK470	4.1 Mb	27170 bp	CCAAAACGGCCAAGTATCAG	TTGCACTCTTCTCCTTCCG	-	328+100+ 72+40bp	DraI
X	ZC449	5.0 Mb	4683 bp	ATTGTGACGAATCGGAACCC	AGTAGACTGAGACCGCACAAAC	-	65+80bp	DraI
X	C54H2	5.7 Mb	23555 bp	TTAAAAGCTGGCTCTAGTGTTG	AGCAATTATAGTGTCATTGCCG	96+60+130 +65bp	-	DraI
X	T28B4	6.6 Mb	7490 bp	CACCGAAGATTGACAACCTTTCG	TTGGTTCATACAGAACTTGGTC	250+80bp	-	BglII
X	C01C10	7.4 Mb	13818	TGACCCGTTTTGTAGAACTCCG	GCATCAATGAGCACTTTGTTGG	160+315bp	-	DraI
X	F15G9	9.7 Mb	19169	GTCTTCATTGCATGATGTGGC	TTGGATCTCCGTAGACGTCAC	300+220bp	-	SspI
X	F19C6	9.9 Mb	30255	TGTGAACGAACCCTCTCAAGC	TCTAGCACGCAAAGTTTCCAC	30+20+25 +191bp	-	TaqI
X	C05C9	11.1 Mb	8685	CGCACTGACTTTTTTCCAGC	ACACTAGAATCTCCACACCTCC	-	161+450bp	DraI
X	F46C3	11.4 Mb	haw107527*	GCGCGTGAATAGGCATATATC	TGAGGAGCGAGGCTCAACGGAG	-	242+2+ 252bp	NdeI
X	C35C5	11.5 Mb	haw107582*	GTGTTTGTCAAACCTTGTTCGG	GAGAGGATCGGAATGAGAATGC	160+242bp	-	SspI
X	C44C10	11.7 Mb	haw107641*	CGTTCAGTGCAATGTATTCTC	AGATCGTGTGAGACATACCAG	232+74bp	-	TaqI
X	B0198	12.0 Mb	692	GTCTATTGCCTCTGCCATCAAG	TTGAAGCCTAAATCGCTTGC	300+86bp	-	EcoRI
X	F22E10	12.7 Mb	snp_F22E10*	TTAAAACCATACAATTCTTCTCAGC	GAATCCCAATCAACAGAGAGC	341+126bp	-	DraI
X	F11C1	12.9 Mb	20912	ATCGACCCCAACAATGCAC	TCCGTCATCCAAATCTCCG	-	252+223bp	Asel
X	F46G10	13.3 Mb	pkP6132*	ACTGTTTACCGCTCTTCTGC	CCGTGTATATAAGAAAATGTGTTCCG	318+191 +37bp	509+37bp	DraI
X	T24C2	14.5 Mb	uCE6-1459*	GCTGGGATTTTGAAGAGTTGTT	CAGTGAATCATCCGTTGAATTT	409+34bp	302+107 + 34bp	DraI
X	H13N06	15.5 Mb	uCE6-1554*	CAAATACCAAAGTTGATCGTGG	TTGTTGCAATTAATCAAACGG	358+134bp	-	DraI
X	W09B12	16.4 Mb	8860 bp	CCTCAGGATTTACCAGTGACAC	TTAGTCTTGCGCCCCTAGAG	-	217+112bp	BglII

All primer sequences are presented from 5' to 3'. The restriction enzymes used for each SNP are indicated. Locations of SNPs are specified by the name of the cosmid and the position within this cosmid with the exception of * marked SNPs, that are specified by the SNP wormbase ID.

Supporting information figure S2: Wild type and *t5669* sequences of an amplified genomic PCR product harbouring the mutation site in the *sams-1* gene.

A

>C49F5.1.1 unspliced + UTR (2168 bp)

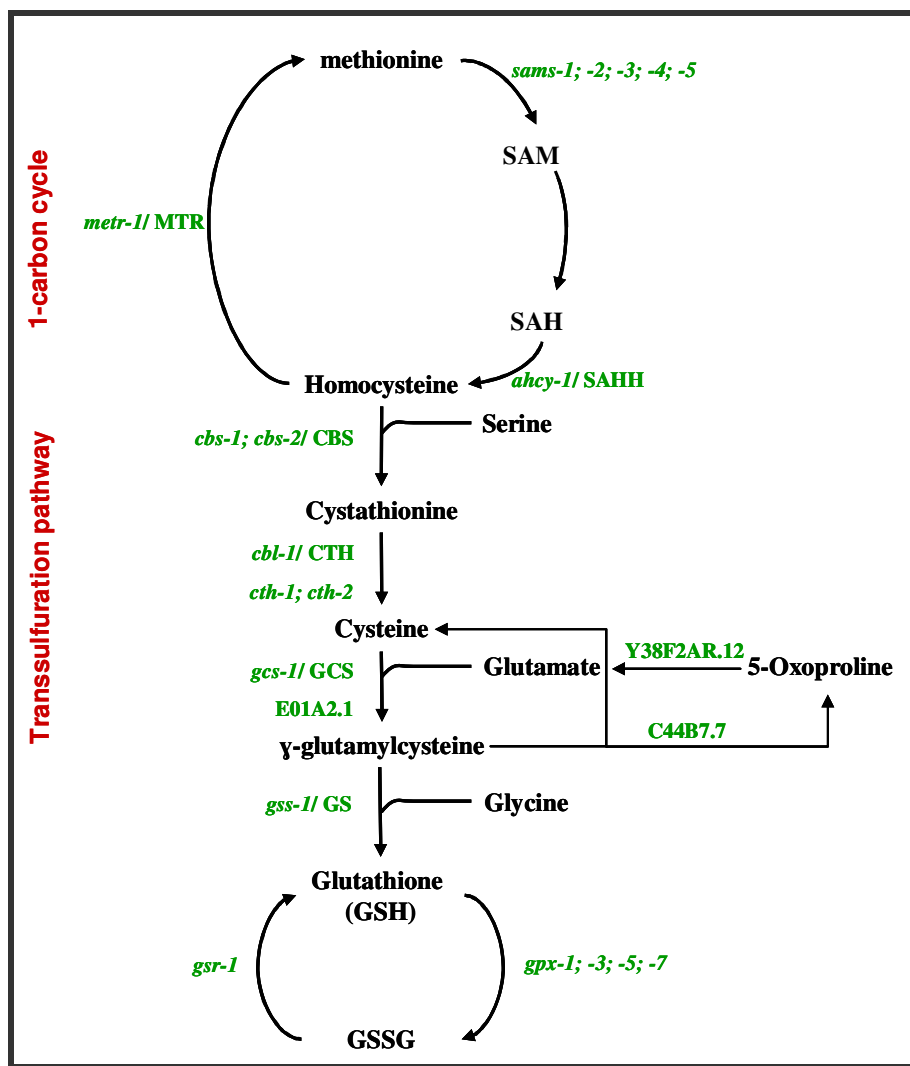
ataaaggcagtggtccgactgtgcgacaagccattctaatacgcttctcagctcttaaaactcagaa**ATGTCCTCCAATT**
CCTTTTCACCAGTGAATCTGTGTCCGAGGGGCATCCAGACAAAATGTGCGATCAA**g**taagtttttttgttttatttatt
 taattttatctatttctgttttttttag**ATTCTGACGCCGTCTCGATGCTCATCTTAAGCAAGATCCAAATGCAAAGG**
TTGCTTGCAGACCGTAACAAAACCTGGTATGGTTATGCTCTGCGGAGAAATACCTCCAAGGCTGTTGTTGACTATCAA
GTTCTCGTCCGTGTCATCGAAAAGATTGGATTACCCGACTCCAGCATTGgtagtttatagaatcttgctttattat
 tagcttgtttcaatgtttttgttcag**GATTGACCCACAAGACCTGCAACGTGCTTGTGTGCTTCTGAGCAACAATCTCCAG**
AAATTGCTGCCGGAGTTCACGTCAACAAGGACGGAGAAGATGTCGGAGCAGGAGATCAAGGAATCATGTTCCGGATATGCA
ACCGACGAGACCGAAGAGACCATGCCATTGACTCTCATTCTTTCCACAAGATCAACGCTGAGCTTACAAGCTCCGCCG
TAACGGAACCTTCCATGGTCCGCCAGACTCCAAGTCTCAAGTACCATTGAGTACGAGTCCCGCCACGGAGCAACCA
TTCCACTCCGCTTACACTGTTGTGGTCTTACCCAACACTCTCCAGATGTTACTCTTGAGAACTCCGCGAGACCATC
CTCGCTGATGTTATCAAGAAGGTCATCCCAGCTTCTCTTTGGACGAGTCTACTGTCTTCCACATCAACCCATGCGGAAC
 CTTTCATCGTTGGAGGACCAATGGGAGACGCAGGAGTACCCGGACGTAAGATCATCGTTCGACACCTACGGAGGATGGGGAG
 CTCACGGAGGAGGTGCTTTCTCTGGAAGGACCAACCAAGTTCGATCGCTCTGCTGCCTACGCTGCCCCTGGGTAGCAG
 ACCTCATTGGTCAAGGCTGGACTTGTAAAGCGCTCCTCGTCCAACCTTCTACGCTATTGGAATCGCCAAGCCAATCTC
 AGTTTTGGTCTATGCTTTCCGAACTTCCCACTCACCGACGAAGAGCTTACCAGATCGTCGAAGACTCCTTCGATCTTA
CCCCAGGAAAAATTATCAAgtaagtgaatacagctagataggagaaatttcattggttttttacag**GGAGCTCGACTCA**
AGAGACCAATCTACGAGAAGACCGCCGAGAACGGTCACTTCGGTCACTCTGAGTTCATGGGAGCAGCCAAAAGCTCTC
AAGATTTCTCCAGCACTTCTCGAGAAGGCCAAGGGAAACCAATCCAGCCACATCTGCTATCGCTCACTAAtttttttg
 cctcggatgcaaaaacttttttttaataatcaatctcgttttattgtatgctaggccaatagtttaatttagtccg
 attttgtagtagacccttgaaaaaactgaaaaaaaacaaagttagagtataaatttagtttaggcaactaattaca
 ttttcaattcagctagatgaccaacacctgcgctatttaaaaaaacgattaacgtatttgacctttcccttct
 cccccaccagcctcttactctgatgcatcccccaatctgtcccttctgttcaactgatgatgtgcaactctcagag
 catttttcaacagtgccctctcttttttaagtccccggtttccgctaccgctgagctgtctgacttttagaatagctt
 cattttcaaaaaattcatatataaaaaaaacatcacaacgcaaaaaaatagttcttgacagtttctaatgcccgaaacat
 attttctccaattacatagattataatcctttctcataacttctcattgctcaatgtctcaactgccaccaactgag
 tggatcgtacgatttttaagcaccatcaaatctttgggtataattaatacatattttgttaaatgtataatccttcg
 gtggtagttcagtaattgcttatttccattcataaattatgcttgacatttaactttgggaaataaagttttaaaatata
 aatttttc

B

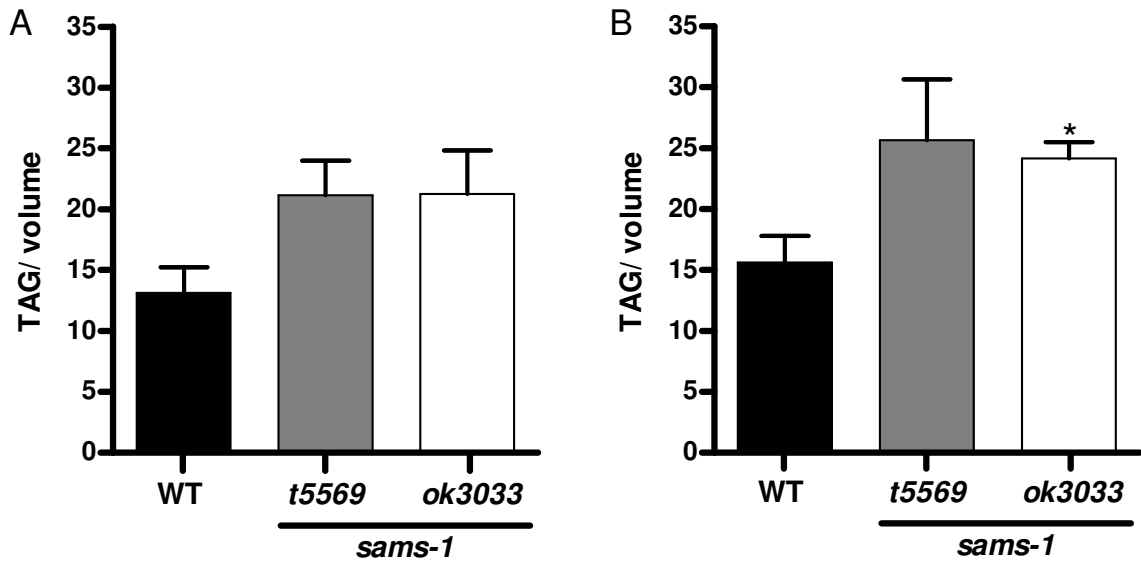
t5669	21TGTGCGATCAAGTAAGTTTTTTTTGTTTTATTTATTTAATTTTATCTATTTCTGT	75
N2	13	ACAAATGTGCGATCAAGTAAGTTTTTTTTGTTTTATTTATTTAATTTTATCTATTTCTGT	72
t5669	76	TTTTTTTAGATTTCTGACGCCGTTCTCGATGCTCATCTTAAGCAAGATCCAAATGCAAAG	135
N2	73	TTTTTTTAGATTTCTGACGCCGTTCTCGATGCTCATCTTAAGCAAGATCCAAATGCAAAG	132
t5669	136	GTTGCTTGCAGACCGTAACAAAACCTGGTATGGTTATGCTCTGCGGAGAAATACCTCC	195
N2	133	GTTGCTTGCAGACCGTAACAAAACCTGGTATGGTTATGCTCTGCGGAGAAATACCTCC	192
t5669	196	AAGGCTGTTGTTGACTATCAAGTCTCGTCCGTCGTGTCATCGAAAAGATTGGATTACCC	255
N2	193	AAGGCTGTTGTTGACTATCAAGTCTCGTCCGTCGTGTCATCGAAAAGATTGGATTACCC	252
t5669	256	GACTCCAGCATTGGTTAGTTTATAGAATCTTGCTTTATTATTAGCTTGTTCGAATGTTTT	315
N2	253	GACTCCAGCATTGGTTAGTTTATAGAATCTTGCTTTATTATTAGCTTGTTCGAATGTTTT	312
t5669	316	TGTTCCAGGATTCGACCACAAGACCTGCAACGTGCTTGTGCTCTTGAGCAACAATCTCCA	375
N2	313	TGTTCCAGGATTCGACCACAAGACCTGCAACGTGCTTGTGCTCTTGAGCAACAATCTCCA	372
t5669	376	GAAATTGTTGCCGGAGTTCACGTCAACAAGGACGGAGAAGATGTCGGAGCAGGAGATCAA	435
N2	373	GAAATTGTTGCCGGAGTTCACGTCAACAAGGACGGAGAAGATGTCGGAGCAGGAGATCAA	432
t5669	436	GGAATCATGTTCCGGATATGCAACCGACGAGACCGAAGAGACCATGCCATTGACTCTCATT	495
N2	433	GGAATCATGTTCCGGATATGCAACCGACGAGACCGAAGAGACCATGCCATTGACTCTCATT	492
t5669	496	CTTTCCACAAGATCAACGCTGAGCTTACAAGCTCCGCCGTAACGGAACCTTCCATGG	555
N2	493	CTTTCCACAAGATCAACGCTGAGCTTACAAGCTCCGCCGTAACGGAACCTTCCATGG	552
t5669	556	GTCCGCCAGACTCCAAGTCTCAAGTACCATTGAGTACGAGTCCCGCCACGGAGCAACC	615
N2	553	GTCCGCCAGACTCCAAGTCTCAAGTACCATTGAGTACGAGTCCCGCCACGGAGCAACC	612
t5669	616	ATTCCACTCCGCGTTCACACTGTTGTGGTCTTACCCAACACTCTCCAGATGTTACTTCT	675
N2	613	ATTCCACTCCGCGTTCACACTGTTGTGGTCTTACCCAACACTCTCCAGATGTTACT_CT	671
t5669	676	TGA...	678
N2	672	TGAGAACTCCGCGAGACCATCCTCGCTGATGATT	706

Wild type and *t5669* sequences of an amplified genomic PCR product harbouring the mutation site in the *sams-1* gene. (A) Genomic sequence of C49F5.1.1 coding for the *sams-1* transcript. Coloured capital letters represent exons. Introns and UTRs are depicted by lowercase sequences. Bold letters indicate the primer sequences used for amplification of a genomic 742 bp PCR product that harbours the mutation site (red letter, underlined). (B) Wild type and *sams-1(t5669)* sequences of the amplified genomic PCR product. Sequencing was done by Eurofins MWG Operon (Ebersberg, Germany). The mutation site is highlighted by an orange bar.

Supporting information figure S3: Schematic representation of the connection between the one-carbon cycle and the transsulfuration pathway.

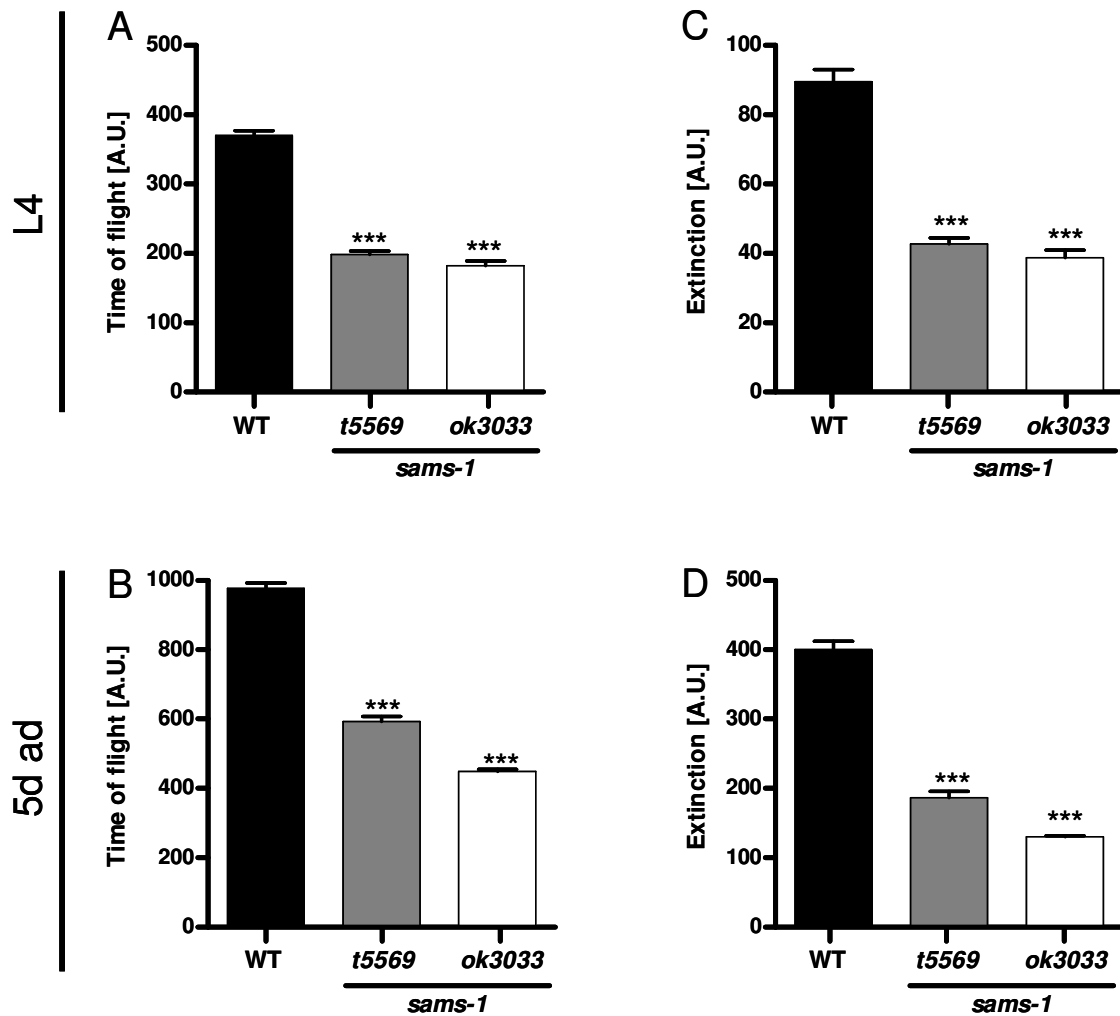


The one-carbon cycle and the interconnected transsulfuration pathway are shown. *C. elegans* genes and proteins, which are involved in respective reactions are indicated in green. Abbreviations: *sams* = S-adenosylmethionine synthetase; *ahcy*/SAHH = S-adenosylhomocysteine hydrolase; *cbs*/CBS = cystathionine β-synthase; *cbl*/CTH = cystathionine β-lyase; *cth* = cystathionine γ-lyase; *gcs*/GCS = γ-glutamylcysteine synthetase; *gss*/GS = glutathione synthetase.

Supporting information figure S4: TAG level adjusted to body volume of *sams-1* mutants and wild type worms.

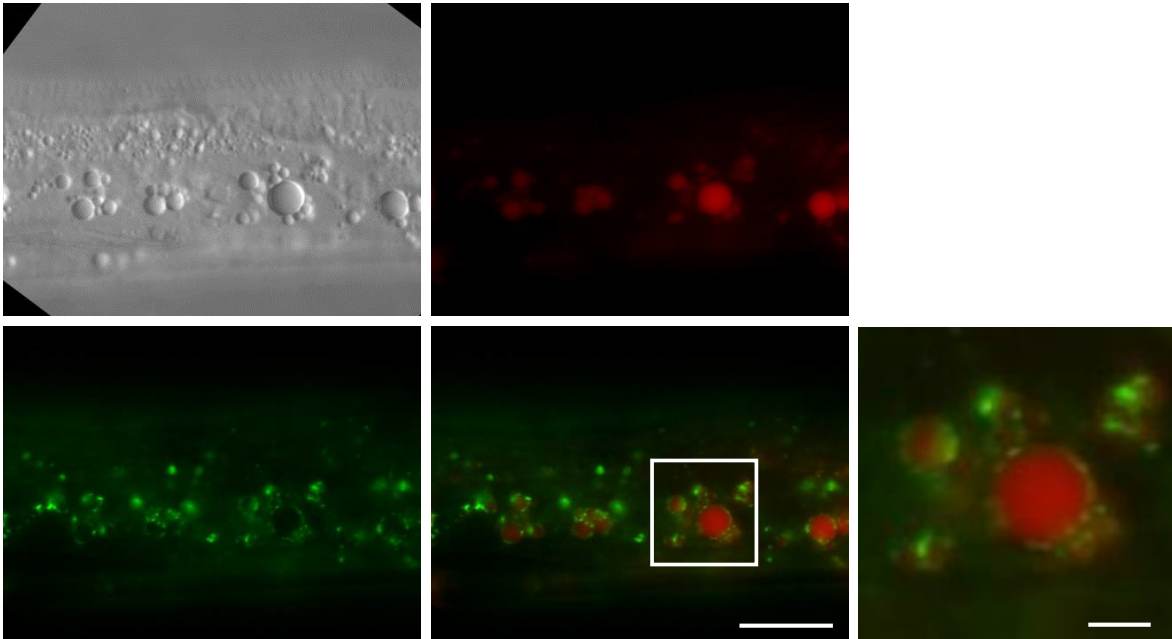
TAG level of wild type worms and *sams-1* mutants were adjusted to the respective body volume. Calculations were made for L4 larvae (A) and 5d-old-adults (B). TAG levels were determined by total lipid extraction from 2000 (WT) to 4000 (*sams-1* mutants) worms and lipid separation by thin layer chromatography. Body volume was determined by analysis of bright-field microscopy images. Images of 10 worms per strain and experiment were analyzed. Bars represent mean \pm SEM of 3 to 5 independent experiments. Significant differences were analyzed between WT and the respective *sams-1* mutant using unpaired t-test (* $p < 0.05$).

Supporting information figure S5: Time of flight and extinction values of wild type worms and *sams-1* mutants.

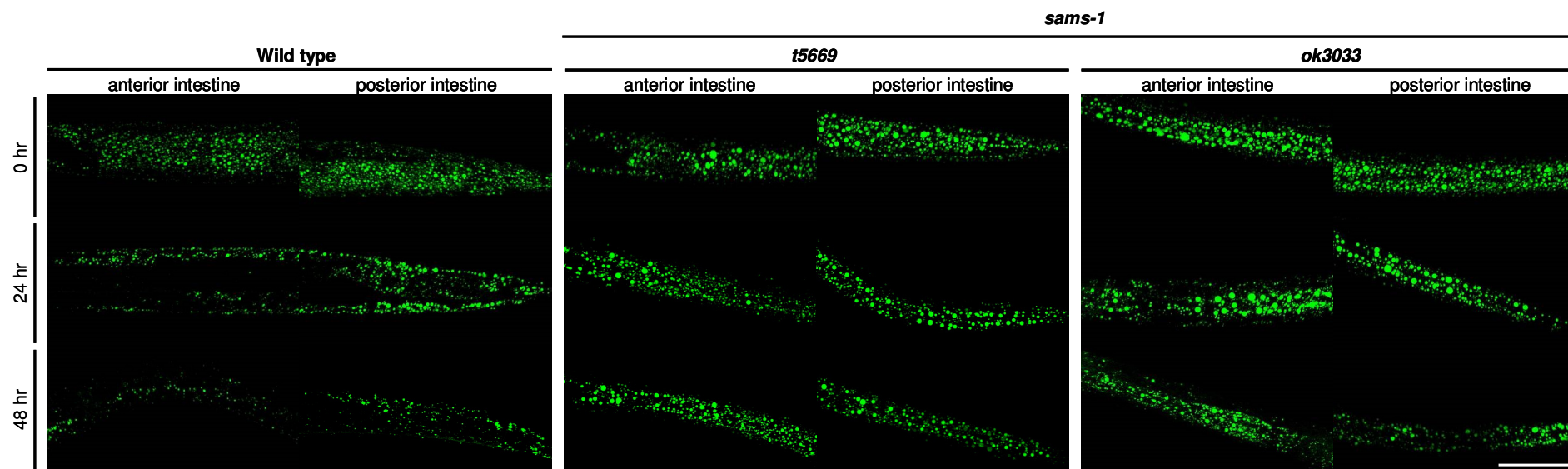


Time of flight (A-B) and extinction values (C-D) of wild type worms *sams-1* mutants at the L4 stage (A, C) and the 5d ad stage (B, D). Data were derived from large particle flow cytometry using COPAS Biosort system. Time of flight and extinction are approximate values for the axial length and for the volume of single worms, respectively [86]. Bars represent mean \pm SEM of at least 3 independent experiments. Biological samples of each experiment comprised \sim 2000 (wild type) and \sim 4000 (*sams-1* mutants) worms. Significance asterisks refer to differences between wild type worms and the respective *sams-1* mutant and were determined by an unpaired t-test ($***p < 0.001$).

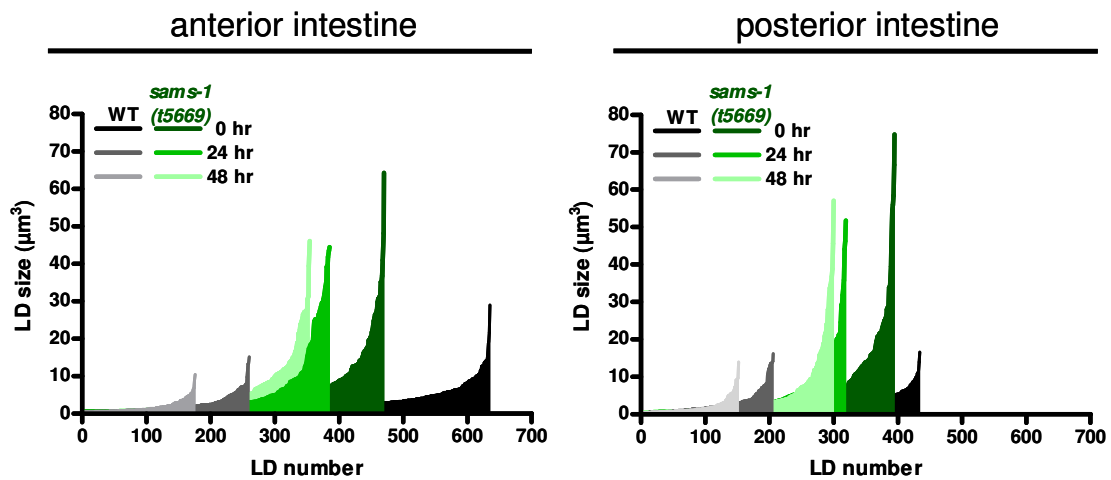
Supporting information figure S6: ATGL-1::GFP as marker for lipid droplets in *sams-1(t5669)* mutants.



Colocalization between ATGL-1::GFP and lipid droplets in *sams-1(t5669)* mutants. *sams-1(t5669)* mutants were crossed with males of the strain VS20 (*hjls67*) expressing an ATGL-1::GFP fusion protein [*atgl-1p::atgl-1::GFP*]. F2 progenies showing the "vacuole" phenotype as well as GFP fluorescence were used for colocalization studies. *sams-1(t5669);atgl-1p::atgl-1::gfp* worms were vitally stained with LipidToxRed (1:200; Invitrogene). Scale bars: 10 μm in the total view; 2 μm in the detailed view.

Supporting information figure S7: Starvation-induced alterations in LD size and LD number in wild type worms and *sams-1* mutants.

LDs of wild type and *sams-1* larvae fed *ad libitum*, starved for 24 hr and starved for 48 hr. LDs have been visualized via fixative BODIPY™ 493/503 fat staining and subsequent 3D fluorescence microscopy. Images of the anterior intestine (left panel for each strain) and the posterior intestine (right panel for each strain) are represented as maximum projections of 10-25 plane images from a z-stack (1 μm interval) depending on the respective strain. Scale bar represents 50 μm .

Supporting information figure S8: Alterations of LD number and LD size during starvation in wild type worms and *sams-1* mutants.

LDs of wild type and *sams-1(t5669)* larvae fed *ad libitum*, starved for 24 hr and starved for 48 hr have been visualized via fixative BODIPY[™] 493/503 fat staining and subsequent 3D fluorescence microscopy. LD number and LD volume have been determined by use of the 3D object counter plugin of the ImageJ software. For one representative worm per strain, the volume of each lipid droplet plotted as a function of the total LD number in the anterior intestine and in the posterior intestine, respectively.

Supporting information table S3: Relative number of lipid droplets classified by size in *ad libitum* fed and starved wild type worms and *sams-1* mutants.

		relative number of lipid droplets (%)					
LD class	time of starvation	anterior intestine			posterior intestine		
		WT	<i>sams-1</i>		WT	<i>sams-1</i>	
			<i>t5669</i>	<i>ok3033</i>		<i>t5669</i>	<i>ok3033</i>
<2 μm^3	0 hr	67.2 \pm 1.2	58.5 \pm 1.4	57.9 \pm 1.7	65.4 \pm 1.1	52.2 \pm 1.3	53.3 \pm 2.4
	24 hr	72.2 \pm 2.0	57.3 \pm 1.5	59.1 \pm 1.6	61.9 \pm 1.4	51.6 \pm 1.7	58.9 \pm 1.9
	48 hr	75.9 \pm 2.7	58.6 \pm 1.1	62.8 \pm 1.5	65.4 \pm 1.7	50.9 \pm 1.5	57.1 \pm 3.0
2-5 μm^3	0 hr	22.0 \pm 0.8	21.4 \pm 0.6	22.2 \pm 0.8	23.2 \pm 0.9	22.6 \pm 0.8	22.8 \pm 1.1
	24 hr	20.2 \pm 1.2	21.7 \pm 0.6	21.4 \pm 0.7	24.3 \pm 0.9	23.6 \pm 0.6	21.8 \pm 0.6
	48 hr	18.9 \pm 1.6	20.8 \pm 1.0	21.3 \pm 1.1	23.9 \pm 1.6	24.5 \pm 1.1	23.6 \pm 2.6
5-10 μm^3	0 hr	7.4 \pm 0.3	9.8 \pm 0.4	10.4 \pm 0.6	8.1 \pm 0.5	11.4 \pm 0.4	12.1 \pm 0.9
	24 hr	5.7 \pm 0.7	11.3 \pm 0.9	9.8 \pm 0.8	9.1 \pm 0.6	12.9 \pm 0.5	10.3 \pm 1.0
	48 hr	4.7 \pm 1.1	9.9 \pm 0.5	8.8 \pm 1.0	8.4 \pm 0.6	11.9 \pm 0.6	9.7 \pm 1.1
10-30 μm^3	0 hr	3.3 \pm 0.5	7.7 \pm 0.6	7.5 \pm 0.8	3.2 \pm 0.6	11.2 \pm 0.6	9.5 \pm 0.9
	24 hr	1.8 \pm 0.4	7.4 \pm 0.4	7.8 \pm 0.7	4.2 \pm 0.5	9.3 \pm 1.1	6.8 \pm 0.7
	48 hr	1.1 \pm 1.6	8.6 \pm 0.7	7.6 \pm 0.6	2.4 \pm 0.4	10.5 \pm 1.5	8.1 \pm 1.2
>30 μm^3	0 hr	0.1 \pm 0.0	2.8 \pm 0.5	2.3 \pm 0.3	0.1 \pm 0.1	2.5 \pm 0.3	2.4 \pm 0.6
	24 hr	0.1 \pm 0.0	2.5 \pm 0.3	2.7 \pm 0.6	0.0	2.6 \pm 0.3	2.3 \pm 0.6
	48 hr	0.1 \pm 0.1	2.6 \pm 0.6	2.0 \pm 0.2	0.0	2.1 \pm 0.6	1.8 \pm 0.4

The relative number (%) of LDs that are <2 μm^3 , 2-5 μm^3 , 5-10 μm^3 , 10-30 μm^3 and >30 μm^3 in volume are shown. Changes in the relative distribution of LD classes are compared between *ad libitum* fed (0 hr) and starved (24 hr; 48 hr) wild type worms and *sams-1* larvae. Values represent mean \pm SEM of at least 10 individual worms from three independent experiments.

7 Appendix

Body size of wild type worms and *sams-1* mutants.

Parameter	wild type			<i>sams-1(t5669)</i>			<i>sams-1(ok3033)</i>			
	Mean	SEM	N	Mean	SEM	N	Mean	SEM	N	
Body length (μm)	L4	782.3	± 22.9	14	599.2	± 16.9	19	581.4	± 13.6	27
	5d ad	1552.0	± 31.7	10	1092.0	± 18.2	25	992.3	± 20.2	24
Body width (μm)	L4	40.9	± 1.9	14	27.2	± 0.9	19	28.3	± 0.7	18
	5d ad	99.4	± 1.3	10	68.7	± 1.1	25	61.3	± 1.5	24
Body volume ($\times 10^3 \text{ mm}^3$)	L4	0.8	± 0.1	14	0.3	± 0.02	17	0.2	± 0.02	12
	5d ad	8.1	± 0.4	10	2.6	± 0.1	25	1.8	± 0.1	25
^a Time of flight [A.U.]	L4	370.2	± 6.6	6	198.5	± 5.3	6	182.2	± 7.0	7
	5d ad	977.0	± 15.2	6	592.8	± 14.4	6	448.9	± 6.8	6
^a Extinction [A.U.]	L4	89.6	± 3.5	6	42.8	± 1.8	6	38.8	± 2.1	7
	5d ad	400.1	± 12.0	6	186.4	± 9.8	6	130.3	± 1.6	6

Different parameters, which describe body size in *C. elegans*, were compared between wild type worms and *sams-1* mutants at the L4 stage (L4) and at fifth day of adulthood (5d ad). ^a Time of flight and extinction are approximate values for axial worm length and body volume, respectively. For these parameters, N represents number of experiments. Each experiments comprised 2000 - 4000 worms. A.U. = arbitrary unit. For body length, body width and body volume N represents number of worms. All parameters were determined as described in Material and Methods.

Reproductive capability of wild type worms and *sams-1* mutants.

Parameter	wild type			<i>sams-1(t5669)</i>			<i>sams-1(ok3033)</i>		
	Mean	SEM	N	Mean	SEM	N	Mean	SEM	N
Hatching rate (% larvae hatched)	95.3	± 1.2	19	81.5	± 1.4	20	69.2	± 8.1	11
Number of progenies	308.2	± 12.1	10	53.8	± 6.4	10	53.3	± 10.8	7

Hatching rate describes the proportion of larvae that hatched from a defined number of eggs. Number of progeny describes the total number of vital larvae, which derived from a single worm during its entire reproductive phase. Both parameters were determined as described in Material and Methods.

Survival rate of wild type worms and *sams-1* mutants exposed to arsenite.

Strain	% survivals		
	Mean	SEM	N
WT	81.8	± 2.4	3
L4440	78.7	± 8.1	3
<i>gcs-1(RNAi)</i>	3.9	± 0.3	3
<i>sams-1(RNAi)</i>	42.3	± 5.3	3
<i>sams-1(t5669)</i>	4.4	± 2.9	3
<i>sams-1(ok3033)</i>	9.2	± 4.9	3

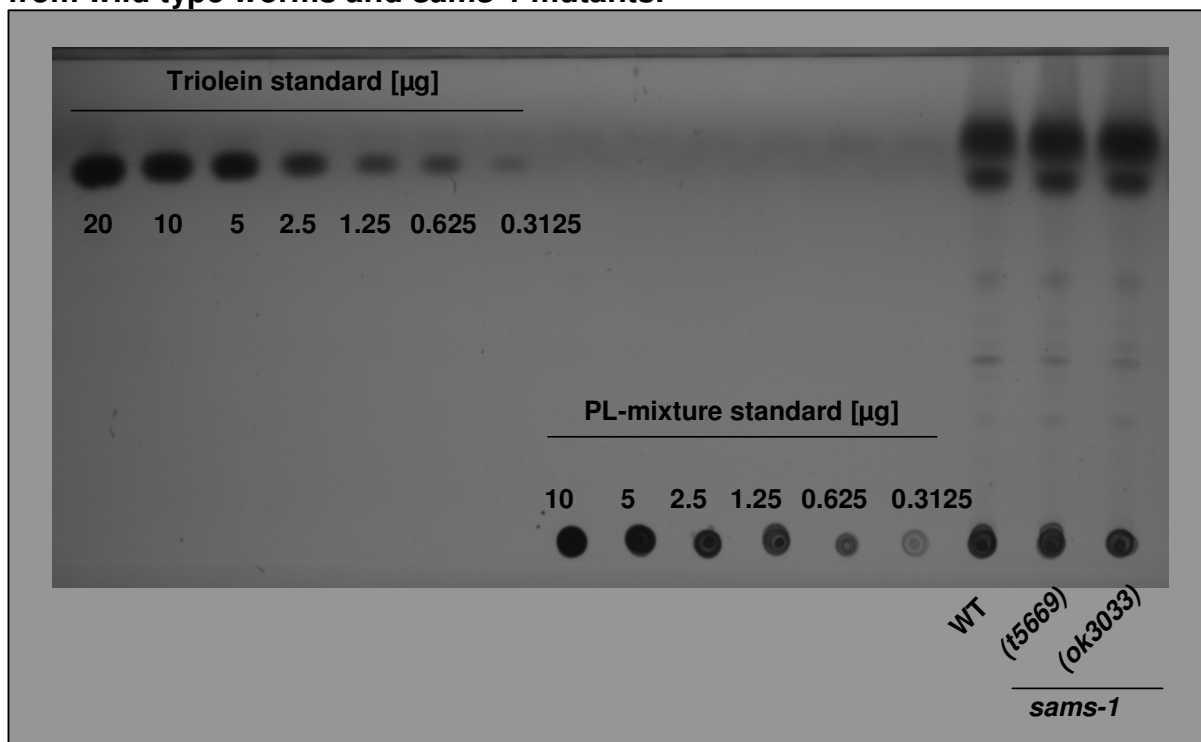
"Percent survivals" describes the proportion of worms, which survived 24 hr of 4 mM NaAsO₂ exposure. WT = wild type. L4440 = wild type fed the control RNAi feeding vector. N = number of experiments. Each experiment comprised 30 worms. For experimental procedure, see Material and Methods.

Lipid fractions of wild type worms and *sams-1* mutants.

Parameter	wild type			<i>sams-1(t5669)</i>			<i>sams-1(ok3033)</i>				
	Mean	SEM	N	Mean	SEM	N	Mean	SEM	N		
TAG	(ng/worm)	L4	10.7	± 1.7	5	6.2	± 0.8	5	4.9	± 0.8	5
		5d ad	126.3	± 17.7	4	65.5	± 12.7	5	52.4	± 9.2	4
	(%)	L4	57.3	± 9.1	5	62.2	± 8.3	5	60.1	± 10.2	5
		5d ad	58.7	± 8.2	4	75.9	± 14.7	5	75.6	± 13.3	4
PC	(ng/worm)	L4	3.8	± 0.2	6	1.6	± 0.2	5	1.5	± 0.2	6
		5d ad	43.7	± 3.5	5	6.8	± 1.3	5	6.6	± 0.8	5
	(%)	L4	20.5	± 1.2	6	16.3	± 1.5	5	17.7	± 1.9	6
		5d ad	20.3	± 1.6	5	7.9	± 1.5	5	9.5	± 1.1	5
PE	(ng/worm)	L4	4.1	± 0.4	6	1.9	± 0.4	6	1.8	± 0.3	6
		5d ad	45.0	± 4.8	5	14.0	± 1.8	3	10.3	± 0.4	5
	(%)	L4	22.1	± 1.9	6	21.0	± 2.8	5	22.2	± 3.1	6
		5d ad	20.9	± 2.2	5	16.2	± 2.0	3	14.9	± 0.6	5

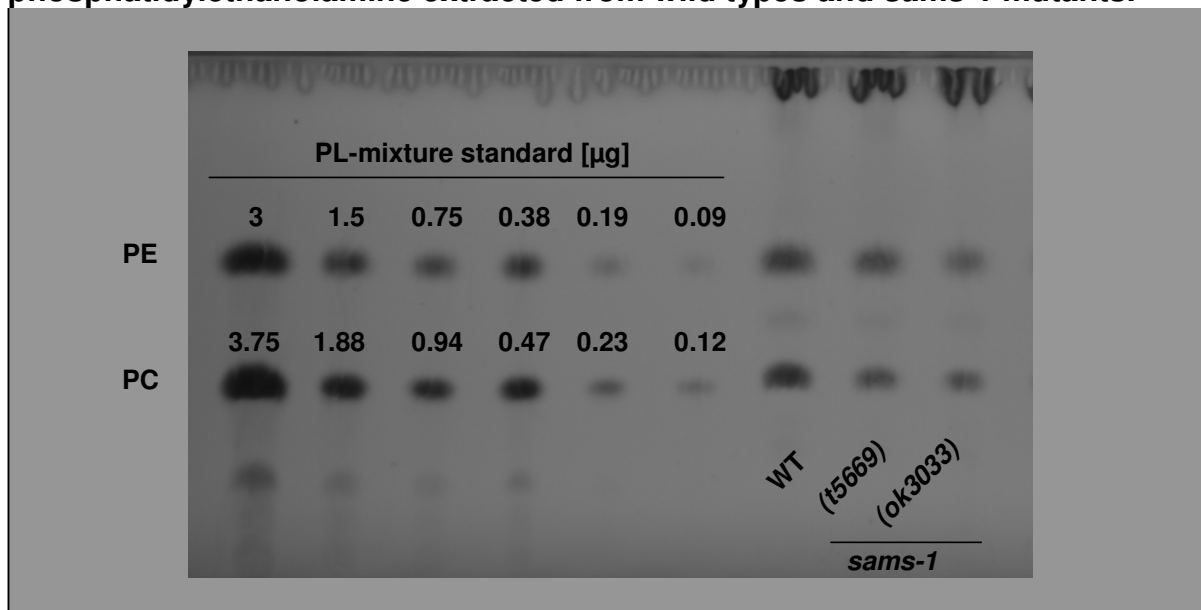
Lipid fractions were compared between wild type worms and *sams-1* mutants at the L4 stage (L4) and at fifth day of adulthood (5d ad). TAG (triacylglycerol), PC (phosphatidylcholine) and PE (phosphatidylethanolamine) fractions are indicated as amount per worm and as relative proportion. Lipid fractions were determined as described in Materials and Methods.

Thin layer chromatogram of triacylglycerides and total phospholipids extracted from wild type worms and *sams-1* mutants.



Representative thin layer chromatogram for the quantification of triacylglycerol and total phospholipid contents of 5-day-old adult wild type worms and *sams-1* mutants. Lipid extraction and separation was performed as described in Material and Methods.

Thin layer chromatogram of phosphatidylcholine and phosphatidylethanolamine extracted from wild types and *sams-1* mutants.



Representative thin layer chromatogram for the quantification of the phosphatidylcholine and the phosphatidylethanolamine contents of 5-day-old adult wild type worms and *sams-1* mutants. Lipid extraction and separation was performed as described in Material and Methods.

Starvation-induced alterations of triacylglycerol and protein level in wild type worms and *sams-1* mutants.

Parameter	time of starv.	wild type			<i>sams-1(t5669)</i>			<i>sams-1(ok3033)</i>			
		Mean	SEM	N	Mean	SEM	N	Mean	SEM	N	
TAG	ng/worm	0 hr	5.4	± 0.9	3	3.4	± 0.3	3	3.9	± 0.8	3
		24 hr	1.2	± 0.3	3	1.7	± 0.1	3	1.2	± 0.3	3
		48 hr	0.4	± 0.1	3	1.1	± 0.04	3	0.5	± 0.4	3
	% of control	0 hr	100.0	± 18.1	3	100.0	± 8.1	3	100.0	± 20.1	3
		24 hr	21.8	± 3.7	3	48.7	± 1.9	3	32.8	± 4.2	3
		48 hr	6.7	± 0.3	3	34.0	± 2.6	3	16.7	± 13.2	3
protein	ng/worm	0 hr	25.8	± 1.2	3	15.5	± 0.6	3	17.6	± 0.7	3
		24 hr	19.8	± 1.5	3	13.8	± 0.9	3	14.5	± 1.4	3
		48 hr	19.7	± 2.1	3	13.3	± 1.1	3	14.3	± 1.2	3
	% of control	0 hr	100.0	± 4.8	3	100.0	± 3.8	3	100.0	± 4.2	3
		24 hr	76.4	± 5.7	3	89.5	± 5.2	3	81.8	± 4.9	3
		48 hr	75.3	± 5.2	3	85.6	± 6.3	3	80.9	± 4.2	3

Triacylglycerol (TAG) and protein contents were compared between *ad libitum* fed (0 hr) and starved (24 hr; 48 hr) wild type worms and *sams-1* mutants. "% of control" indicates the relative proportions of TAG and protein in starved worms referred to respective *ad libitum* fed worms. Protein and TAG were determined as described in Material and Methods.

Starvation-induced alterations of lipid droplet number, mean lipid droplet volume and total lipid droplet volume in the anterior intestine of wild type worms and *sams-1* mutants.

Parameter	time of starv.	wild type			<i>sams-1(t5669)</i>			<i>sams-1(ok3033)</i>				
		Mean	SEM	N	Mean	SEM	N	Mean	SEM	N		
anterior intestine	number of LDs	0 hr	611.2	± 49.5	9	436.8	± 18.3	12	455.1	± 52.3	9	
		24 hr	254.2	± 37.6	13	389.8	± 23.9	8	312.8	± 18.9	9	
		48 hr	159.2	± 36.9	10	384.6	± 21.4	10		± 16.5	3	
	Mean LD volume	μm ³	0 hr	2.4	± 0.1	9	4.6	± 0.3	10	4.4	± 0.3	11
			24 hr	1.9	± 0.2	13	4.6	± 0.3	10	4.5	± 0.4	9
			48 hr	1.8	± 0.2	10	4.6	± 0.4	10	4.3	± 0.3	4
	total LD volume	μm ³	0 hr	1488.5	± 143.9	9	2127.9	± 289.5	10	2228.1	± 272.2	11
			24 hr	561.8	± 105.3	13	1933.3	± 166.2	10	1340.1	± 101.4	10
			48 hr	319.0	± 90.9	10	1776.6	± 188.1	10	1081.4	± 181.8	5
		% of control	0 hr	100.0	± 9.6	9	100.0	± 13.6	10	100.0	± 12.2	11
			24 hr	37.7	± 7.1	13	73.9	± 4.9	10	60.2	± 4.5	10
			48 hr	21.4	± 6.1	10	70.5	± 8.0	10	48.5	± 8.2	5

LD = lipid droplet. LD number, mean LD volume and total LD volume of the anterior intestine were compared between *ad libitum* fed (0 hr) and starved (24 hr; 48 hr) wild type worms and *sams-1* mutants. Changes in total LD volume (LD number multiplied by mean LD volume) are shown as relative proportion (% of control) referred to the respective control (0 hr starvation).

Starvation-induced alterations of lipid droplet number, mean lipid droplet volume and total lipid droplet volume in the posterior intestine of wild type worms and *sams-1* mutants.

Parameter	time of starv.	wild type			<i>sams-1(t5669)</i>			<i>sams-1(ok3033)</i>		
		Mean	SEM	N	Mean	SEM	N	Mean	SEM	N
posterior intestine	number of LDs	μm^3	0 hr	383.4 ± 40.5	10	404.7 ± 23.7	11	409.9 ± 36.2	11	
			24 hr	218.9 ± 20.1	10	355.7 ± 33.9	10	303.4 ± 25.5	11	
			48 hr	151.9 ± 20.8	10	301.9 ± 25.2	9	252.0 ± 23.1	4	
	Mean LD volume	μm^3	0 hr	2.5 ± 0.1	10	5.1 ± 0.2	11	4.8 ± 0.4	11	
			24 hr	2.6 ± 0.1	10	5.0 ± 0.3	10	4.5 ± 0.4	10	
			48 hr	2.4 ± 0.1	10	4.7 ± 0.5	10	4.2 ± 0.3	5	
	total LD volume	μm^3	0 hr	942.4 ± 96.3	10	2036.0 ± 141.7	11	1864.0 ± 118.5	11	
			24 hr	632.4 ± 81.7	11	1780.3 ± 180.5	10	1258.8 ± 121.7	11	
			48 hr	361.7 ± 49.9	10	1505.7 ± 235.4	9	982.0 ± 148.2	5	
		% of control	0 hr	100.0 ± 10.2	10	100.0 ± 6.9	11	100.0 ± 6.4	11	
			24 hr	60.1 ± 5.6	10	75.5 ± 9.3	7	67.5 ± 6.5	11	
			48 hr	38.4 ± 5.3	10	59.2 ± 8.2	7	52.7 ± 7.9	5	

LD = lipid droplet. LD number, mean LD volume and total LD volume of the anterior intestine were compared between *ad libitum* fed (0 hr) and starved (24 hr; 48 hr) wild type worms and *sams-1* mutants. Changes in total LD volume (LD number multiplied by mean LD volume) are shown as relative proportion (% of control) referred to the respective control (0 hr starvation). For experimental procedure, see Material and methods.

Size classification of lipid droplets of the anterior intestine from *ad libitum* fed and starved wild type and *sams-1* larvae.

LD class	time of starv.	wild type			<i>sams-1(t5669)</i>			<i>sams-1(ok3033)</i>				
		Mean	SEM	N	Mean	SEM	N	Mean	SEM	N		
anterior intestine	<2 μm^3	absolut	0 hr	408.4	± 31.5	9	265.9	± 24.6	10	267.4	± 35.2	9
			24 hr	175.7	± 24.1	13	242.3	± 17.9	10	188.0	± 14.6	9
			48 hr	113.3	± 23.5	10	223.9	± 10.7	10	163.8	± 21.3	5
		%	0 hr	67.2	± 1.2	9	58.5	± 1.4	10	57.9	± 2.1	9
			24 hr	72.2	± 2.0	13	57.3	± 1.5	10	59.8	± 1.6	9
			48 hr	75.9	± 2.7	10	58.6	± 1.1	10	62.8	± 1.5	5
	2-5 μm^3	absolut	0 hr	135.3	± 12.9	9	96.2	± 8.2	10	100.8	± 12.5	9
			24 hr	55.5	± 9.4	13	91.2	± 6.5	10	63.9	± 4.5	9
			48 hr	33.7	± 9.6	10	80.5	± 6.5	10	59.2	± 8.5	5
		%	0 hr	22.0	± 0.8	9	21.4	± 0.6	10	22.1	± 0.9	9
			24 hr	20.2	± 1.5	13	21.6	± 0.6	10	20.5	± 0.9	9
			48 hr	18.0	± 1.7	10	20.8	± 1.0	10	22.6	± 1.6	5
	5-10 μm^3	absolut	0 hr	45.9	± 4.7	9	44.2	± 4.1	10	47.7	± 5.7	9
			24 hr	16.9	± 3.3	13	47.3	± 4.2	10	29.7	± 2.8	9
			48 hr	10.2	± 3.7	10	38.5	± 3.7	10	23.2	± 3.7	5
		%	0 hr	7.4	± 0.3	9	9.8	± 0.4	10	10.6	± 0.7	9
			24 hr	5.7	± 0.7	13	11.3	± 0.9	10	9.5	± 0.8	5
			48 hr	4.8	± 1.1	10	9.9	± 0.5	10	8.8	± 1.1	5
	10-30 μm^3	absolut	0 hr	20.9	± 3.5	9	35.2	± 4.4	10	30.9	± 2.9	9
			24 hr	5.7	± 1.6	13	31.4	± 3.0	10	23.8	± 2.3	9
			48 hr	1.9	± 0.9	10	33.3	± 3.4	10	16.8	± 3.8	5
		%	0 hr	3.3	± 0.5	9	7.7	± 0.6	10	7.4	± 1.0	9
			24 hr	1.8	± 0.4	13	7.4	± 0.4	10	7.7	± 0.8	5
			48 hr	1.1	± 0.5	10	8.6	± 0.7	10	6.2	± 0.9	5
>30 μm^3	absolut	0 hr	0.7	± 0.3	9	12.6	± 2.9	10	8.3	± 1.9	9	
		24 hr	0.5	± 0.3	13	10.1	± 1.5	10	7.4	± 1.6	9	
		48 hr	0.1	± 0.1	10	8.3	± 2.0	10	4.8	± 1.1	5	
	%	0 hr	0.1	± 0.04	9	2.6	± 0.5	10	2.0	± 0.4	9	
		24 hr	0.2	± 0.1	13	2.4	± 0.3	10	2.5	± 0.6	5	
		48 hr	0.2	± 0.2	10	2.2	± 0.6	10	1.7	± 0.3	5	

LD = lipid droplet. This table shows starvation-induced alterations in the composition of LD classes of the anterior intestine. The absolute and the relative (%) number of LDs that are <2 μm^3 , 2-5 μm^3 , 5-10 μm^3 , 10-30 μm^3 and >30 μm^3 are indicated for *ad libitum* fed larvae (0 hr starvation) as well as for 24 hr and 48 hr starved wild type and *sams-1* larvae. For experimental procedure, see Material and methods.

Size classification of lipid droplets of the posterior intestine from *ad libitum* fed and starved wild type and *sams-1* larvae.

LD class	time of starv.	wild type			<i>sams-1(t5669)</i>			<i>sams-1(ok3033)</i>				
		Mean	SEM	N	Mean	SEM	N	Mean	SEM	N		
posterior intestine	<2 μm^3	absolut	0 hr	252.5	\pm 28.8	10	210.8	\pm 13.0	11	223.5	\pm 27.4	11
			24 hr	138.7	\pm 14.2	10	184.4	\pm 20.2	10	180.4	\pm 17.1	11
			48 hr	99.1	\pm 13.6	10	152.3	\pm 11.6	9	130.8	\pm 11.1	5
		%	0 hr	66.4	\pm 1.1	10	52.2	\pm 1.3	11	53.3	\pm 2.4	11
			24 hr	61.9	\pm 1.4	10	51.6	\pm 1.7	10	58.9	\pm 1.9	11
			48 hr	65.4	\pm 1.7	10	50.9	\pm 1.5	9	57.1	\pm 2.9	5
	2-5 μm^3	absolut	0 hr	87.8	\pm 8.7	10	92.2	\pm 7.1	11	93.2	\pm 8.7	11
			24 hr	51.3	\pm 3.6	10	83.3	\pm 7.8	10	65.4	\pm 4.9	11
			48 hr	36.4	\pm 5.9	10	73.4	\pm 5.9	9	56.6	\pm 11.0	5
		%	0 hr	23.2	\pm 0.9	10	22.6	\pm 0.8	11	22.8	\pm 1.1	11
			24 hr	24.3	\pm 0.9	10	23.6	\pm 0.6	10	21.8	\pm 0.6	11
			48 hr	23.9	\pm 1.6	10	24.5	\pm 1.1	9	23.6	\pm 2.7	5
	5-10 μm^3	absolut	0 hr	31.0	\pm 3.2	10	46.5	\pm 3.9	11	48.2	\pm 4.1	11
			24 hr	20.2	\pm 2.5	10	45.7	\pm 4.3	10	31.7	\pm 4.9	11
			48 hr	12.9	\pm 2.1	10	36.1	\pm 3.5	9	23.0	\pm 3.8	5
		%	0 hr	8.1	\pm 0.5	10	11.4	\pm 0.4	11	12.1	\pm 0.9	11
			24 hr	9.1	\pm 0.6	10	12.9	\pm 0.5	10	10.3	\pm 1.0	11
			48 hr	8.4	\pm 0.6	10	11.9	\pm 0.6	9	9.7	\pm 1.1	5
	10-30 μm^3	absolut	0 hr	11.8	\pm 2.2	10	45.2	\pm 3.5	11	36.5	\pm 2.6	11
			24 hr	8.7	\pm 1.1	10	32.9	\pm 3.9	10	19.7	\pm 2.1	11
			48 hr	3.5	\pm 0.7	10	33.2	\pm 6.1	9	18.6	\pm 2.7	5
		%	0 hr	3.2	\pm 0.6	10	11.2	\pm 0.6	11	9.5	\pm 0.9	11
			24 hr	4.2	\pm 0.5	10	9.3	\pm 1.1	10	6.8	\pm 0.7	11
			48 hr	2.4	\pm 0.4	10	10.5	\pm 1.5	9	8.1	\pm 1.2	5
>30 μm^3	absolut	0 hr	0.3	\pm 0.2	10	10.0	\pm 1.4	11	8.6	\pm 1.7	11	
		24 hr	0.0	\pm 0.0	10	9.1	\pm 1.3	10	6.2	\pm 1.5	11	
		48 hr	0.0	\pm 0.0	10	6.8	\pm 2.2	9	4.2	\pm 1.4	5	
	%	0 hr	0.07	\pm 0.05	10	2.5	\pm 0.3	11	2.4	\pm 0.6	11	
		24 hr	0.02	\pm 0.02	10	2.6	\pm 0.3	10	2.3	\pm 0.6	11	
		48 hr	0.0	\pm 0.0	10	2.1	\pm 0.6	9	1.8	\pm 0.4	5	

LD = lipid droplet. This table shows starvation-induced alterations in the composition of LD classes of the posterior intestine. The absolute and the relative (%) number of LDs that are <2 μm^3 , 2-5 μm^3 , 5-10 μm^3 , 10-30 μm^3 and >30 μm^3 are indicated for *ad libitum* fed larvae (0 hr starvation) as well as for 24 hr and 48 hr starved wild type and *sams-1* larvae. For experimental procedure, see Material and methods.

Danksagung

Es war ein langer Weg von meiner Entscheidung zur Promotion bis zum Erschaffen dieser Arbeit. Neben zahlreichen schönen und inspirierenden Erfahrungen, hat mich auch der ein oder andere Zweifel am Gelingen begleitet. Um so mehr möchte ich die Gelegenheit nutzen, mich bei einigen Personen zu bedanken, ohne die die Arbeit in der vorliegenden Form nie entstanden wäre.

In erster Linie bedanke ich mich bei meinem Doktorvater Prof. Dr. Frank Döring, der mich mit seinem Enthusiasmus erst für das Projekt "Forschung" begeistern konnte. Ich bedanke mich für die Überlassung eines spannenden und manchmal nervenzerreißenden Themas, für die langjährige Betreuung und insbesondere für das entgegengebrachte Vertrauen in mich und meine Arbeit.

Ein ganz besonderer Dank gilt Prof. Ralf Schnabel, der mich nicht nur für einige Zeit liebevoll in seiner Arbeitsgruppe beherbergt und mir die Durchführung der Mutagenese ermöglicht hat, sondern auch stets für konstruktive Kritik und hilfreiche Anregungen zur Verfügung stand.

Bei Gregory Minevich und Alexander Boyanov bedanke ich mich für die Durchführung und Auswertung des "Whole Genome Sequencing".

Ich danke den derzeitigen und ehemaligen Mitgliedern der Molekularen Prävention für die gute Zusammenarbeit, für ihre Hilfsbereitschaft und für die angenehme gemeinsame Zeit.

Meiner lieben Hausgemeinschaft und der "Langenbecker Umgebung" danke ich dafür, daß sie mich und meine Launen ertragen haben. Danke für die fürsorgliche Verpflegung, die Schulter zum Anlehnen und das unterhaltsame Freizeitprogramm.

Mein größter Dank gilt meiner Familie, die immer an mich geglaubt und mich liebevoll und unermüdlich in allen Lebenslagen unterstützt hat. Ich freue mich darauf in Zukunft wieder mehr Zeit mit ihnen verbringen zu können.

Lebenslauf

Persönliche Daten

Name	Madeleine Ehmke
Geburtstag	06.08.1983
Geburtsort	Eberswalde, Brandenburg
Staatsangehörigkeit	deutsch

Promotion

04/2009 – 07/2013	Promotion (Dr. oec. troph) Christian-Albrechts-Universität zu Kiel, Institut für Humanernährung und Lebensmittelkunde, Abteilung Molekulare Prävention betreut durch Prof. Dr. Frank Döring
-------------------	--

Studium

03/2007 – 03/2009	Masterstudium Ökotrophologie (M. Sc.) Christian-Albrechts-Universität zu Kiel <i>Masterarbeit:</i> "Relationship between reproduction and fat metabolism in the nematode <i>Caenorhabditis elegans</i> "; betreut durch Prof. Dr. Frank Döring
-------------------	--

10/2003 – 03/2007	Bachelorstudium Ökotrophologie (B. Sc.) Christian-Albrechts-Universität zu Kiel <i>Bachelorarbeit:</i> "Die Bedeutung von PPAR γ als Transkriptionsfaktor und dessen natürliche und synthetische Liganden"; betreut durch Prof. Dr. Gerald Rimbach
-------------------	---

Schulische Bildung

06/2003	Abitur Gymnasium Alexander von Humboldt, Eberswalde
---------	---